EXPERIMENTAL RESEARCH ON SEISMIC RETROFITTING OF R/C CORNER BEAM-COLUMN-SLAB JOINTS UPGRADED WITH CARBON FIBER REINFORCED POLYMER (CFRP) SHEETS

by

İbrahim Topcu

B.S. in Civil Engineering, Boğaziçi University, 2005

Submitted to the Institute for Graduate Studies in

Science and Engineering in partial fulfillment of

the requirements for the degree of

Master of Science

Graduate Program in Civil Engineering

Boğaziçi University

2008

To my family

ACKNOWLEDGEMENTS

Foremost, I am deeply indebted to my supervisors Asst. Prof. Cem Yalçın and Assoc. Prof. Azadeh Parvin. Without their help, invaluable suggestions, advice, guidance, and encouragement, this work would not be possible.

I would like to convey my appreciation to Prof. Uğur Ersoy, Asst. Prof. Kutay Orakçal, and Asst. Prof. Şevket Özden (members of the thesis committee) for reviewing this thesis and offering helpful comments.

I would like to say a big 'thank you' to my friends and colleagues, Erdal Gökgöz, Selçuk Altay, and Osman Kaya for their help, contributions and suggestions throughout this study. It would be hard to succeed if they do not give me the feeling of being at home at the laboratory. I would also like to express my gratitude to Begüm Altay and Onur Ertaş and thank to other Structures Laboratory assistants, Serap Altın and Savaş Atmaca. I want to express special thanks to technicians Hasan Şenel and Hamdi Ayar for their assistance during the experiments and for giving me such a pleasant time when working together with them.

I wish to thank to my friends, Nurihan Amuce and Salih Çakır. It would be hard to manage any difficulties occurred during this study whether they do not go about with me.

The financial supports for this research by the National Science Foundation through grant OISE-0535294; and TUBITAK through grant İÇTAG-1597-NSF (103I026) are gratefully appreciated. I am also grateful to BASF-YKS for providing strengthening materials and AKÇANSA for providing ready-mixed concrete used in this research.

Last, but not least, I would like to dedicate this thesis to my family. My special thanks, of course, go to my brothers for their loving support. Finally, and most importantly, I wish to thank my parents. They have always supported and encouraged me to do my best in all matters of life.

ABSTRACT

EXPERIMENTAL RESEARCH ON SEISMIC RETROFITTING OF R/C CORNER BEAM-COLUMN-SLAB JOINTS UPGRADED WITH CARBON FIBER REINFORCED POLYMER (CFRP) SHEETS

An experimental study was conducted on seismically deficient RC corner connections with and without floor slab in order to examine the behavior under seismic action and to develop proper strengthening techniques. Four 2/3 scale specimens were tested which were designed according to pre 1970's USA design codes. The specimens were designed to simulate non-ductile detailing characteristics of pre-seismic codes construction. Therefore, they contained some typical detailing deficiencies; 1) lapped splices of column reinforcement just above the joint region, 2) widely spaced column ties, 3) no transverse reinforcement within the beam-column joint, and 4) discontinuous positive beam reinforcement with a short embedment length into the column. Carbon fiber reinforced polymers (CFRP), which were placed around potential hinging zones, were used to strengthen the specimens with floor slab in order to overcome these deficiencies. The specimens were tested under constant axial load, with a magnitude of 700 kN (30% of axial load capacity of the column), and reversed cyclic lateral load.

The test results showed that RC corner connections with above mentioned deficiencies were subjected to the brittle joint shear and bond-slip failures under seismic action. The tested strengthening techniques were successful in delaying and limiting the joint shear and bond-slip failures. CFRP application also improved lateral load versus drift response, energy dissipation potential and stiffness degradation characteristics of deficient subassemblies.

ÖZET

DÖŞEMELİ BETONARME KÖŞE BİRLEŞİM BÖLGELERİNİN KARBON FİBER TAKVİYELİ POLİMER MALZEMELERLE SİSMİK GÜÇLENDİRİLMESİ

Sismik yetersizliği bulunan döşemeli ve döşemesiz betonarme köşe birleşimlerin sismik etki altındaki davranışının belirlenmesi ve uygun bir güçlendirme tekniğinin geliştirilmesi üzerine yapılan bir deneysel çalışmadır. Bu çalışma kapsamında 1970 öncesi Amerikan kodlarına gore dizayn edilmiş 4 adet 2/3 ölçekli numune test edilmiştir. Numuneler deprem yönetmeliklerinden önce inşa edilen yapılarda bulunan sünek olmayan detaylandırma karakteristiklerini simule edebilecek şekilde dizayn edilmişlerdir. Bu nedenle bazı tipik detaylandırma yetersizliklerini bulundurmaktadırlar; 1) birleşim bölgesinin hemen üstünde kolon donatısında bindirmeli ekler, 2) aralıkları geniş kolon etriyeleri, 3) etriyesiz kolon-kiriş birleşim bölgesi, ve 4) kolona yeteri boyda ankrajlanmamış süreksiz kiriş alt donatısı. Döşemeli betonarme köşe birleşimlerindeki bu yetersizliklerin aşılarak numunelerin güçlendirilmesi amacıyla muhtemel mafsallaşma bölgelerine CFRP sarılmıştır. Numuneler sabit 700 kN eksenel yük (kolon eksenel yük kapasitesinin %30'u) altında, tersinir tekrarlı periyodik yanal yüklere tabi tutularak, test edilmiştir

Deney sonuçlarına göre, yukarıda belirtilen yetersizliklere sahip betonarme köşe birleşimleri mesnetteki aşırı kesme etkisi ve kiriş alt donatılarının sıyrılması nedenleriyle gevrek çökmelere maruz kalmışlardır. Bu çalışma kapsamında test edilen güçlendirme teknikleri, gevrek davranışı geciktirmeyi ve sınırlandırmayı başarmıştır. CFRP uygulaması aynı zamanda numunelerin yatay yük-kat ötelenmesi davranışını, enerji sönümleyebilme potansiyellerini ve rijitlik kaybı karakteristiklerini geliştirmiştir.

TABLE OF CONTENTS

LIST OF FIGURES

LIST OF TABLES

LIST OF SYMBOLS / ABBREVIATIONS

a	Height of the undeformed joint
b	Width of the undeformed joint
C_c	Concrete compression force
d_b	Depth of the beam
D_c	Diagonal compression force
D_s	Diagonal steel force
D_l	Length of the undeforment joint diagonal
e	Eccentricity
f_{ult}	Ultimate strength of steel
$f_{ult\ avg}$	Average ultimate strength of steel
f_y	Yield strength of steel
$f_{y\ avg}$	Average yield strength of steel
H_i	Maximum horizontal force at the i^{th} cycle
L	Span length
l_{dh}	Development length of the hooked bars
M_b	Maximum moment of the beam
M_c	Maximum moment of the column
M_r	Moment strength ratio
T	Tensile force
T_s	Steel tension force
T_c	Steel compression force
V_b	Beam shear force
V_c	Column shear force
V_{jh}	Horizontal joint shear force
V_{jv}	Vertical joint shear force
w	Distributed load
x	Distance from support to the contraflexure point
α	Angle
Δ	Displacement

Δ_α	Change in the angle
Δ_i	Maximum displacement at the i^{th} cycle
ΔD_1	Change in the dimension of joint diagonal
ΔD_2	Change in the dimension of joint diagonal
^0C	Centigrade degree
με	Micro strain
ε_r	Rupture strain of steel
$\varepsilon_{r\ avg}$	Average rupture strain of steel
Ø	Diameter of rebar
τ	Torsional moment

arctan	Arc tangent
ACI	American Concrete Institute
CFRP	Carbon fiber reinforced polymer
FRP	Fiber reinforced polymer
GFRP	Glass fiber reinforced polymer
LVDT	Linear variable differential transformer
RC	Reinforced concrete
USA	United States of America
sqrt	Square root
2-D	Two dimensional

1. INTRODUCTION

1.1. General

Beam-column joints of existing reinforced concrete (RC) structures that have been designed according to pre 1970s national design codes pose serious danger in moderate to severe earthquakes. The vulnerability of these structures is due to the fact that they have been designed for gravity loads and the amounts of lateral force levels that are much lower than those specified by the current codes. Also, the lack of seismic detailing has caused non-ductile behavior. As a result, excessive lateral deformation demands could not be accommodated, and thus, failure mechanisms toward total collapse easily occur.

Beres *et al.* (1996) have determined typical seismic deficiencies in joint regions and members of RC frame structures. They are as follows:

- Longitudinal reinforcement ratio in the columns is less than 2%.
- Lapped splices of column reinforcement are furnished just above the construction joint at the floor level where maximum moments and plastic hinges occur.
- Widely-spaced column ties provide little or no confinement to the joint region.
- Little or no transverse reinforcement within the beam-column joint.
- Discontinuous positive beam reinforcement with a short embedment length into the column.
- Construction joints below and above the beam-column joint.
- Columns with bending moment capacity less than that of the beams (weak column-strong beam case).

Most desired mode of failure for RC frame structures in an earthquake is when first plastic hinging occurs in the beam, and thus, energy due to earthquake forces could be absorbed. However, because of these deficiencies, brittle mode of joint failures is experienced before beams reach their ultimate capacities. This results in undesirable features like sudden degradation of strength and stiffness, and poor seismic energy

dissipation due to joint damage which should be eliminated since the joint is part of the column and its damage has a direct effect on the overall response and stability of the frame. It is therefore important to evaluate the performance of deficient beam-column joints and to devise effective retrofitting techniques towards improved seismic behavior of lateral load resisting moment frames.

Many researchers have conducted experimental studies in order to investigate the effects of these deficiencies on seismic behavior of RC frame structures. These researches generally involve testing of 2-D beam-column joint subassemblies, with no transverse beams and slabs, under simulated seismic action. Transverse beams framing into the joint, confine the joint region which may help to prolong joint shear failures. Likewise, slab contribution may increase the moment capacity of the longitudinal beam, and accordingly, would impede the beam hinging. Therefore, in order to evaluate the performance more realistically, the effects of transverse beams and floor slabs should also be investigated. In light of performance-based researches, strengthening techniques for improving poor performance of deficient joints have also been investigated in similar studies. A variety of techniques applicable to concrete elements have also been applied to joints where RC and steel jackets are among the most commonly applied retrofitting techniques. However, these techniques have been characterized by some disadvantages such as difficulty of ensuring perfect bond and interaction between the old and new parts, labor-intensive procedures, loss of floor spaces, excessive construction time, and increased mass. Research efforts on upgrading existing beam-column joints have focused on the use of fiber reinforced polymer (FRP) composites in recent years. The technique involves the use of FRP composites as externally bonded reinforcement in critical regions of RC members. There are many favorable characteristics of FRP composites, including; high strength-weight ratio, corrosion resistance, ease of application, low labor cost, and no significant increase in member sizes.

In this study, the results of a comprehensive experimental program are presented, and the emphasis was given to seismic performance evaluation of deficient RC corner beam-column joints by considering the effects of transverse beam and slab, and assessing

the applicability of using CFRP composites as an effective technique for the seismic rehabilitation of these deficiencies.

1.2. Research Objectives and Scope

Prior researches have showed the significance of beam-column joints on the seismic behavior of deficient RC frame structures (Beres et al. 1996, El-Amoury and Ghobarah 2002). A substantial portion of these researches have been conducted on the two dimensional specimens without transverse beams and floor slabs. However, in order to evaluate the performance of deficient beam-column joints more precisely, the effects of transverse beams and floor slabs should also be considered. In addition, methods for strengthening of seismically deficient RC frame structures by CFRP composites are tested using simplified two dimensional beam-column joint specimens that do not reflect the real-life situation. This experimental study was mainly focused on the development of an applicable FRP retrofitting technique by taking into consideration the presence of transverse beam and slab.

The research objectives can be summarized as follows:

- To investigate the behavior of seismically deficient RC corner beam-column joints;
- To evaluate the effects of transverse beam and slab on the behavior of seismically deficient RC corner beam-column joints;
- To investigate the effectiveness of CFRP composite materials for rehabilitation of seismically deficient RC corner beam-column joints;
- To develop applicable CFRP retrofitting techniques in order to overcome especially anchorage and shear deficiencies of seismically deficient RC corner beam-column joints by taking into consideration the presence of transverse beam and slab;
- To come up with a rational and practical way to wrap the CFRP fabric around the joint.

In this study, four 2/3 scale RC corner beam-column joint specimens with deficiencies mentioned above were tested under constant axial load and reversed cyclic

loading following a pre-defined displacement history. In the first phase of the study, two control specimens, namely; one with transverse beam only and the other with both transverse beam and slab, were tested in order to investigate the effects of these members on seismic behavior separately. Taken into account of these test results, another CFRP retrofitted specimen, with both transverse beam and slab, was also tested in order to overcome the mentioned deficiencies and to evaluate the effectiveness of the retrofitting scheme. After the test observations of the specimen with first retrofitting scheme, another CFRP wrapping procedure was developed for the last specimen. A total of four tests were performed.

2. LITERATURE REVIEW

2.1. Introduction

Seismic retrofitting is an important task in order to overcome vulnerable effects of earthquakes on non-seismically designed structures. On the other hand, it is also a complicated task which involves more effort than installing a new shear walls or jacketing columns. Detailed investigation, proper design and qualified labor are required to provide adequate performance of structure for seismic effects. First of all, a general sense of expected building performance should be developed. Because of that, many experimental researches have investigated the behavior of existing structures under seismic actions. Some of these studies have concluded that beam-column joints of RC frames that were designed according to pre-1970s codes due to deficiencies already mentioned may have potential for severe damages under seismic action. The publications related to the beam-column joint behaviors and retrofitting techniques by FRP were examined and their summary was presented in this chapter in order to gain more detailed understanding before starting the experimental study.

2.2. Methodology of Previous Experimental Studies

Over the past few decades, the researchers have focused on the seismic behavior of beam-column joints since they were inadequately detailed and ultimately became the weakest links in the lateral load resisting systems of RC framed structures in recent earthquakes. Effects of various parameters on seismic behavior of these weak links have been investigated through numerous experimental studies performed on beam-column subassemblies with typical beam-column joint subassemblies that have been designed to represent interior or exterior joints in a typical RC frame according to pre 1970s design and construction practice. Investigators have selected exterior joints more commonly since they are most vulnerable and are normally expected to fail first. Test specimens have been designed by assuming that points of contraflexure occur in the mid-height of columns and mid-span of beams. Thus, members of subassemblies have always spanned as per assumed

inflection points. Test specimens have been tested either with columns in vertical position or beams with vertical position in a test set-up which has been designed in order to simulate the boundary conditions of the subassembly of a real structure.

One of the main concerns of these experimental researches is to introduce a lateral load-displacement to simulate the seismic loading. Shake table testing is a realistic experimental method for assessing the performance of a frame since an actual earthquake demand could be implemented. However, there are many limiting factors of shake table testing such that unavailability of the equipment and instrumentation in many laboratories. Also, size limitations are often cause problems. Usually, structural subassemblies are tested under quasi-static cyclic loading in order to investigate the behavior and the capacity of specimens.

2.2.1. Quasi-Static Cyclic Loading

In any quasi-static cyclic loading, the specimens are subjected to predetermined numbers of displacement-controlled loading cycles as shown in Figure 2.1, and these load reversals are applied slowly in order to eliminate the effects of material strain rate (Sin 2004). It gives conservative estimates of the real strength of the structure or structural assemblage, since an increase in the strain rate due to the dynamic effects, the real earthquake loads result in an increase in the strength of the materials. Researchers have applied quasi-static loading cycles in terms of displacement ductility or interstorey drifts. Displacement ductility may be defined as the ratio of the maximum displacement to the displacement reached at the yield. Therefore, at first, it is required to define the yield deformation so that the displacement ductility levels that could be imposed to the specimen during the experiment could be determined. Interstorey drift, which is obtained by dividing the interstorey horizontal displacement to the storey height, is commonly used among the United States and Japanese researchers since it avoids the difficulty of the defining the yield displacement level. However, care should be taken in the use of interstorey drift as a test criterion since the level of imposed interstorey drift should depend on the stiffness of the structure and the level of ductility factor to be imposed (Park 1989).

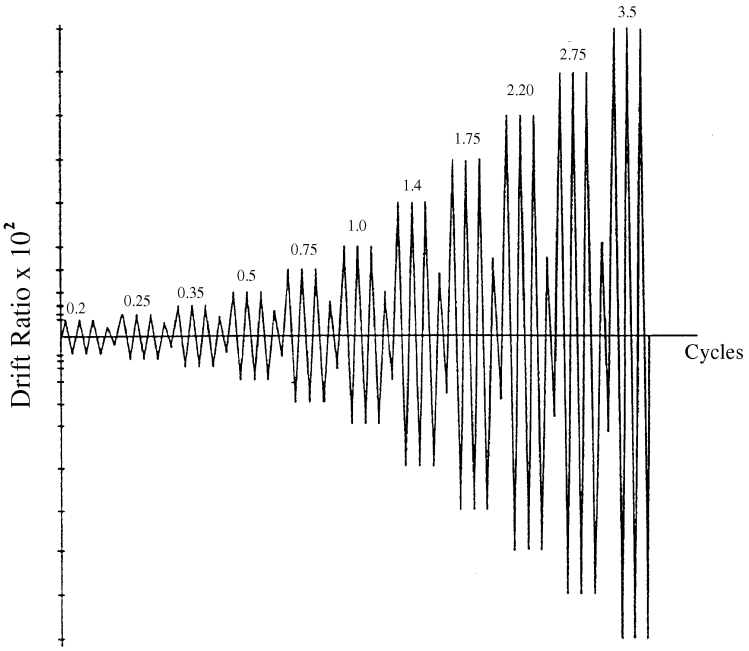

Figure 2.1. Example of test sequence of displacement controlled cycles (ACI T1.1 01 2001).

ACI T1.1 01 (2001) is a guideline on the structural testing of moment frames, and has recommended a test sequence expressed in terms of interstorey drift (Figure 2.1). This sequence is intended to ensure that the displacements are increased gradually in steps that are neither too large nor to small. Too large steps result with that the drift capacity of the system may not be determined with sufficient accuracy. Furthermore, if the steps are too small, the system may be unrealistically softened by loading repetitions and also the results could mask undesirable brittle failure modes that might occur in the inelastic response range during a major event.

2.3. Main Factors Affecting Beam-Column Joint Behavior

2.3.1. Relative Column versus Beam Flexural Strength

Reinforced concrete frame structures that are subjected to strong earthquake ground motions should possess an appropriate collapse mechanism in order to absorb the seismic energy through inelastic deformations. Column hinging, which result in a soft story mechanism, should be avoided since it leads very high ductility demands at the plastic hinges and causes fatal collapse of the building (Figure 2.2(b)). Overall sway mechanism

(Figure 2.2(c)), in which all plastic hinges form in beams, is desirable if the plastic hinge regions are designed properly in order to undergo some large deformations without losing much of their strength and stiffness.

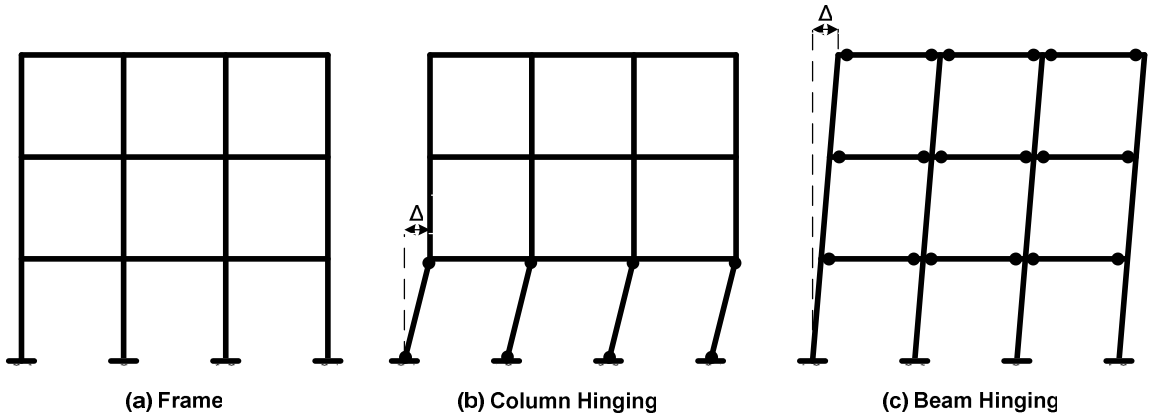

Figure 2.2. Mechanisms in multistory frames

Relative beam to column flexural strength ratio, M_r, is a significant parameter to predetermine the failure hierarchy in reinforced concrete buildings under seismic actions. Many researchers have investigated the effects of different M_r values on failure type of beam-column joints (Ehsani and Wight 1985a, 1985b, Durrani *et al.* 1987, French and Moehle 1991, Di Franco *et al.* 1995). ACI 352 R-02 (2002), in the light of all these experimental studies, proclaims that the sum of the nominal flexural strengths of the column sections above and below the joint should not be less than 1.2 times the sum of the nominal flexural strengths of the beam sections at the joint. This way, a "strong column-weak beam" philosophy could be achieved. However, this condition does not ensure that the column will not yield nor suffer damage if the structure is pushed into the inelastic range. Therefore, much higher M_r ratios are needed (on the order of 2.0 for uniaxial case and 3.0 for biaxial case) in order to achieve this goal, particularly if the structure is flexible and higher modes contribute to the response.

ACI 352R-02 (2002) confirms that slab contribution should also be considered in the evaluation of beam flexural strengths if slab reinforcements are adequately anchored. Strength of majority of bars placed in slabs that interact monolithically with the beams is mobilized as a result of large earthquake-induced displacements. Therefore, neglecting the

contribution of slab reinforcements will cause an underestimation of beam flexural strength, which in turn may risk the performance of components that were intended to remain elastic. Current design codes recommend effective slab width which contributes to the flexural capacity of the beam by considering different connection geometries (ACI 318.02 2002).

2.3.2. Discontinuous Beam Reinforcement with Short Embedment Length

One of the main deficiencies of beam-column joints in gravity load designed structures is the discontinuity of positive beam reinforcement having a short embedment length into the column. Longitudinal beam positive reinforcements are under compression at the joint region only when the gravity load is taken into account. Therefore, it is meaningful to not to concern about an effective anchorage length for these bars since significant bond stresses will not be induced under compressive action. However, moment reversals are to be expected at joint region during seismic action that cause stress reversals in beam, column and slab longitudinal reinforcements at the connection (Figure 2.3). Hence, anchoring longitudinal bars passing through the joint becomes a significant concern, since sufficient bond strength is required to resist resultant tensile forces of negative seismic moments. If it is not considered, an undesirable anchorage failure may occur which considerably reduces energy dissipation capacity and stiffness of the joint.

Insufficient anchorage length for beam longitudinal bars has been studied by Beres *et al.* (1996) as a characteristic deficiency of the existing buildings in the United States that were designed according to pre 1970s code requirements. In this study, the specimens tested with reinforcement embedment of 150 mm. into the column have exhibited limited cracking until their peak resistance was reached. This has been followed by rapid drop in the strength due to the pullout of embedded bars, which has caused a brittle type of failure while forming a hinging mechanism at the beam-column interface instead of ductile, yielding type of beam hinging at a distance away from the column surface. Because of the effect of pullout on slip and crack opening, the neutral axis in the beams migrates upwards causing a smaller compressive block to resist the essentially constant tension force, significantly increasing the compressive stresses and strains in the upper region of the cross section, and potentially leading the crushing of concrete. Large crack openings at the

beam-column interface also causes pinching in the hysteresis loops and rapid degradation of strength and stiffness that results undesirable energy dissipation characteristic of specimens. Also Biddah *et al.* (1997) and El-Amoury and Ghobarah (2002) have studied on this topic and results of these studies are similar.

Altay *et al.* (2007) investigated the bond-slip behavior of inadequately embedded beam bars with experimental and analytical studies. The experimental results had revealed that drift capacity of the test specimen mainly depended on the anchorage capacity of the shortly embedded beam bottom longitudinal reinforcement bars into the column. Comparisons are made between experimental results, and an existing bond stress-slip model in the literature. Based on the observed behavior, in general, analysis results using the developed backbone curve for bond stress-slip relationship pertaining only to this study was in good agreement with experimentally obtained moment-slip rotation results.

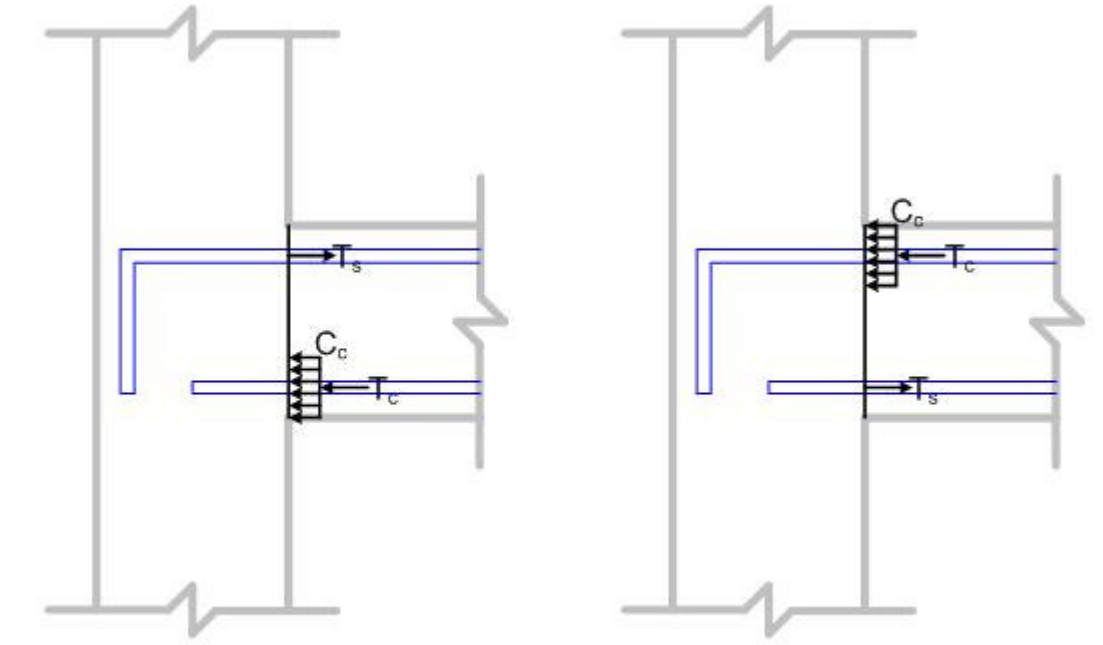

Figure 2.3. Stress reversals at longitudinal beam bars at the joint region

2.3.3. Anchorage Deficiencies in Continuous or Bent Column and Beam Bars

For typical beam-column joints, not only the slippage of inadequately anchored beam bottom bars could be fully eliminated but also the slippage of beam and column bars passing through the joint could not be avoided as well. Kaku and Asakusa (1991a) have outlined the anchorage performances of longitudinal bars passing through beam-column joints based on the results of experimental researches performed in the United States, New Zealand and Japan. In particular, they have studied the effects of bond and anchorage of the longitudinal bars passing through the interior joints and bent in the exterior joints. For both cases, bond deterioration has caused undesirable phenomena such as pinching in the hysteresis loops, increasing the slip deformation at the beam-column interface, moving the shear transfer mechanism in the joint core, and decreasing the flexural strength of the adjoining members. For the case of interior joints, column depth to bar diameter ratio was observed to be effective on the bond behavior of longitudinal bars. They have pointed out that for the case of lower value of this ratio, not only pull-out slip but also push-in slip increases with the loading repetition while greater of this value stops the push-in slip. However, to increase the value of this ratio, excessively beyond a certain limit, was not too effective to reduce the bar slip. Furthermore, they have also demonstrated that since the crack pattern in the joint region is different for bonded and unbonded specimens, shear capacity of the bonded specimen may be less than that of the unbonded one as a result of the excessive damage of concrete strut. For the case of bent bar anchorage in exterior joint, they have studied on the effect of development length, l_{dh}, of hooked bars. They have observed that if the value of l_{dh}/d_b is greater than 10, the maximum tensile forces occurred at longitudinal beam bars at almost all specimens is greater than the yielding forces. In addition, they have concluded that the push-in slip does not occur for the hooked bar which stops the pinching of hysteresis curve due to bond deterioration.

Several researchers have also investigated the effects of longitudinal bar diameter passing through the joint and sizes of the adjoining members on the bond-slip characteristics of beam-column joint subassemblies. Paulay *et al.* (1978) have suggested that smaller reinforcing bars tend to reduce the bond deterioration under reversed cyclic loading. Durrani and Wight (1987) have found out that the presence of flexural hinges at

the face of joint is more important source of the bond deterioration when it is compared with the cracking of the joint core due to shear. The cracking zone, associated with these flexural hinges, was extended into the joint that resulted in a partial loss of bond in the column bars during the tests. They concluded that, the loss of bond and the slippage of bars are unavoidable for normal column sizes unless these flexural hinges are moved away from the joint. As a result, they studied the effects of joint depth-to-bar diameter ratio that is recommended by the codes in order to limit this deficiency. In this study, the difference between anchorage failure characteristics of bottom and top reinforcing bars was investigated for one of the specimens which had joint depth-to-bar diameter ratio of 19 and 16, respectively. Since recommendations for the design of connections have required this ratio of equal to or larger than 20 to control the slippage of bars through the joint, bottom bars should perform better than the top bars. However, the test results have showed just the opposite behavior since the amount of the top steel in the main beam was more than that of the bottom bars. This means the amount of reinforcement worked in tension during the loading affects significantly the bond deterioration and bond slip problems. Finally, ACI 352R-02 (2002) has recommended values for the ratio of column depth to bar diameter to limit the slippage of bars from the joint on the basis of similar studies (Durrani and Wight 1985, Hakuto *et al.* 2000).

Effect of joint confinement on the bond-slip characteristics of longitudinal bars passing through the joint region is another investigated parameter in many experimental studies. Durrani and Wight (1985) have tested three interior beam-to-column connections to examine the effect of joint hoop reinforcement and joint shear stress on the behavior of beam-column joints under seismic action. In this study, joint confinement and the level of joint shear stress improved the bond-slip characteristic of beam main reinforcement that is passing through the joint core significantly, and hence limited the pinching of the hysteresis loops and increased the energy dissipation capacity of the beam-column subassemblies. Similarly, Ehsani and Wight (1985a) have found that joint shear reinforcement in specimens without transverse beams improve the slippage characteristic of the main beam longitudinal bars. Furthermore, in another study of Ehsani and Wight (1985b), improved confinement provided by transverse beams stopped the pullout of beam longitudinal bars. However, the slippage of column longitudinal bars could not be stopped

in this study. Though, the test results showed an increase in the joint transverse reinforcement resulting in a delay of column longitudinal bar slippage in the specimens, both with and without transverse beams and slab.

2.3.4. Joint Shear

Structural design mainly consists of estimating internal and external loads that the structure are be subjected to and developing the most proper design according to the most severe case caused by combinational effects of these loads. Accordingly, beam-column joints should also be designed properly in order to be able to transmit all possible resultant forces acted by adjacent members in the framing. However, gravity load-designed structures have some joint deficiencies as a result of the improper structural analysis due to the lack of seismic consideration.

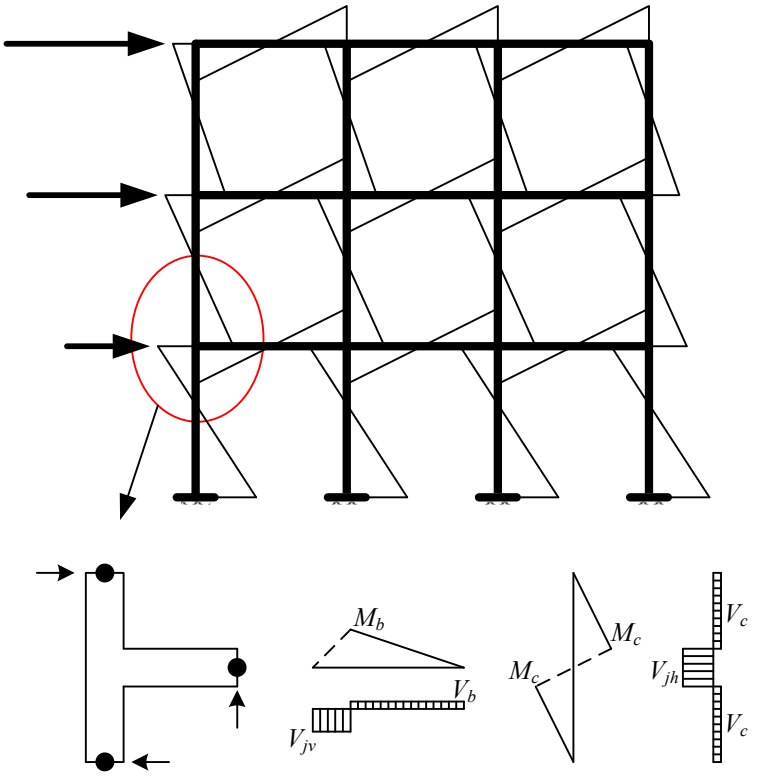

Figure 2.4. Horizontal and vertical joint shear forces

As a result of the seismic action, the joint region is subjected to significant horizontal and vertical shear forces due to moment reversals in the adjacent members

across the joint. As it is shown in Figure 2.4, the magnitude of joint shear forces are much larger than those in the beams and columns that may lead to a brittle joint shear mechanism as a results of strength and stiffness degradation when subjected to cyclic loading in the inelastic range. Additionally, strength degradation within the joint, which is also a part of the column, could also jeopardize the capacity of the column causing total collapse of the building.

Paulay *et al.* (1978) have postulated that there are two shear resisting mechanisms; truss mechanism and a linear concrete strut, which may develop in a beam-column joint, as it is shown in Figure 2.5. Diagonal compression strut mechanism transmits the single diagonal compression force D_c acted on the joint as a resultant of the compression forces of beams and columns at diagonally opposite corners of the joint. However, all the remaining longitudinal steel forces, which should also be in equilibrium, induce significant bond forces within the joint that will introduce shear stresses into the core concrete. That will result in diagonal tension stresses in the joint core which induce diagonal cracks in the majority of cases since the diagonal tension capacity of the joint core concrete will be reached. After that, with the contribution of horizontal and vertical joint shear reinforcements, truss mechanism can be developed in which the core concrete supplies the necessary diagonal compression field with a capacity of D_s. Contribution of these two existing mechanisms to joint shear strength was also investigated in this study. The shear resistance is primarily due to the diagonal strut until plastic hinges form in the beams adjacent to the column faces. However, shear transfer by diagonal compression strut is diminished by full depth cracking at the face of the column and by yield penetration caused by the cyclic loading. Therefore, contribution of truss mechanism is increased that will necessitate more horizontal shear reinforcement.

Ehsani and Wight (1985a, 1985b) studied the effect of joint shear reinforcement percentage and the joint shear stress levels on the behavior of exterior beam-column subassemblies both with and without transverse beams and slabs. In these studies, it was reported that the percentage of joint shear reinforcement or decrease in joint shear stress level improve the overall behavior significantly in specimens without transverse beams and slabs especially that had larger flexural strength ratios. On the other hand, transverse

beams and slabs provided confinement to the joint and increased effective joint width that resulted in improved overall behavior. Therefore, they diminished the effect of joint shear stress level or joint shear reinforcement with the improved behavior of connection.

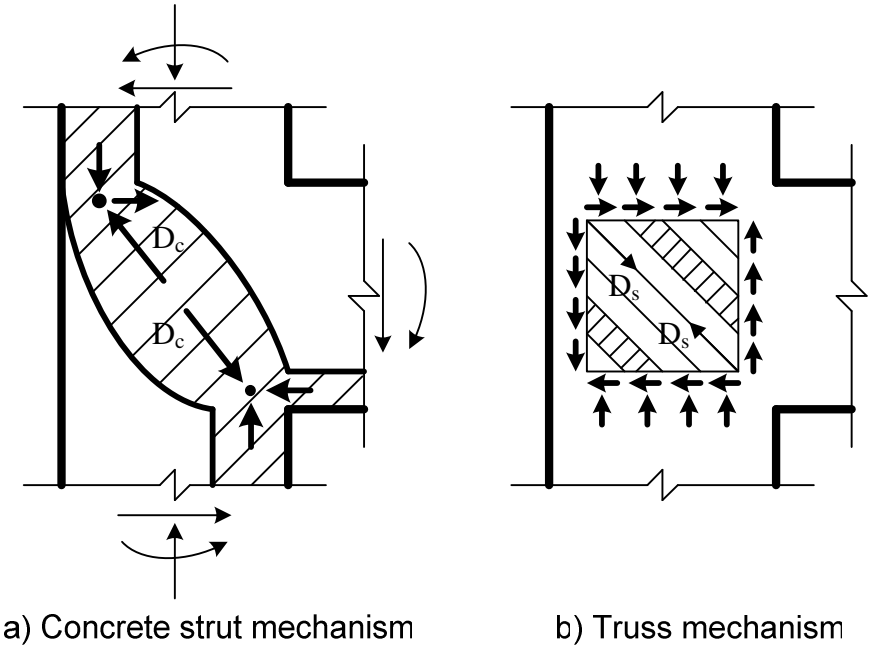

Figure 2.5. RC joint shear resisting mechanisms

The effects of same parameters on the seismic behavior of interior connections were also studied by Durrani and Wight (1985, 1987). They have concluded that joint shear stress has a significant effect on strength and stiffness of subassemblies at larger ductility levels while joint hoop reinforcement was more effective for lower ductility levels, if transverse beams and slabs are not to be considered. However, for the specimens including transverse beams and slabs, the test results showed that joint behavior was not sensitive to changes in the amount of joint transverse reinforcement and joint shear stress level for relative drift levels of less than 2%. At larger deformation levels, the amount of joint transverse reinforcement has become more important than joint shear stress level. Nonetheless, as it was concluded for exterior connections, while transverse beams and slabs have improved the behavior, joint transverse reinforcement and shear stress level was not as effective as they were for specimens without transverse beams and slabs. Likewise,

Hakuto *et al.* (2000) studied the one-way interior beam-column joints with substandard reinforcing details and confirmed the conclusions of these studies.

2.3.5. Axial Load

Effect of axial load on the seismic behavior of beam-column joints have also been investigated in related experimental researches. Cheung *et al.* (1991) have tested interior and exterior beam-column joint subassemblies with floor slabs which have been designed for earthquake resistance by considering the effect of axial load on joint core behavior. They have concluded that, at large inelastic cyclic displacements the shear resistance provided by the diagonal concrete compression strut across the joint core diminishes while that by a truss mechanism formed by the joint core reinforcement becomes dominant if the axial load on the column is low. However, this degradation of the diagonal compression strut mechanism is not so apparent when the axial column load is large. Therefore, in order to simulate the worst case of the joint core behavior, they have not applied axial compression force to the columns of subassemblies. On the other hand, the increase of column axial load level has had no clear effects on ultimate joint shear capacity of specimens tested by Fujii and Morita (1991) while it has been beneficial to reduce the amount of joint shear reinforcement when joint shear failure is surely prevented and column load is kept constant during the disturbance.

Not only shear behavior but also bond-slip characteristic of joint may change with different column axial load levels. It has been investigated by Kaku and Asakuso (1991a) that the reduction of not only absolute slip but also the ratio of deflection due to slip to total deflection has been observed with increasing column axial load which confines the concrete surrounding the development length zone of bent bars in exterior joint. The results of another experimental study conducted by Kaku and Asakusa (1991b) have showed that higher column axial loads retain a spindle type hysteresis loop and maintain a good energy absorption capacity even after excessive lateral displacements. On the contrary, pinching has been observed at the hysteresis loops of specimens with lower axial column loads. They have also studied the effect of tensile axial column force and have found that pinching occurs at an early load stage with the remarkable decrease of load

carrying capacity, compared with the specimens those having the same reinforcement detailing with different axial load level. This implies that also the influence of tensile axial force can not be neglected which is likely to occur in exterior beam-column joints.

Beres *et al.* (1996) have observed minor strength increase and decreased pinching in the columns subjected to higher axial forces from enhanced crack closure and bond along the reinforcement anchored in or passing through the joint. Moreover, they have concluded that the deformability rather than the strength is affected by the presence of axial load.

2.4. Effects of Transverse Beams and Slab

Since the presence of transverse beams and slab may fundamentally affect the seismic behavior of joints, some investigators primarily have focused on this parameter. The outcomes of experimental studies considering additional effects of these members are presented below.

The experimental studies have illustrated that longitudinal bars, which were included in effective width of the slab, contribute the flexural strength of the main beam, if they are adequately anchored. As a result of slab contribution, strength and stiffness of specimens with a slab are higher than the specimens without a slab in both direction of loading. In the study of Durrani *et al.* (1987), the stiffness has increased 60-70% for some specimens with the inclusion of a slab when compared the ones without a slab. As a result of strength and stiffness increase, the specimens with a slab have dissipated 40% more energy than the specimens without a slab in this study. On the contrary, slab contribution may adversely affect the behavior as a result of the increase in the flexural strength of the beam by changing the failure hierarchy to “strong beam-weak column.” Since it is important to determine the flexural strength of the main beam exactly for ensuring a desirable failure hierarchy, an effective slab width should be established properly. Researchers have attributed many factors influence the extent of slab participation. Di Franco *et al.* (1995) have established that torsionally stiff transverse beams result in larger amounts of effective slab width and hence stronger main beams. Moreover, Pantazopolou and French (2001) have concluded that not only the stiffness of transverse beam but also

magnitude of imposed deformation demand; longitudinal and transverse reinforcement distribution in the slab; aspect ratio and boundary conditions of the slab panel; and load history influence the extent of slab participation.

Researchers have also investigated the effects of transverse beams on joint behavior. Ehsani and Wight (1985a) have found that transverse beams provide additional confinement to the joint region which improves the joint behavior significantly. Additionally, they have observed that some of the joint shear stresses are resisted by the concrete outside the joint core thus leaving a smaller percentage of the shear stresses to be resisted by the joint transverse reinforcements. This means that the presence of transverse beams also increases the effective joint depth as well. On the other hand, because of the presence of a slab, the torsion-induced transverse beams introduce torsional shear stresses in the joint and also cause additional cracking of concrete near the joint region. In this context, Durrani *et al.* (1987) have observed that after transverse beams reach their torsional cracking strength, the strain in the joint reinforcement increase rapidly, thus indicate loss of joint confinement by the transverse beams which have also acted as an extension of the joint. French and Moehle (1991) have concluded that additional shear demand may be resisted by overall behavior of slab, transverse beams and joint in interior joints. Therefore additional joint shear reinforcement may not be necessary for interior joints whereas it may be required in exterior joints.

French and Moehle (1991) have summarized the observations of beam-column-slab tests in various aspects. Differently from above mentioned, they have concluded that slab action in a continuous structure differs from that in isolated connections tested in laboratories. The difference can easily be observed by comparison of crack patterns that develop in a slab in continuous and isolated connections. It has been found that the slab shear deformations, slab flexural deformations, and transverse slab strains may also differ as a result of the increased restrained in continuous structures. The overall affect of these differences may be that the slab contribution is larger in continuous structures as compared with results from experimental studies. However, they have also highlighted that further study is required before definite conclusions on this subject may be drawn.

2.5. Seismic Retrofitting of Beam-Column Joints

As all of the researches mentioned above illustrate, beam-column joints can be critical regions in reinforced concrete frames under severe seismic effects. Since beam-column joint failures have been observed in recent earthquakes worldwide, concerns for seismic rehabilitation of these 'weak links' grew considerably (Figure 2.6). Although rehabilitation of RC joints is a rather difficult task and many researchers have studied on various techniques included epoxy repair, concrete jacketing, steel jacketing and/or addition of external steel elements, as well as fiber reinforced polymer (FRP) composite applications.

Figure 2.6. Joint Failure (El-Amoury and Ghobarah 2002)

As it was described by Moehle (2000), two approaches generally are considered for a seismic rehabilitation project; (1) global modification of the structural system, (2) local modification of structural components. In the first approach, the modifications to the structural system are designed so that the design demands, often denoted by target displacement, on the existing structural and nonstructural components are less than their capacities. Common modifications include addition of structural walls, steel braces, or base isolators. In the latter approach, the objective is to increase the deformation capacity of deficient components so that they will not reach their specified limit state as the building responds at the design level. Beam-column joint rehabilitation is the one corresponds to

this approach. In this context, many experimental studies have been conducted in order to develop proper retrofitting techniques for beam-column joints.

Researchers who have studied on the retrofitting of beam-column joints have tried to maintain the goal of latter approach by establishing a strength hierarchy between the columns, beams and joints to ensure the formation of ductile beam hinging mechanism instead of column hinging or brittle joint failures. In gravity load-designed structures, where beams are often stronger than columns, strengthening the column is generally not sufficient by itself since the joint then becomes the next weakest link due to nonductile reinforcement detailing in the joint region. Thus, retrofitting scheme should also overcome these deficiencies of joints. Achieving such an improvement is challenging in actual three-dimensional frames because of the presence of adjoining members framing into the joint that limit the accessibility of the joint and because of the difficulties in developing the strength of externally placed reinforcements within the small area of the joint. However, majority of these researches have not accounted for the three dimensional geometry of the actual frame joints (Engindeniz *et al.* 2005).

2.5.1. Repair and Strengthening Techniques for Beam-Column Joints

Several researchers have investigated strengthening of deficient RC beam-column joints using various techniques. Engindeniz *et al.* (2005) have presented a state-of-the-art publication on these strengthening techniques including; 1) epoxy repair, 2) removal and replacement, 3) concrete jacketing, 4) concrete masonry unit jacketing, 5) steel jacketing and addition of external steel elements, 6) strengthening with FRP composite applications. Each method has been reviewed with emphasis on its application details, required labor, range of applicability, and performance. Additionally, relative advantages and disadvantages of each method have been discussed in this study. A brief summary of findings from researches previously conducted on these techniques except FRP composite applications will be given in this part on the basis of this state-of-the-art study.

One of the earliest and the most common solutions for rehabilitation of concrete frames is to encase the existing column, along with the joint region, in new concrete cover with additional longitudinal and transverse reinforcement, namely concrete jacketing. The

continuity of the added longitudinal bars through the joint requires opening the slab at the column corners. The addition of the joint transverse reinforcement makes the process even more labor-intensive, in which case the beams are also confined and in-place bending of the hooks is necessary. Results of the researches conducted on this technique have concluded that concrete jacketing did provide increased joint strength, shifted the failure to the beam, and increased the overall lateral strength and energy dissipation. However, there are some disadvantages which limit the applicability of this method. An apparent disadvantage is labor-intensive procedures mentioned above. Jacketing also increases the member sizes, which reduces the available floor space and increases mass. In addition, the construction procedure disrupts the building occupants, which may well add to the overall cost of the rehabilitation. Finally, such jacketing techniques alter the dynamic characteristics of the building which may cause increased demands at unintended locations, and may require careful re-analysis.

In steel jacketing technique, various configurations of steel jackets, plates, or shapes have been used to increase the strength and ductility of deficient beam-column joints. Steel jackets consisting of flat or corrugated steel plates, or rectangular or circular tubes are prefabricated in parts and welded in place. The space between the jacket and RC frame is grouted with nonshrink or expansive cement mortar. Steel parts are often mechanically anchored to the concrete to improve confinement. In the light of experimental studies, Engindeniz *et al.* (2005) have said that when compared with concrete and masonry jackets, the use of steel jackets can significantly reduce the construction time due to prefabrication. However, disadvantages such as the potential for corrosion, difficulty in handling the heavy steel plates, objectionable aesthetics in the case of corrugated steel plates, and loss of floor space in the case of grouted steel tubes, can not be overlooked. Steel jackets may result in excessive capacity increases, even where only confinement effect is intended, and create unexpected failure modes. Even if these disadvantages are ignored, it seems difficult to apply these schemes to actual three dimensional joints.

More than a decade ago, a new technique for strengthening structural elements emerged. The technique involves the use of FRP composite materials as externally bonded

reinforcement in critical regions of RC elements. In this context, the use of FRP composite applications to retrofit deficient beam-column joints has gained a wide spectrum of applications in recent years. Findings of the experimental studies on this technique have presented below in detail.

2.5.2. FRP Composite Applications

FRP composite applications to retrofit seismically deficient structures have been in the center of attention in the past few years since they offer advantages over structural steel and reinforced concrete. Some of the advantages are the superior resistance to corrosion, high stiffness-to-weight and strength-to weight ratios, the ability to control the material's behavior by selecting the proper orientation of the fibers, ease of application (including limited disruption to building occupancy), low labor costs, and no significant increase in member sizes. All of these features make carbon fiber composites a highly engineered material suitable for infrastructure applications, in spite of the fact that the cost of carbon fibers is much higher than the cost of conventional construction materials (Gergely *et al.* 2000 and Engindeniz *et al.* 2005).

The bond between the concrete surface and the composite sheets is critical for FRP composite applications as in every retrofitting procedure involving externally attached materials to existing members. Gergely *et al.* (2000) have mentioned that the quality of the concrete surface, from the adhesion point of view, depend greatly on the quality of the finish, the concrete strength, and the presence of materials deposited on the surface (paint, dust, oil, loose material etc.). They have investigated the effects of two different surface preparation; namely wire brushing and water jetting, on the effectiveness of FRP composite applications. Superior performance has been achieved by water jetting the concrete surface and using a high strength adhesive which indicates the improved effect of proper bond between composite and concrete surface. In conclusion, in order to obtain required bond between the FRP composite and concrete surface, Engindeniz *et al.* (2005) have pointed that the concrete surface should be thoroughly cleaned, a penetrating epoxy primer should be applied, and each ply should be placed between two coats of resin.

Gergely *et al.* (2000) have focused on a retrofitting technique for beam-column joints based on externally applied CFRP sheets and have tested 14 specimens by considering the following variables: the composite curing process, the CFRP layout, and the surface preparation of the concrete specimens. In general, the test results have showed that CFRP sheets improve the overall damage control, and the joints have proved to have a minimal residual strength at the end of the test sufficient to support dead load. The observed failure modes have been function of the composite layout, the surface preparation, and the number of layers. For control specimens, shear damage in the beam-column joint region has caused failure at low lateral load. For retrofitted specimens, because CFRP sheets have gradually delaminated from the face of the beam and have left the joint with no effective external reinforcement, a similar but contained damage has occurred. However, the peak lateral load has significantly increased. Delamination of the FRP sheets has been observed to start from the top and bottom of the joint, which have reinforced the importance of proper anchorage. Delamination has occurred at stress levels of only a fifth of the composite's capacity which has shown that adding more inclined layers without enhancing the anchorage of sheets would not improve the behavior. Elevated temperature curing system has not improved the joint shear behavior when it is compared with the room temperature cure system. Most effective FRP orientation in the joint region has been observed to be inclined at 45^0 which is the direction of the principal planes.

Granata and Parvin (2001) conducted an experimental study on FRP strengthening of beam-column joint. This study was performed specifically for evaluating the moment capacity of the beam-column connections wrapped with Kevlar fiber composite fabric. Experimental results demonstrated significant improvement of flexural capacity of beam-column connections and provided certain guidelines for the proper FRP fabric thickness. It was also concluded that the addition of FRP overlays to the bottom of the beam-column connections provided the mechanism for shear transfer between the beam and column elements.

Ghobarah and Said (2002) have tested four exterior joint which represent existing pre-1970 construction. Following the practice before the seismic design codes available, no

transverse reinforcement has been installed in joint region. In order to improve the shear deficiency of the beam-column joint, 4 different rehabilitation techniques have been investigated by using uni-directional or bi-directional glass fiber reinforced polymer (GFRP) sheets. Two control specimens, namely T1 and T2, which have subjected to different axial column loads have behaved in a similar manner and have failed in classical joint shear-failure mode. The results from the testing of joint T4 have shown that unanchored GFRP does not contribute much to the shear strengthening since joint-shear failure has occurred after the delamination of FRP. Therefore, they have pointed the importance of anchorage in order to develop strength of the fiber and in providing confinement to the joint. Therefore, specimens T1R and T2R, previously damaged in the joint region and repaired, have been provided with mechanical anchorage using steel plates and threaded rods core-drilled through the joint. Specimens T1R, T2R, and T9 have performed well in eliminating or delaying the shear mode of failure. Instead, the failure mode has been transferred to flexural hinging of the beam, which is a ductile mode of failure. Thus, the rehabilitated specimens have exhibited energy dissipation characteristics superior to those of the control specimens T1 and T2.

El Amoury and Ghobarah (2002) have used GFRP sheets to strengthen exterior joint in a typical concrete frame which have design and detailing deficiencies under seismic loads namely; no transverse reinforcement in joint region and inadequate anchorage length for the bottom reinforcement of the longitudinal beam. In order to upgrade the shear strength of the joint, the joint has been wrapped with two U-shaped composite layers which have anchored using steel plates and tie rods driven through the joint. For upgrading the steel bars' bond slip, GFRP sheets have been applied to the beam bottom face and have extended along the inner column face. Steel plates have been used to enhance the bond between the GFRP and the concrete and to overcome debonding of these sheets from the concrete surface at the beam-column corner. They have concluded that the rehabilitation techniques have eliminated the brittle joint shear failure, have improved the bond conditions of the beam top reinforcement, have delayed the slippage of the bottom steel bars, have increased the energy dissipated by the specimen, and have reduced the stiffness degradation of the joint.

Antonopoulos and Triantafillou (2003) have investigated the effect of various parameters on the behavior of shear critical exterior RC joints strengthened with FRP by testing 18 specimens. The results have demonstrated the important role of mechanical anchorages in limiting premature debonding, and they have provided important information on the investigated parameters, including: area fraction of FRP, distribution of FRP between the beam and the column, column axial load, internal joint (steel) reinforcement, initial damage, carbon versus glass fibers, sheets versus strips, and the effect of transverse beams. In this study, debonding has dominated the behavior of FRP unless very low area fractions are employed or proper mechanical anchorages are provided. Concerning this, mechanical anchorages and wrapping of longitudinal FRP sheets with transverse layers have increased the effectiveness of both strips and sheets. However, they have pointed that for the same area fraction, flexible sheets are more effective than strips. Additionally, both the strength and the dissipated energy have increased considerably with -but not proportionally (due to premature debonding) to- the number of FRP layers. On the other hand, they have also concluded that increasing the FRP area fraction only in the beam is nearly as effective as it is for equal increase in both the beam and the column, implying that the effectiveness of column FRP is rather limited. Though, the effectiveness of FRP sheets in joints with a transverse beam or with joint shear reinforcement has been reduced when it is compared to planar system with no shear reinforcement. Antonopoulos and Triantafillou (2002) have also modeled FRP strengthened joints analytically. The models provide equations for stresses and strains at various stages of the response (before or after yielding of the beam or column reinforcement) until the ultimate capacity is reached, defined by concrete crushing or FRP failure due to fracture or debonding. Analytical predictions of shear strength have been found to be in good agreement with these experimental results. Moreover, a few parametrical study carried out in this study have indicated that even low quantities of FRP materials may provide significant enhancement of the shear capacity.

Mukherjee and Joshi (2004) have conducted an experimental study on the FRP composite retrofitting of two different types of interior RC beam-column joints; (1) adequately designed and detailed joints, (2) joints with anchored deficient beam bottom reinforcements. In this study, the control specimens have also been rehabilitated after

testing to investigate the effectiveness of retrofitting technique for damaged specimens. They have used both glass and carbon composite materials and have concluded that both of them can be efficiently used for seismic retrofitting as well as rehabilitation of reinforced concrete joints. However, specimens strengthened using CFRPs have shown stiffer behavior than GFRP strengthened specimens because the stiffness of carbon is considerably higher than that of glass. Considerable increases in yield load and initial stiffness have been achieved regardless of reinforcement detailing and damage state. Test on rehabilitated specimens have suggested that FRP not only restores original strength of specimen but also there is considerable enhancement in its yield load, initial stiffness and energy dissipation capacity.

Balsamo *et al.* (2005) have tested a full-scale RC dual system which consists of two frames. Two tests have been performed on the original structure; the first under the design earthquake and the second under 1.5 times more than the design earthquake force. After the damage, the structure has been repaired using CFRP laminates and then subjected to a new series of two tests with the same input accelerograms selected for the original. They have aimed at assessing the opportunity of using composite materials as an effective technique for seismic repair of RC frames. They have focused on the local modification of components which is based on the upgrade of single members characterized by unsatisfactory performance. The experimental outcomes have pointed out that the repaired structure has not attained any local mechanism above the foundation, but its failure has been controlled by the column/wall-footing interface. The occurrence of such local crisis due to the termination of the CFRP laminates at the bottom of the columns/walls has not allowed the repaired structure to show the capacity increase that could be potentially attained due to the FRP strengthening. However, CFRP composites have allowed the repaired structure to withstand the displacement demand under both design and 1.5 design earthquakes with moderate damage above the foundation. Moreover, the repaired structure has showed a large displacement capacity without exhibiting any loss of strength and with a similar energy dissipation characteristic to that of the original configuration. In particular, the rotations of CFRP repaired joints have always overcame those of original joints under the design earthquake, whereas no significant difference has been measured under the 1.5 design earthquake.

In tests conducted by Ghobarah and El-Amoury (2005), L-shaped FRP orientation has been applied to the beam bottom face and column to overcome the anchorage deficiency of beam bottom reinforcements. Besides, shear deficient joint region has been wrapped by FRP sheets. In order to prevent debonding of FRP sheets, steel plates have been installed in critical locations. The rehabilitation techniques have been found effective in eliminating the brittle joint shear and steel bar bond-slip failure modes. Nonetheless, they have underlined the importance of adequate anchorage system for FRP application to maintain the efficiency of strengthening.

3. EXPERIMENTAL STUDY

3.1. Description of Specimens

In this study, four RC corner beam-column subassemblies, one with transverse beam only and the rest with transverse beam and floor slab, were tested under constant axial and reversed cyclic loading. They were designed according to pre-1970s United States codes since seismic deficiencies of the gravity load designed structures were investigated. Geometrical and reinforcing details of specimens were also chosen amongst typical RC buildings constructed before 1970s in the United States of America. In order to investigate the behavior of as-built structure, two specimens, which were called as control specimens, were tested. The other two were retrofitted through a CFRP application to overcome deficiencies observed in the tests of control specimens. The current investigation is a part of an ongoing experimental research on CFRP application to retrofit seismically deficient RC beam-column joints conducted in Bogazici University Structures Laboratory. The specimens are labeled in accordance with this ongoing research project as shown in Table 3.1.

Here, “US” labeling is chosen, since the details of specimens are commonly observed in seismically deficient RC structures constructed before 1970 in United States. In this project there are several specimens with different seismically deficient reinforcement details. Thus, “3” stands for the third type of reinforcement detailing which was identified as the most critical detailing according to the previously tested specimens in this ongoing project. “C” stands for ‘Corner joint’ and “S” illustrates that specimen has a floor slab. Specimens, which were tested as is, are called as Control while retrofitted specimens are referred as FRP1 and FRP2, representing two different retrofitting schemes developed with a collaborative effort by Dr. Parvin, Dr. Yalçın and the author.

Table 3.1. Description of specimens

Specimen Name	Specimen Sketch	Description
US3-C-Control	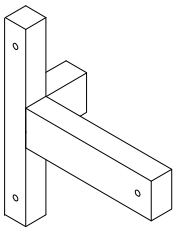	Effects of transverse beam on behavior of 2D beam-column joint subassemblies are investigated.
US3-CS-Control	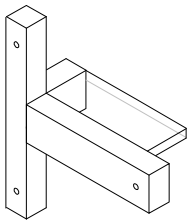	Effects of floor slab on behavior of beam-column joint subassemblies are investigated.
US3-CS-FRP1	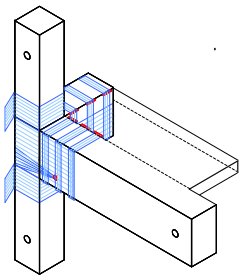	Performance of 1st FRP retrofitting scheme was evaluated.
US3-CS-FRP2	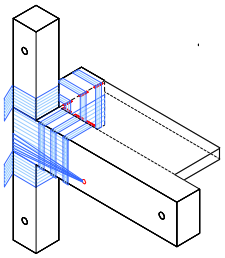	Performance of 2nd FRP retrofitting scheme was evaluated.

3.1.1. Geometry of Specimens

The geometry of specimens represents a typical corner connection of RC structures. In this context, all of the specimens consisted of top and bottom columns framing with two orthogonal beams. As it is shown in the Figure 3.1, the beam that was parallel to the direction of applied lateral load was called as longitudinal beam and the other was called as transverse beam. All specimens except US3-C-Control, were constructed with a floor slab.

Thus, two control specimens were differed from each other to investigate the effects of floor slab on the overall behavior.

A detailed drawing which shows all dimensions of the specimens is given below in Figure 3.3. Under seismic loading, the inflection points are likely to occur in the mid-span of the longitudinal beam and in the mid-height of the columns. Accordingly, column heights and longitudinal beam length were representing the mid-height and mid-span of a typical building, respectively. Span length and story height of a typical RC building was assumed to be 5.5 m and 3 m, respectively. Therefore, longitudinal beam spanned at 1650 mm from the face of the column to the beam end support and the column height was chosen to be 1920 mm from the pin support at the bottom of the column to the location where the lateral load was applied.

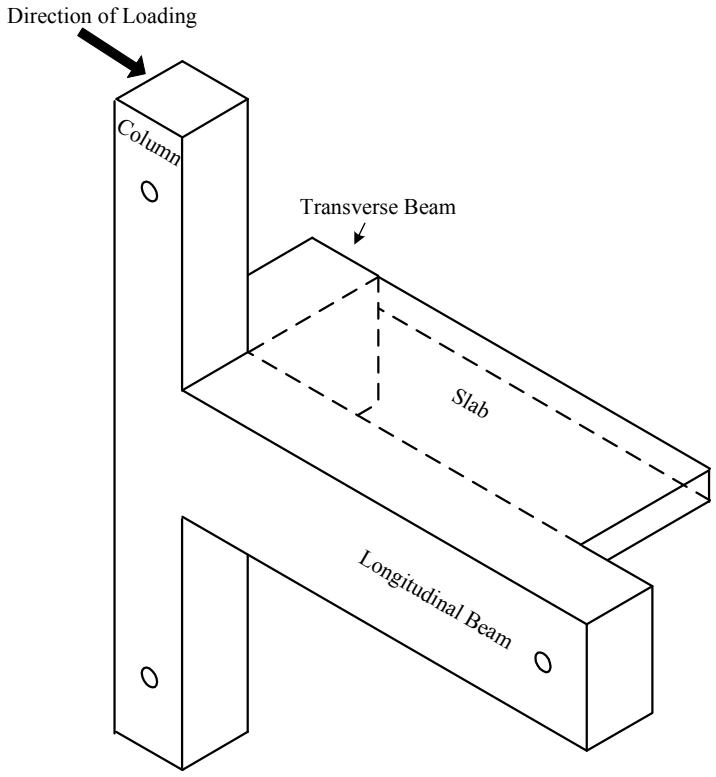

Figure 3.1. 3D view of specimens

Inflection point approach was also applied for determination of the transverse beam length. In the experiments, because of the support conditions, transverse beam was not loaded directly and thus, it was subjected to gravity loads only. Approximate moment

diagrams of beams under gravity loads are given in ACI (Figure 3.2). The distance of the point of inflection to the column face, which corresponds to transverse beam length, was determined by these diagrams. Transverse beam length is equal to subtraction of the column half width from *x*. Therefore, it was found to be more than 265 mm (10.43 in) and less than 700 mm (27.56 in).

On the other hand, transverse beam length should not be smaller than the effective slab width. Therefore, this result was checked by effective slab width requirements of ACI 318-63 (1963). It is recommended that, if beams having a flange on one side only, the effective overhanging flange width shall not exceed 1/12 of the span length of the beam, nor six times the thickness of the slab, nor one-half the clear distance to the next beam. These restrictions resulted with effective slab width of more than 290 mm (11.32 in) and less than 800 mm (31.5 in). In this study, effective width of the slab and the corresponding length of the transverse beam were assumed to be 600 mm which was within the ranges of above mentioned approaches. The slab was 90 mm thick and 1400 mm wide and all specimens had 300 x 300 mm square columns and 300 x 500 mm rectangular transverse and longitudinal beams.

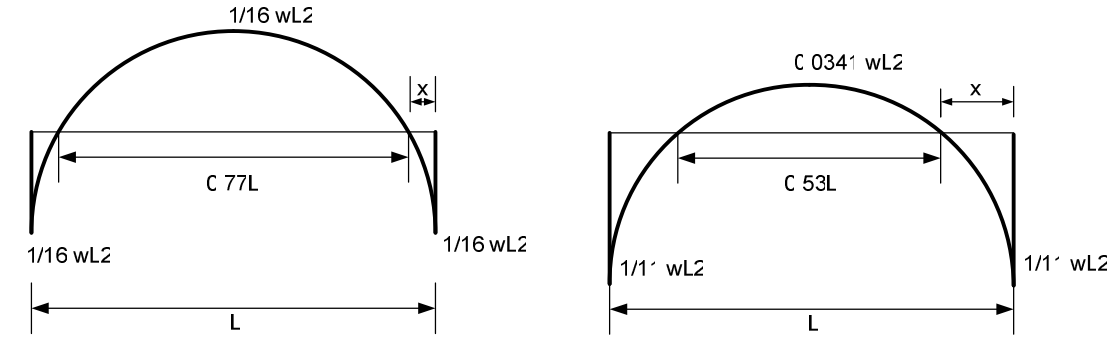

Figure 3.2. ACI Approximate Moment Diagrams

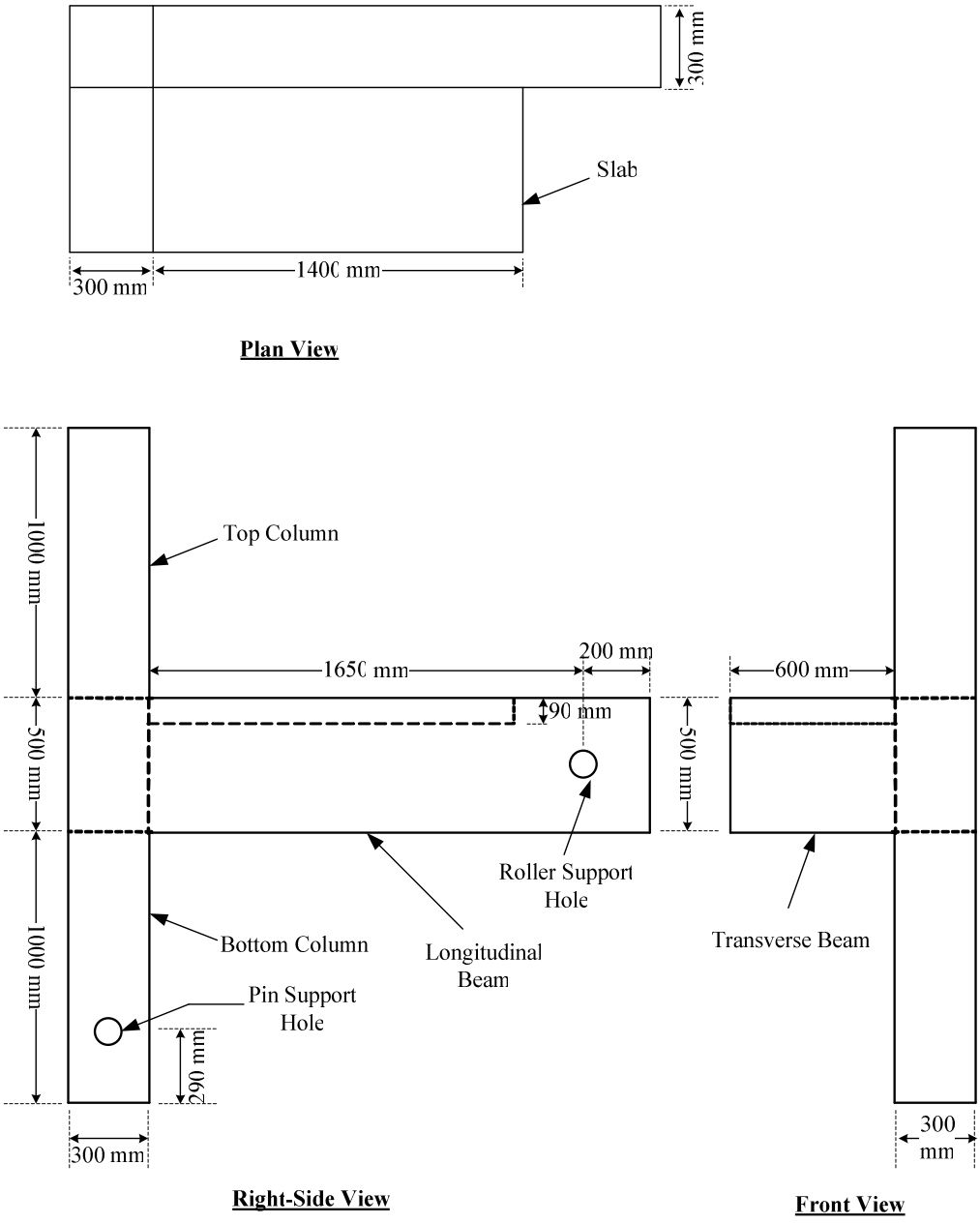

Figure 3.3. Geometrical details of specimens

3.1.2. Reinforcement Details

Reinforcement design and detailing were determined according to ACI 318-63 (1963) and the deficiencies of the gravity load designed buildings given in the study of Beres *et al.* (1996). In Beres' study, the following details were found typical and were judged to be potentially critical in an earthquake for these buildings:

- Lapped splices of column reinforcement at the maximum moment region just above the construction joint at the floor level.
- Widely spaced column ties that provide little confinement to the joint.
- Little or no transverse reinforcement within the beam-column joint.
- Discontinuous positive beam reinforcement with a short embedment length into the column.
- Construction joints below and above the beam-column joint.
- Columns with bending moment capacities less than those of the beams.

All specimens consisted of these deficiencies except that the relative moment ratios of specimens were higher than 1.0. Columns and beams were designed to provide the moment strength ratio of 1.0 without considering the slab contribution to the capacity of longitudinal beam. However, the resulting ratio was not exactly equal to 1.0 because the material properties used for design were not matched exactly with the actual properties of the materials used in the construction. In addition, as recommended in ACI 352 R-02 (2002), slab contribution should be considered in the evaluation of beam flexural strengths since slab reinforcements are adequately anchored. Therefore, capacity calculations of the column and longitudinal beam were revised with actual material properties and contribution of slab. The resulting relative beam-column moment strength ratios are given below in Table 3.2.

Table 3.2. Relative beam-to-column flexural strength ratios

	Relative Beam-to-Column Flexural Strength Ratio	
Specimen	**In Push Direction of Loading**	**In Pull Direction of Loading**
US3-C-Control (without slab)	2,41	1,66
US3-CS-Control/FRP1/FRP2	2,23	1,37

Reinforcement details of specimens which include all detailing deficiencies mentioned above are given in Figures 3.4 to 3.6. In all specimens, columns were reinforced with 6∅20 longitudinal re-bars and with widely spaced stirrups as shown in Figure 3.4. Longitudinal beam had 3∅20 top and 2∅20 bottom reinforcements with 150 mm spaced ∅10 stirrups. However, stirrups were closely spaced at support regions of both longitudinal

beam and column in order to prevent local failures. When only gravity loads were taken into account, reinforcement design and detailing of both transverse and longitudinal beam was same since design loads are same for two orthogonal beams. The floor slab was designed according to ACI 318-63 (1963) under vertical loads (dead and live loads) which resulted in minimum reinforcement (∅10@250 mm). Slab reinforcements were adequately anchored to the beams as shown in Figure 3.6.

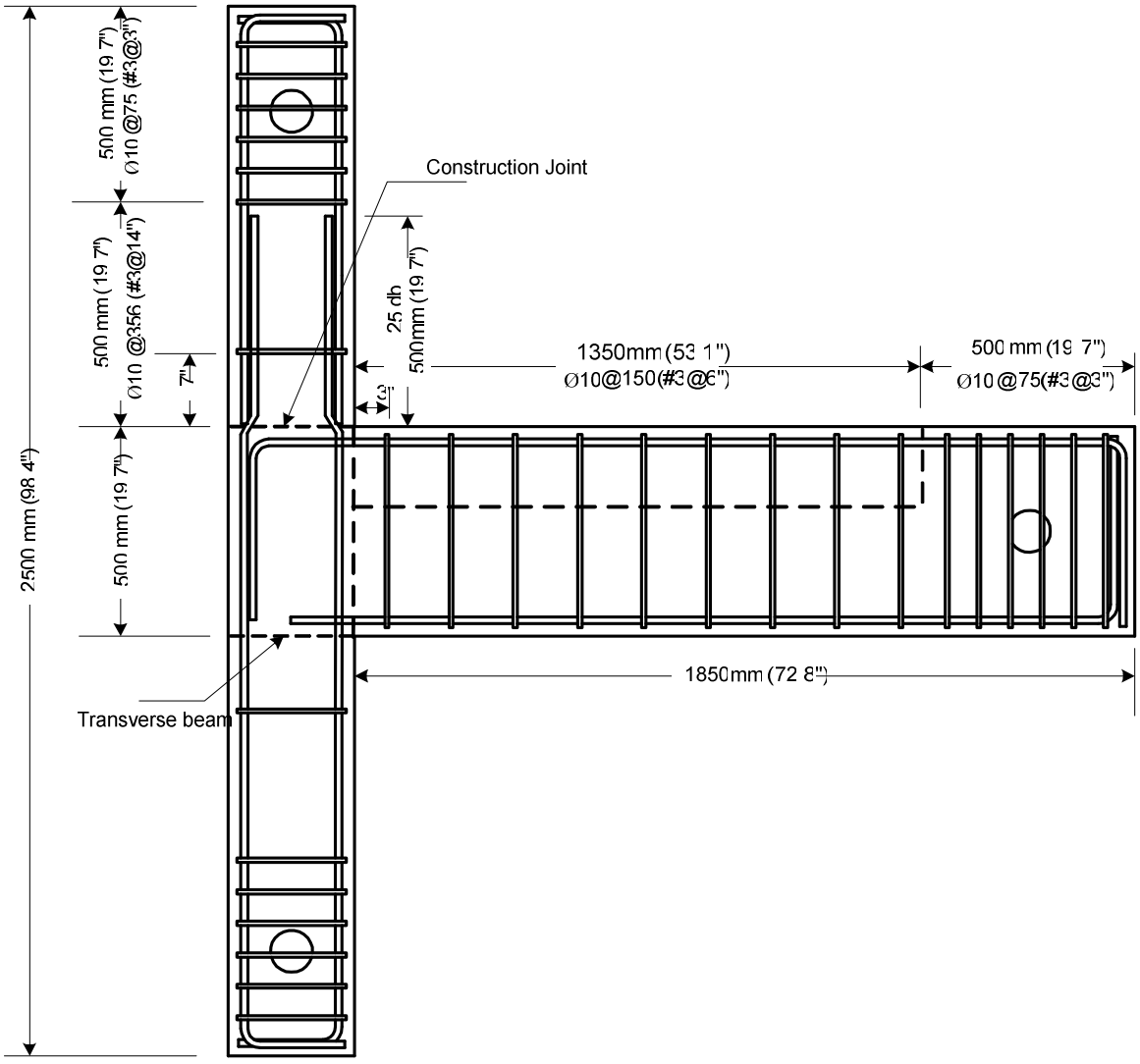

Figure 3.4.Reinforcement details of longitudinal beam and column

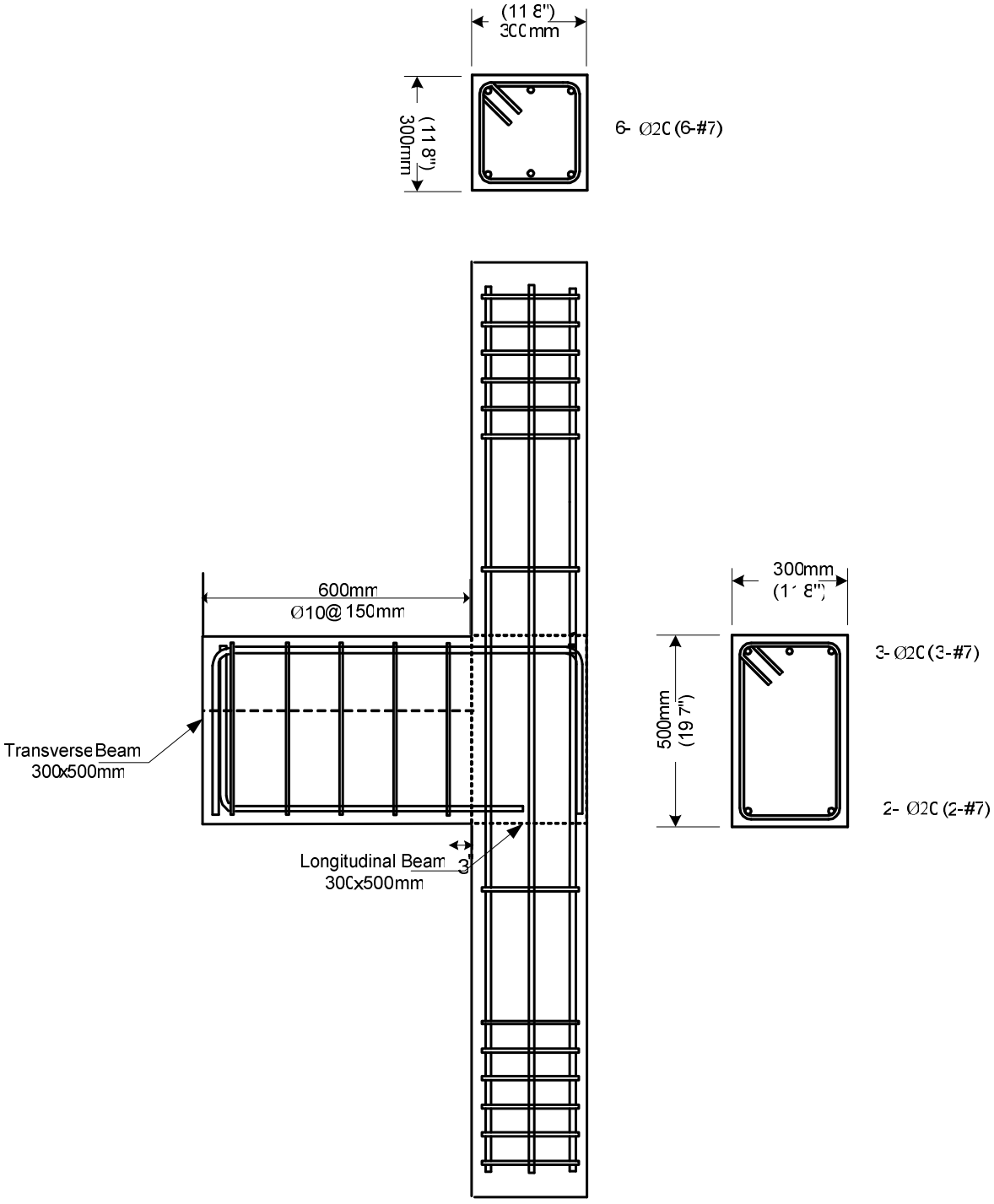

Figure 3.5.Reinforcement details of transverse beam

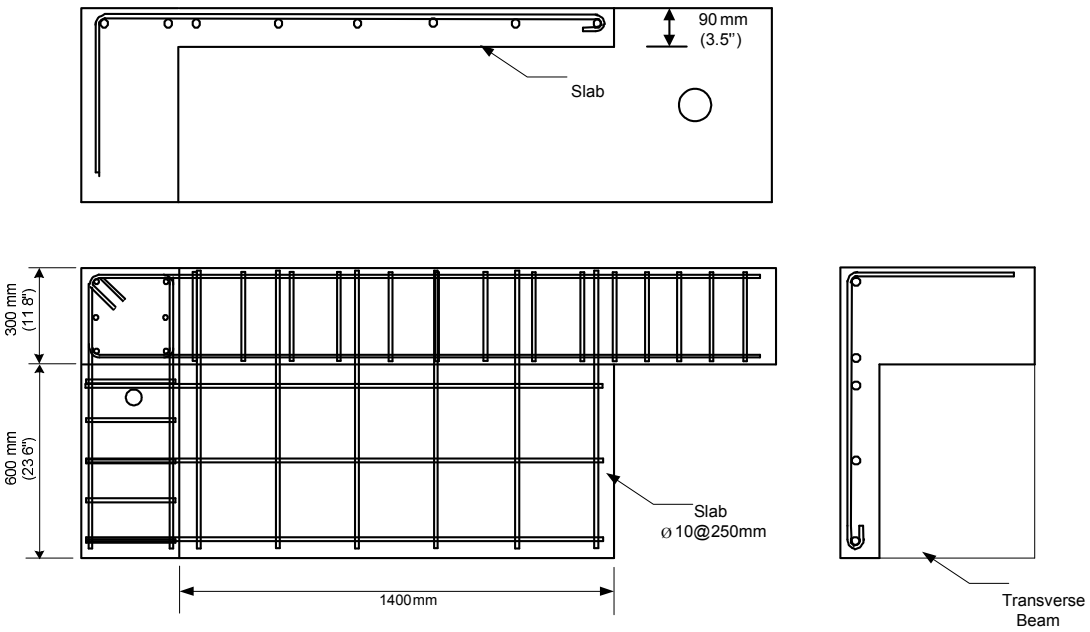

Figure 3.6. Reinforcement details of slab

3.2. Construction of Specimens

The specimens were constructed and cast at the Boğaziçi University's Structural Engineering Laboratory (Figure 3.7). For each subassembly, all members were cast at one time in wooden formworks made of plywood and lumbers. Steel pipes were embedded into the formwork in order to form the holes for hinge and pin supports of the members. Besides, PVC pipes were embedded into formworks for placement of steel rods used for the application of axial load. The form was oiled prior to concrete casting with the aim of ease in formwork removal process. Reinforcement cages for members were prepared at the laboratory and strain gauges were mounted to the bars at predetermined critical locations. Reinforcement cages of columns and beams were first assembled on the ground and then were placed in formworks. Slab bars were tied in the formwork after the placement of column and beam reinforcement cages. The concrete was poured in the upright position of formwork to simulate the field application and was carefully vibrated with electrical vibrator in order to provide proper consolidation. The curing was made by water spraying for 7 days, continuously. After 7 days, formworks were removed and subassemblies were lifted and placed in the laboratory.

Figure 3.7. Construction of test specimens

3.3. Material Properties

3.3.1 Concrete

Ready mix concrete, which was ordered from a local supplier, was used. While casting of subassemblies, 21 samples of cylinders were taken from the mix to be tested for determination of compressive strength of the concrete. The cylinder specimens were kept in molds for 1 day and after the removal of molds they were cured in the same manner as it was done for subassemblies. 3 cylinder samples were tested in 28^{th} day, and tests results are given in Table 3.3. Compressive test machine is shown in Figure 3.8.

Table 3.3. 28th day concrete compressive strength test results

Test Specimen	**Compressive Strength (MPa)**
SP1	31.17
SP2	27.15
SP3	29.23
SP4	29.00
SP5	29.14
Average	**29.14**

Figure 3.8. Compression Testing Machine

3.3.2 Reinforcing Steel Bars

St420 deformed re-bars were used for both longitudinal and transverse reinforcements of all members. ∅20 re-bars were used for longitudinal reinforcements and ∅10 re-bars were used for transverse ones. To evaluate the mechanical properties of steel bars, tensile tests were conducted on 3 samples of each diameter. 600 mm long samples were tested under monotonically increasing load in Dinç Makina Testing Machine, which is shown in Figure 3.9. Mechanical properties of ∅20 and ∅10 re-bars are given in Table 3.4.

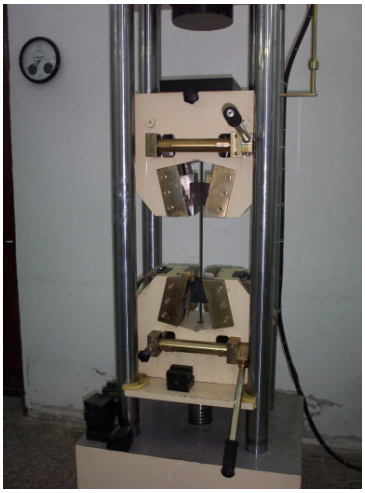

Figure 3.9. Tensile Testing machine

Table 3.4. Mechanical properties of rebars

Rebar Diameter (mm)	Yield Strength (f_y) (MPa)	$f_{y\,avg}$ (MPa)	Ultimate Strength (f_{ult}) (MPa)	$f_{ult\,avg}$ (MPa)	Rupture Strain (ε_r) (mm/mm)	$\varepsilon_{r,avg}$ (mm/mm)
10	397,3	397,3	621,3	624,9	0,18	0,22
	397,3		628,5		0,21	
	397,3		624,9		0,24	
20	440,5	440,0	512,4	513,4	0,23	0,21
	434,3		515,5		0,20	
	445,2		512,4		0,22	

3.3.3. FRP Material

FRP is a new class of composite material manufactured from fibers and resins and has proven to be efficient and economical for the development and repair of new and deteriorating structures in civil engineering. In this study, it was used to enhance seismic behavior of deficient RC corner beam-column joint subassemblies.

CFRP application can be summarized briefly as mounting of CFRP sheets to concrete surfaces by special resins. Installation of CFRP sheets need special care and only trained technicians can install them for proper application. Generally, environmental conditions of CFRP application process must be examined carefully during the winter season and/or cold zones. CFRP should not be applied when ambient temperatures are lower than 5^0C. Similarly, when temperatures are in excess of 20^0C, care shall be taken with batch life of epoxies and special precautions may be necessary.

Before the application, a proper surface preparation is required where CFRP retrofitting will be applied. Surface preparation consists of below mentioned requirements;

- Surfaces must be clean and free of moisture and frost.
- When the fiber sheets have to run perpendicularly to corners, concrete corners must be rounded.

- Existing uneven surfaces must be filled with an appropriate repair mortar or must be ground smooth.
- Dust from surface preparation must be removed using an air blower or other suitable means. If the dust is removed by means of water washing, the surface must be thoroughly dried.

The procedure followed for installing the CFRP sheets to the subassemblies was as following:

- ***Preparing the surface of the specimen***: All the faces of specimen, where CFRP retrofitting is to be applied, were first smoothened with wire brushing technique. If gaps still existed after smoothening process, they were filled with an appropriate repair mortar (MBrace Rasatura Putty). After the curing of repair mortar, smoothening process is repeated for finishing. The corners are rounded to a radius of 20 mm. Finally, the subassemblies were cleaned from dust by using air blower and water washing to obtain a clean surface.

- ***Application of the primer:*** Concrete surface was dried after water washing since the presence of moisture may inhibit adhesion of primer. A primer (MBrace Pimer) which improves the adhesion of CFRP and concrete was applied to the surfaces with roller brush in sufficient quantity that produce a non-porous film in the surface after full penetration. 24 hour curing time passed prior to CFRP application on the primer.

- ***Application of the CFRP with epoxy:*** CFRP sheets were cut beforehand into prescribed sizes using appropriate scissors. After the primer got dry, two component epoxy adhesive of CFRP, MBrace Adesivo (Saturant), was prepared and CFRP fabrics were installed to the subassemblies in accordance with the predetermined orientation. Firstly a coat of MBrace Saturant was applied to the primed surface in sufficient quantity by using a roller brush. Then the CFRP sheet was placed on the surface and the surface of adhered sheet was squeezed in the fibre longitudinal direction using the roller brush in order to impregnate resin into

the fabric material and remove any air bubbles. In the case where more than one layer CFRP sheets must be used, this process was repeated. The epoxy was applied to the fabric prior to any thickening or gelling.

Mechanical properties of above mentioned materials (primer and saturant) used for FRP application is given below in Table 3.5 to 3.7. These values were taken from the manufacturer product data sheet. In this study, CFRP fabric produced by BASF, MBrace CF 130, was used. Stress-strain relationship and mechanical properties of this fabric are given below in Table 3.8 and Figure 3.10, respectively.

Table 3.5. Mechanical Properties of MBT-MBrace Primer

Tensile Strength (N/mm^2)	>12
Bending Strength (N/mm^2)	>24
Tensile Elastic Modulus (N/mm^2)	>700
Bending Elastic Modulus (N/mm^2)	>580
Maximum Elongation	3%
Adherence with Concrete	$>\sigma_{tc}$

Table 3.6. Mechanical Properties of MBT-MBrace Adesivo (Saturant)

Compressive Strength (N/mm^2)	>80
Tensile Strength (N/mm^2)	>50
Bending Strength (N/mm^2)	>120
Tensile Elastic Modulus (N/mm^2)	>3000
Bending Elastic Modulus (N/mm^2)	>3500
Maximum Elongation	2.5%
Adherence with Concrete	$>\sigma_{tc}$

Table 3.7. Mechanical Properties of MBT-MBrace Rasatura Putty

Tensile Strength (N/mm^2)	>12
Bending Strength (N/mm^2)	>26
Tensile Elastic Modulus (N/mm^2)	>1800

Table 3.8. Mechanical Properties of MBrace-CF130

Fibre Reinforcement	Carbon-High Tensile
Fibre Density (g/cm3)	1,70
Fibre Modulus (GPa)	240
Fibre Weight (g/m2)	300
Fibre Thickness (mm)	0,176
Tensile Strength (MPa)	3800
Tensile Elongation, Ultimate	1,55

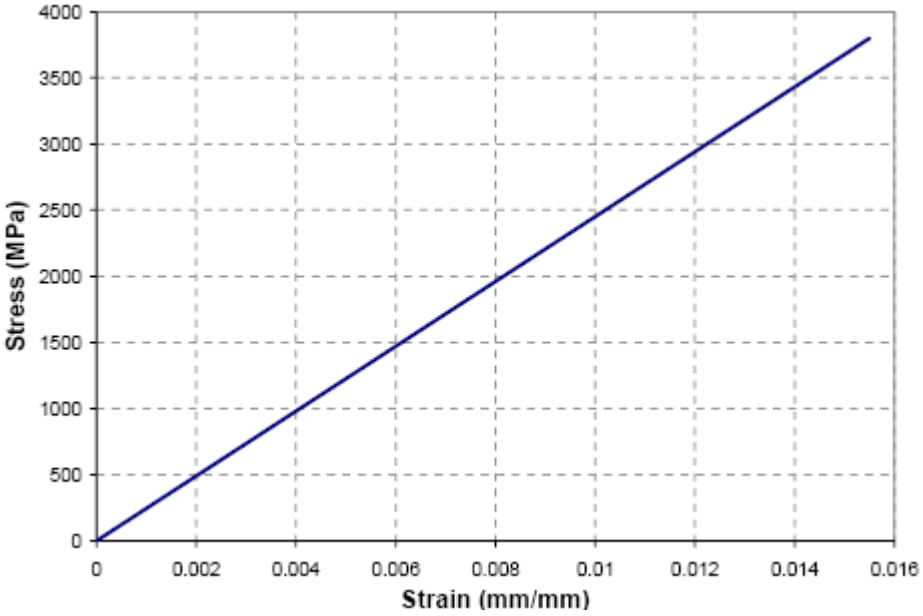

Figure 3.10. Stress-Strain Relationship of CFRP

3.4. Retrofitting Method

3.4.1 Wrapping Orientation for US3-CS-FRP1

In addition to the existing deficiencies, the results of the control specimen tests gave guidance to the evaluation of the first retrofitting scheme. The main problem for the control specimens was the slippage of the longitudinal beam bottom reinforcements which caused a brittle type of failure with rapid strength degradation in the push direction of loading. Inadequate anchorage length of these reinforcements was the reason of the slippage problem. Therefore, in the first retrofitted subassembly (US3-CS-FRP1), one of

the main concerns of the retrofitting was to prevent or delay the slippage which was maintained by the application of FRP belts. As shown in Figure 3.11, six layers of belts which turn around the column and anchored in the drilled hole at the bottom portion of the longitudinal beam were used.

In the pull direction of loading, joint shear deformations governed the behavior of control specimens. In US3-CS-FRP1, six layers of L-shape FRP sheets were applied to the inner and outer sides of the beam-column joint in order to give additional confinement to the joint region to limit shear deformations. It was aimed to prevent joint shear failure in order to delocalize the plastic hinge formation at the longitudinal beam for a ductile failure. Inner and outer L-shape FRP sheets were applied as shown in Figure 3.12.

Figure 3.11. FRP belt

(a) Outer L-Shape FRP Sheets

(b) Inner L-Shape FRP Sheets

Figure 3.12. L-shape FRP sheets

Because column ties were widely spaced, confinement and shear deficiencies occurred at the top and bottom columns close to the joint region during the tests of control specimens. Joint shear and bond-slip cracks were propagated through the top and bottom columns. In the first retrofitting scheme, column wraps were used to avoid these deficiencies by providing additional confinement and improving the shear capacity. 300 mm region of the column from the joint was wrapped with three layer FRP sheets at the top and bottom as shown in Figure 3.13.

Figure 3.13. Column wraps

The importance of proper anchorage for FRP application was mentioned before in Chapter 2. In US3-CS-FRP1, anchorage strips (100 mm wide six layers of FRP sheets) were wrapped around transverse and longitudinal beams in order to prevent the debonding problem of L-shape FRP sheets. These anchorage strips also served as additional shear reinforcement of transverse and longitudinal beams. For passage of anchorage strips, six slots were drilled close to the surfaces of transverse and longitudinal beams on the slab of US3-CS-FRP1. In addition, to anchor FRP belt which was used to prevent slippage problem of longitudinal beam bottom reinforcements, a closed system was maintained by passage of the FRP belt from a hole which was drilled 200 mm away from the column surface at the bottom part of the longitudinal beam. Both anchorage strips and FRP belts

were overlapped 150 mm. Wrapping orientation of the US3-CS-FRP1 is given step by step below in Table 3.9 in the order of application.

Table 3.9. Wrapping orientation of US3-CS-FRP1

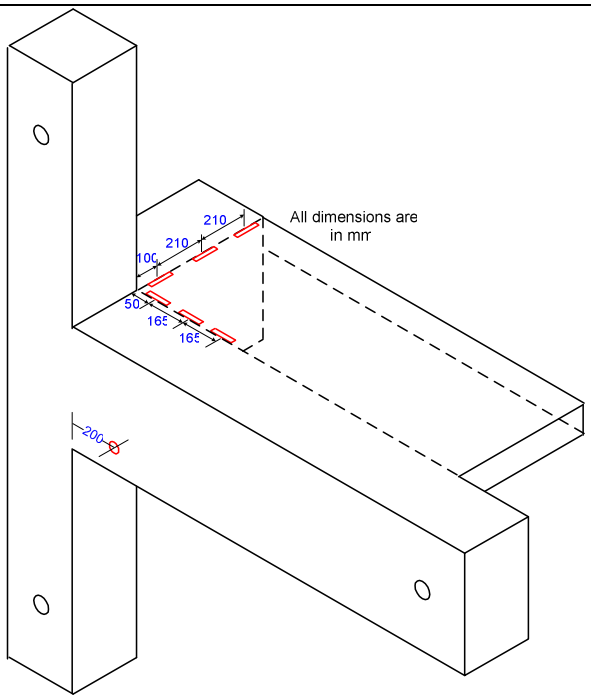

(a) Step 1: Drilling of the holes

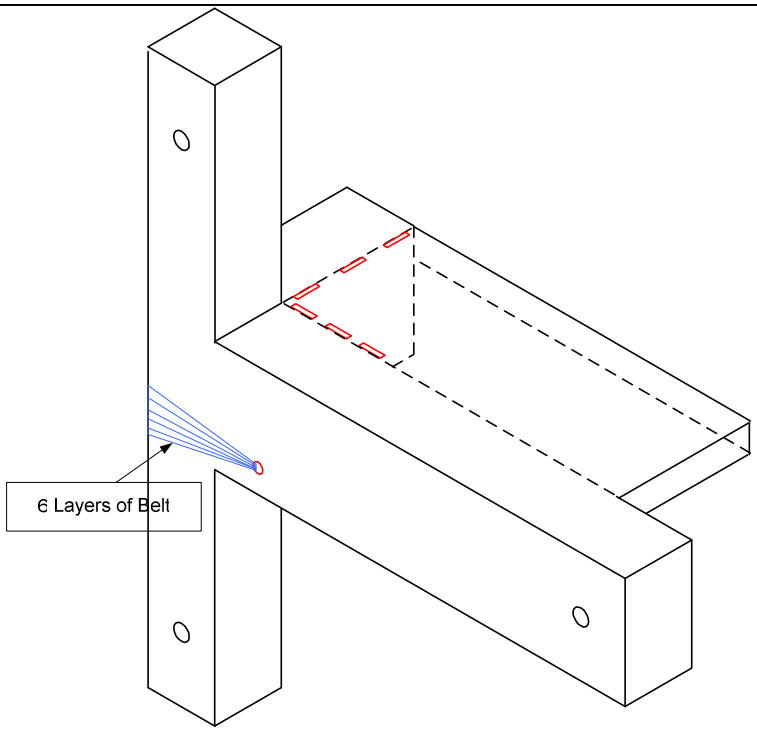

(b) Step 2: Application of the FRP belt

Table 3.9. Wrapping orientation of US3-CS-FRP1 (Cont'd)

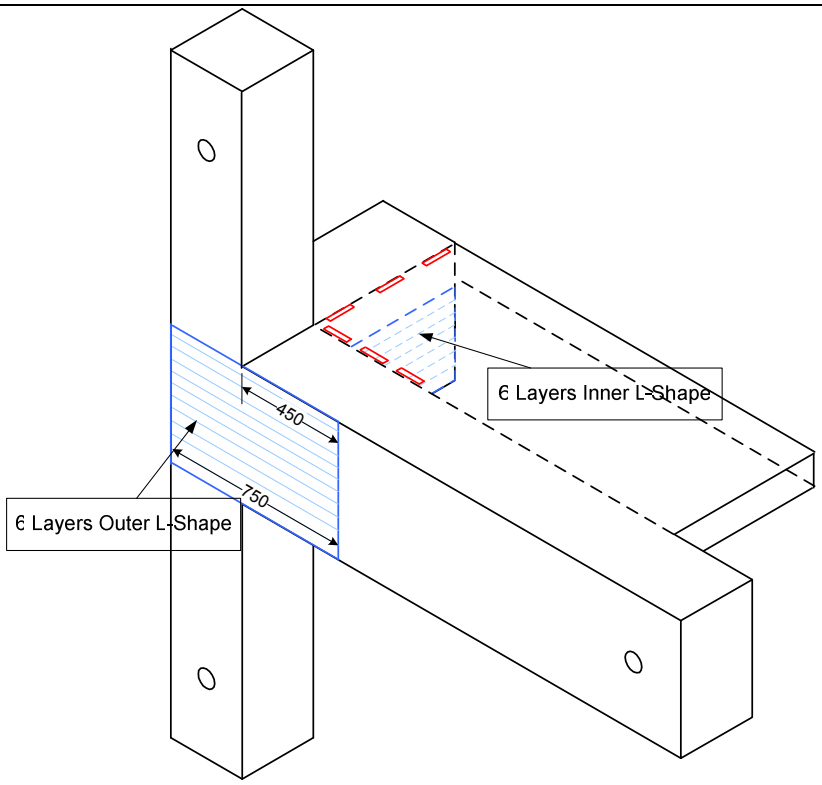

(c) Step 3: Application of the L-shape FRP sheets

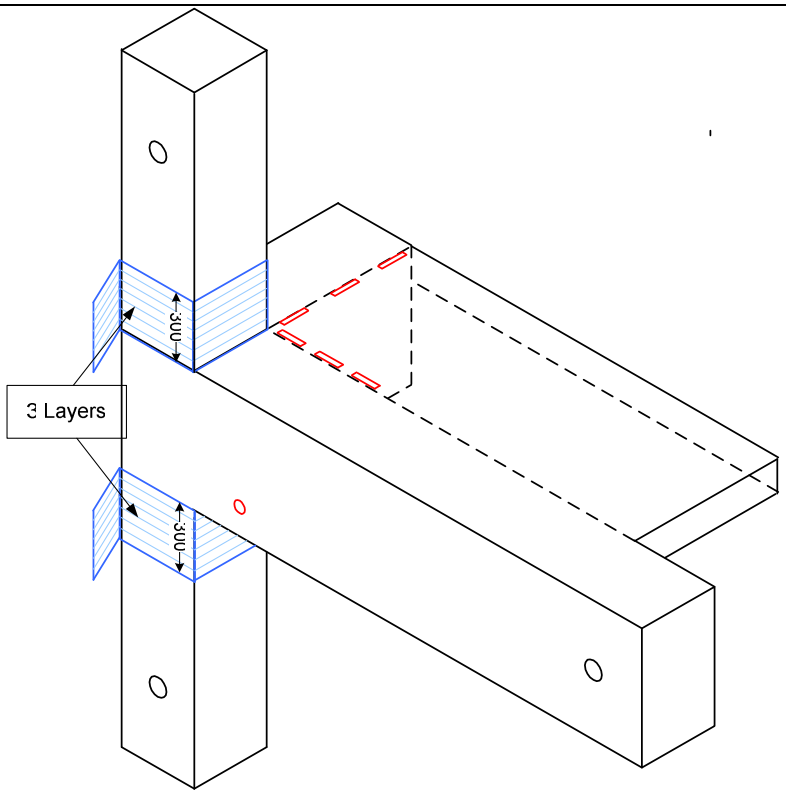

(d) Step 4: Application of the column wraps

Table 3.9. Wrapping orientation of US3-CS-FRP1 (Cont'd)

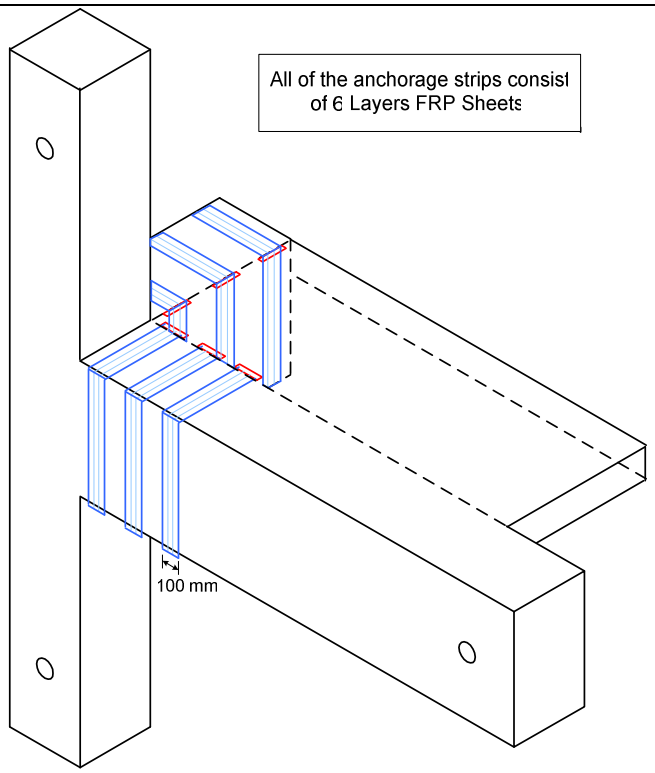

(e) Step 5: Application of the anchorage strips

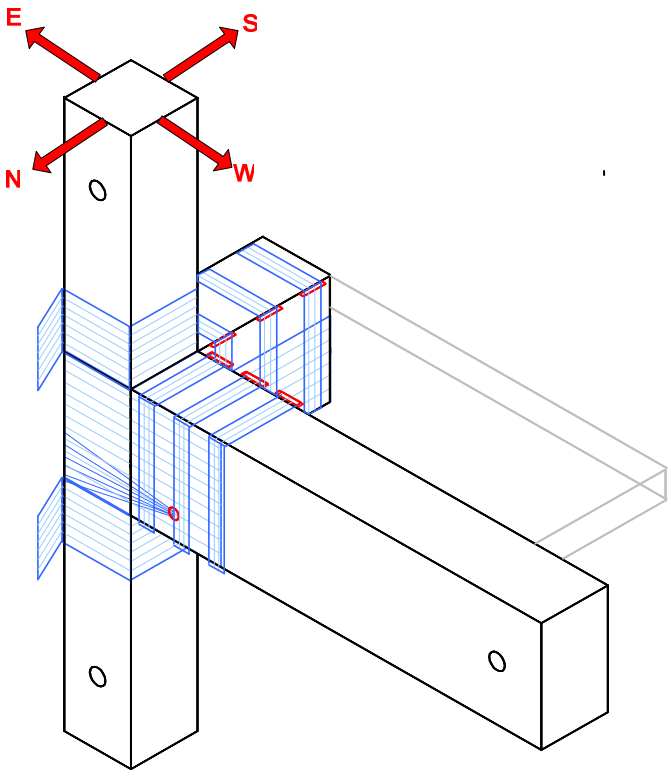

(f) Final view of the retrofitting scheme

3.4.2. Wrapping Orientation for US3-CS-FRP2

FRP strengthening scheme of the second retrofitted specimen, namely US3-CS-FRP2, was developed based on the existing deficiencies and the test results of US3-CS-FRP1. In general, first retrofitting strategy significantly improved the behavior of seismically deficient beam-column-slab subassembly. Inner and outer L-shape FRP-sheets limited the joint shear deformations by providing additional confinement. Column wraps worked efficiently and stopped any undesired deformation at top and bottom columns. Furthermore, bond-slip characteristic of subassembly was also improved by FRP belt application. Test results of US3-CS-FRP1 showed that, anchorage failure was delayed up to 2.75 % drift level but rapid strength and stiffness degradation again occurred at that drift level. By considering the above mentioned results, it was concluded that the behavior of US3-CS-FRP1 was satisfactory. However, brittle anchorage failure in push direction may still be critical although significant slippage was not observed up to an acceptable drift level. Therefore, it was aimed to prevent the slippage of longitudinal beam bottom reinforcements up to a higher drift level in the next retrofitting scheme for US3-CS-FRP2 specimen. In this context, the length of FRP belt was increased and hence, they were anchored 750 mm away from the column surface at the bottom of the longitudinal beam. The rest of the second retrofitted strategy was same with the first one. Retrofitting scheme of US3-CS-FRP2 is given below in Figure 3.14.

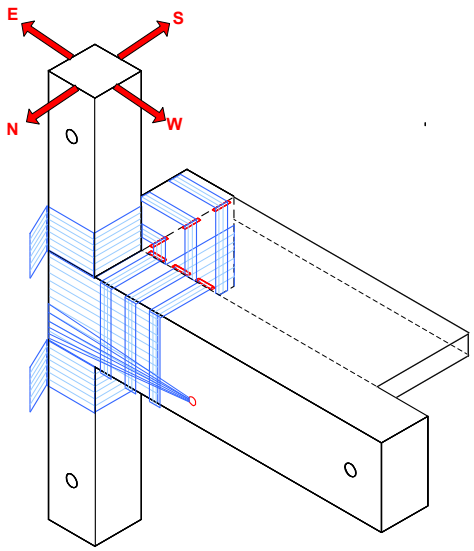

Figure 3.14. Retrofitting scheme of US3-CS-FRP2

3.5. Test Procedure

The subassemblies were subjected to quasi-static cyclic loading in terms of predetermined inter-story drifts expected under earthquake motions for that portion of the frame (Figure 3.15). They were loaded in the direction of longitudinal beam. In addition, constant axial load of 30% of the column axial capacity was applied to the columns throughout the tests. The transverse beam and slab were not loaded directly. 39 loading cycles were applied starting from 0.15 % and reaching to 4 % drift ratio. Three fully reversed cycles were applied at each drift ratio in order to evaluate the strength and stiffness degradation of subassemblies during the repeated cycles.

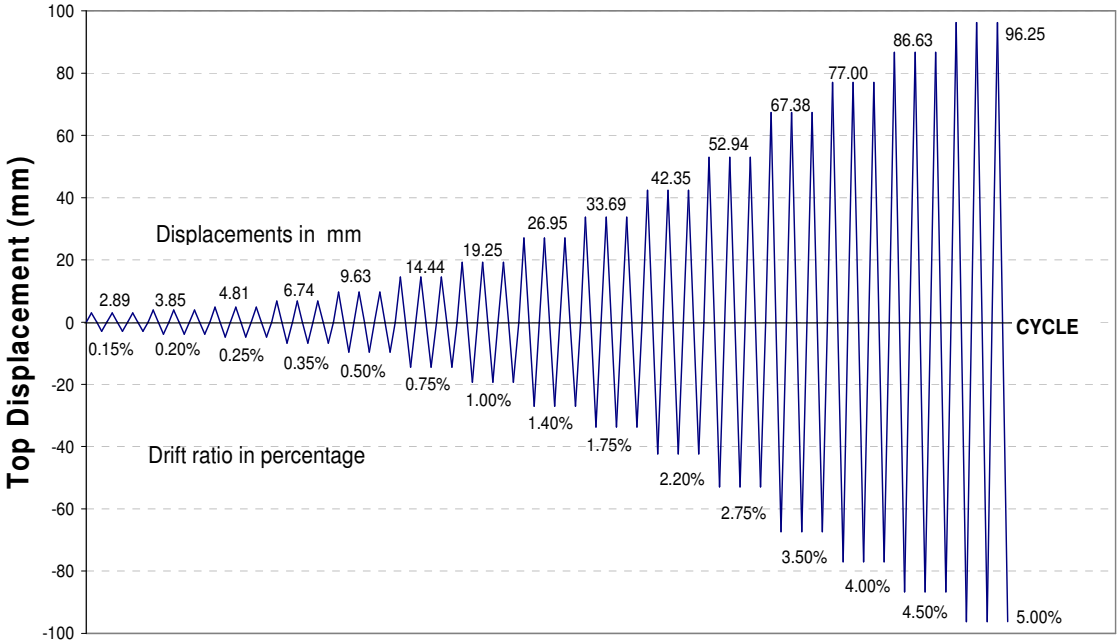

Figure 3.15. Loading pattern

The test set-up is shown in Figure 3.16. The subassemblies were tested in column vertical position and supported by universal pin at the bottom end of the column. The column was also linked to a horizontal hydraulic actuator at the top which has a capacity of 250 kN. Longitudinal and transverse beams were in the horizontal position. Free end of the transverse beam was not supported while longitudinal beam was hinged at the free end. Constant column axial load was applied by a load control with the vertical 1000 kN

capacity actuator. Because subassemblies are not symmetrical about the longitudinal axis of longitudinal beam, an out-of-plane frame was used in order to guide lateral displacements along the longitudinal direction only.

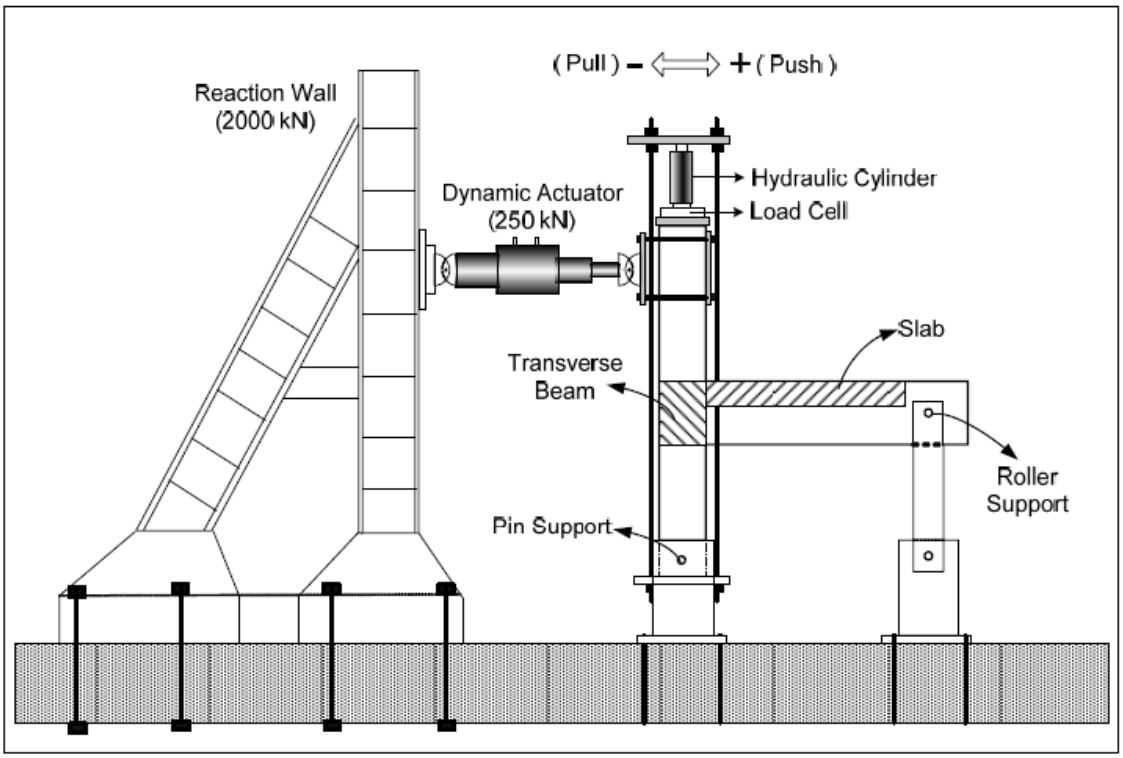

Figure 3.16.Test set-up

During the tests, all data were collected with a TML 602 50 Hz. 50 channel data acquisition box. Besides, observations were noted and photographs were taken for each sequence of three cycles. Moreover, a full cycle was recorded by a camcorder at each drift level.

3.6. Instrumentation

Total of 14 strain gages were mounted on the internal reinforcing bars of US3-C-Control specimen. In addition to these, 15 more strain gauges were mounted on internal bars of slab in US3-CS-Control specimen in order to investigate the contribution of slab in detail. Because of the channel restriction at the data acquisition system, only 4 strain gauges were mounted on the slab bars of retrofitted specimens since 19 additional strain

gauges were mounted on FRP sheets to evaluate the performance of retrofitting technique. Typical strain gauge instrumentation on reinforcing bars and FRP sheets are shown in Figures 3.17 to 3.20. Figure 3.21 shows a picture of strain gauges installed. All strain gages were connected to the data acquisition system and data were obtained in each 3 seconds. In addition to the strain gauges, displacement at the tip of the column, the shear deformation in the joint, and rotations at the longitudinal beam and column were monitored and measured by linear variable differential transducers (LVDTs) and data was transferred to the data acquisition system. Typical LVDT locations were shown in Figure 3.22. Finally, load cells were used in the horizontal actuator and at the top of the column in order to monitor lateral and axial loads, respectively.

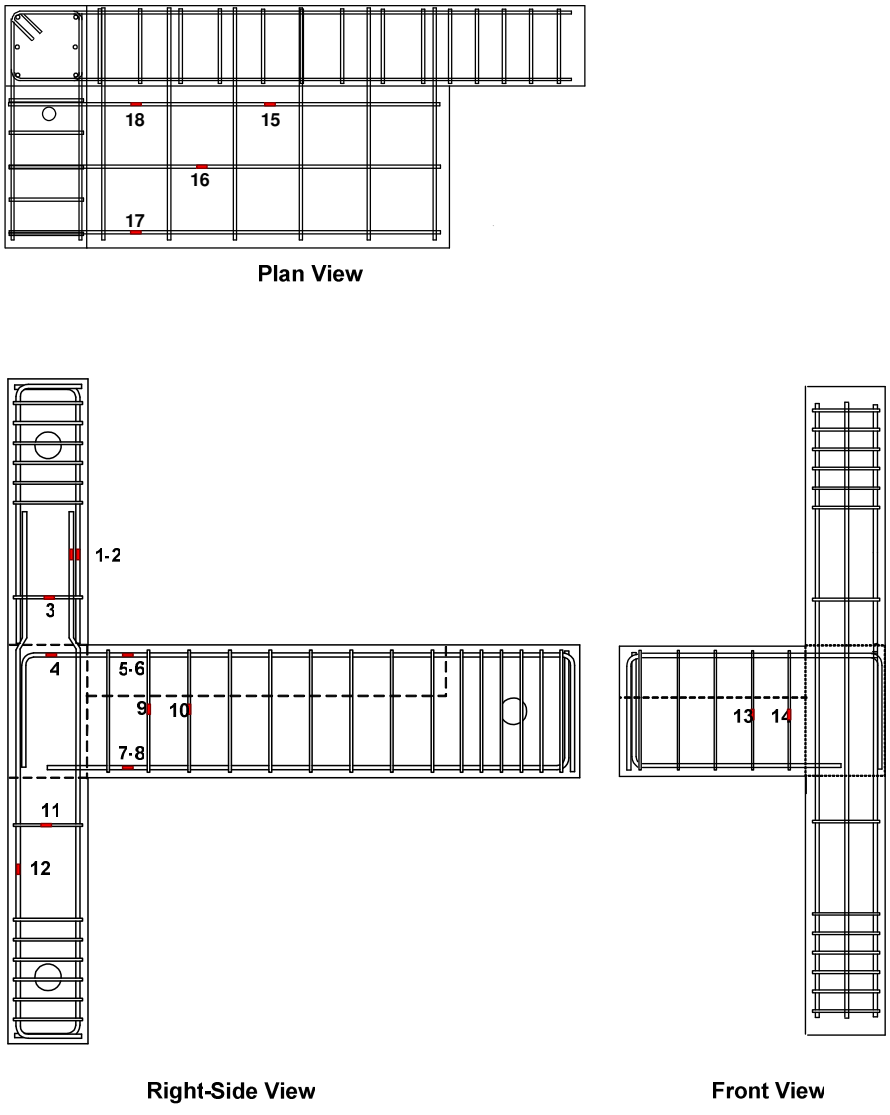

Figure 3.17.Typical strain gage instrumentation on reinforcing bars

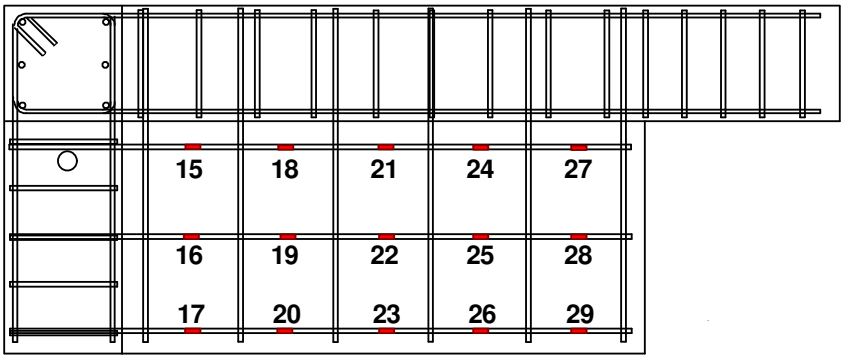

Figure 3.18.Strain gage instrumentation on reinforcing bars of US3-CS-Control slab

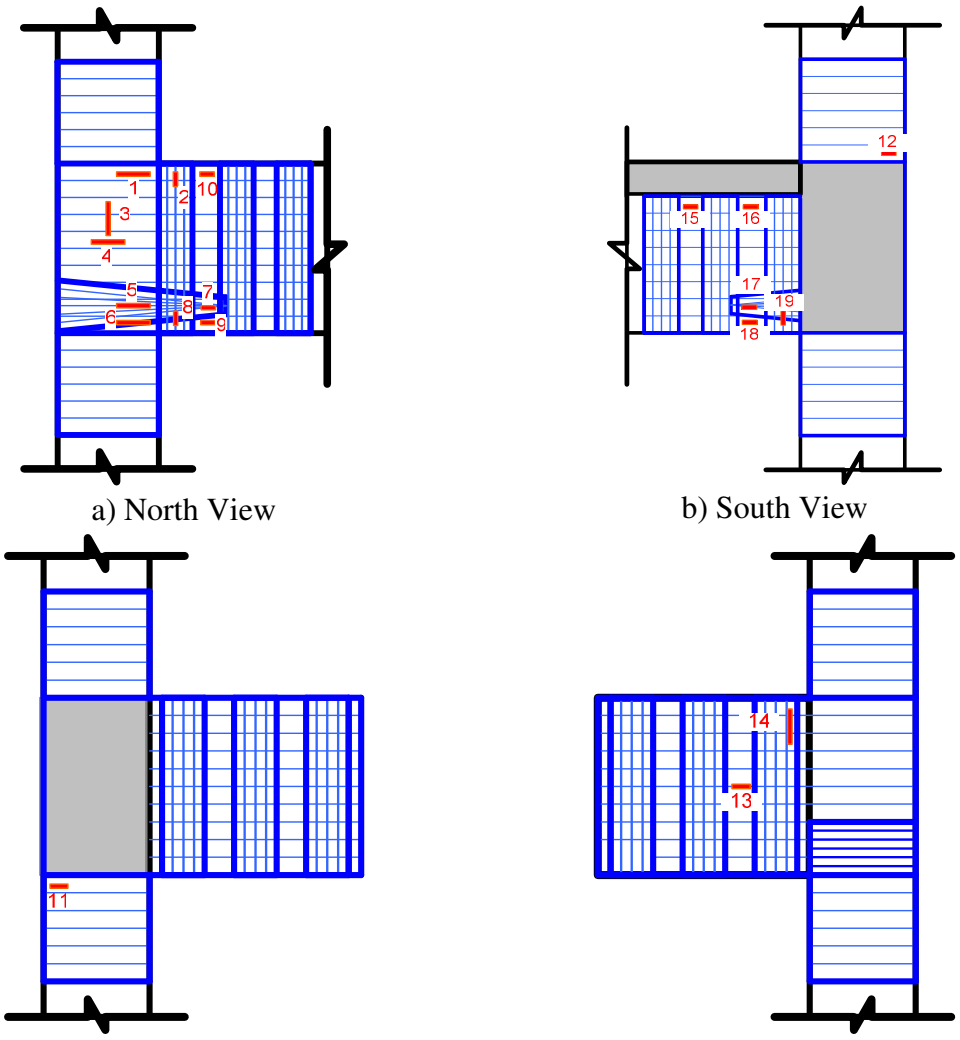

a) North View

b) South View

c) West View

d) East View

Figure 3.19.Strain gage instrumentation on FRP in US3-CS-FRP1

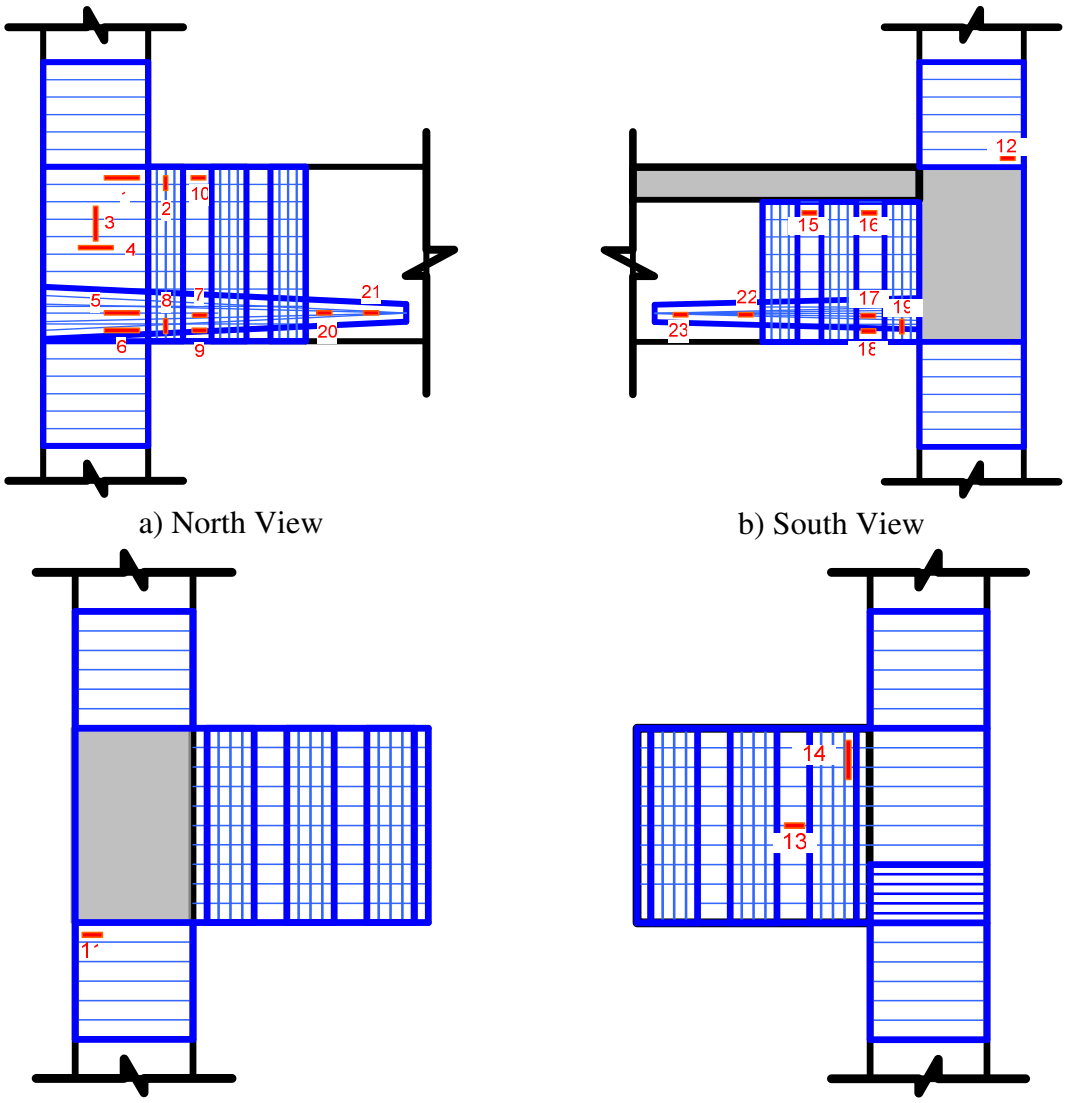

a) North View b) South View

c) West View d) East View

Figure 3.20.Strain gage instrumentation on FRP in US3-CS-FRP2

Figure 3.21.Strain gages installed in US3-CS-Control

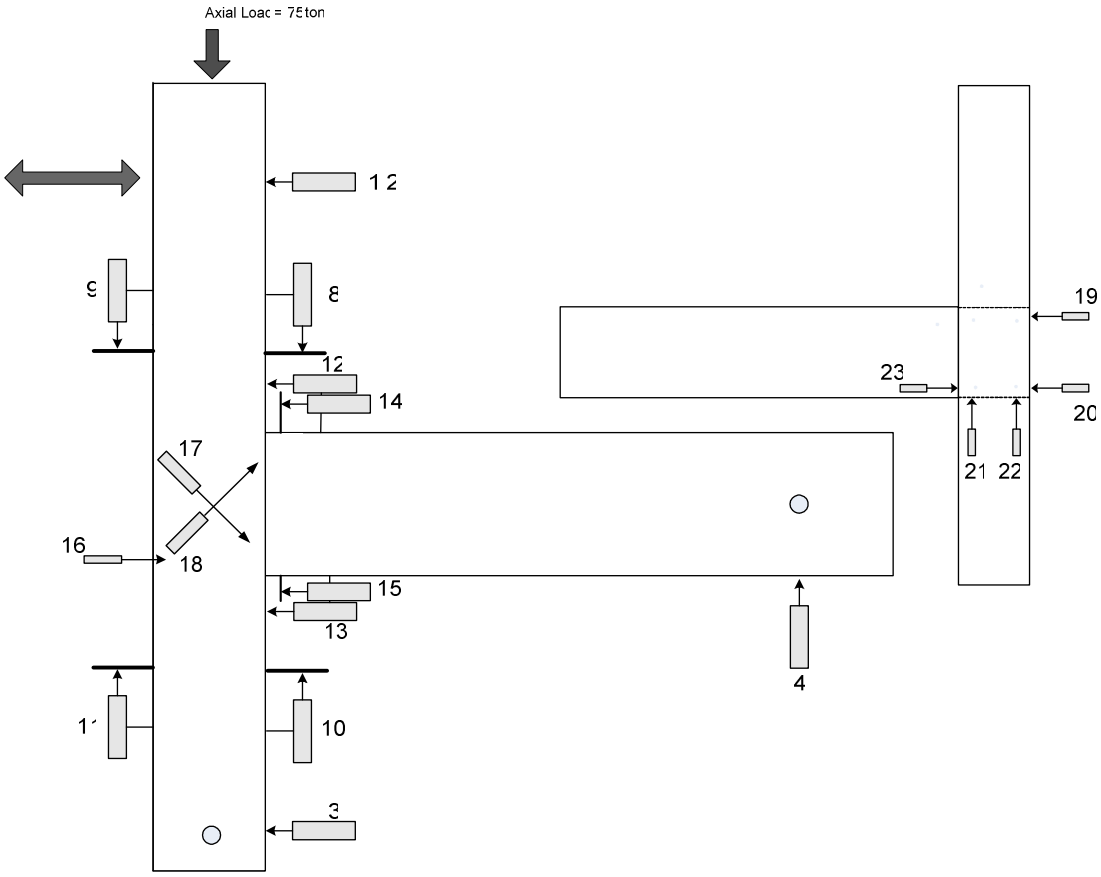

Figure 3.22.Typical LVDT instrumentation

4. TEST OBSERVATIONS

4.1. General

In this chapter, test observations are discussed to give an insight to the overall behavior of the subassemblies. Observations noted during the experiments (for instance; cracking and/or crushing of the concrete and debonding and/or rupture of FRP sheets etc.) are given with related photographs of the damaged subassemblies. Besides, for each subassembly lateral load versus column top displacement graph, which was plotted instantly during the experiments by data acquisition system, is also presented.

4.2. US3-C-Control

The first test was conducted on US3-C-Control subassembly that does not include the slab (Figure 4.1). Under reversed cycling loading, the first crack was the flexural type and occurred in the push direction of loading at the bottom of the longitudinal beam, 90 mm away from the column when the lateral load was 20 kN and the drift was 0.20%. In the same drift level, when the lateral load was 40 kN, the first flexural crack in the pull direction of loading also occurred. This crack was located at the top of the column-longitudinal beam interface. Up to drift level of 0.50% there were mainly flexural cracks observed at the longitudinal beam.

Figure 4.1 View of US3-C-Control subassembly at the test set-up

In push direction of loading, when the interstory drift level was 0.50% and the applied lateral load was 35 kN, a crack was observed at the longitudinal beam-column interface. Insufficient embedment length of the beam bottom longitudinal reinforcements resulted in slippage, and this was the reason of the occurrence of the crack. At the next drift level, 0.75%, lateral load reached the maximum of 37.5 kN in push direction of loading, while the crack at the interface continued extending. After this drift level, in the push direction of loading, lateral load decreased gradually as a result of the significant positive beam reinforcement slippage.

On the other hand, in the pull direction of loading, first diagonal shear crack in the joint region occurred at the drift level of 0.75% when the lateral load was 75 kN. Although diagonal shear cracks in the joint region were observed, the applied lateral load was still increasing up to drift level of 1.40% and reached the maximum of 94 kN. After that drift level, joint shear deformations governed the behavior in pull direction of loading which resulted in gradual decrease of lateral load (Figure 4.2).

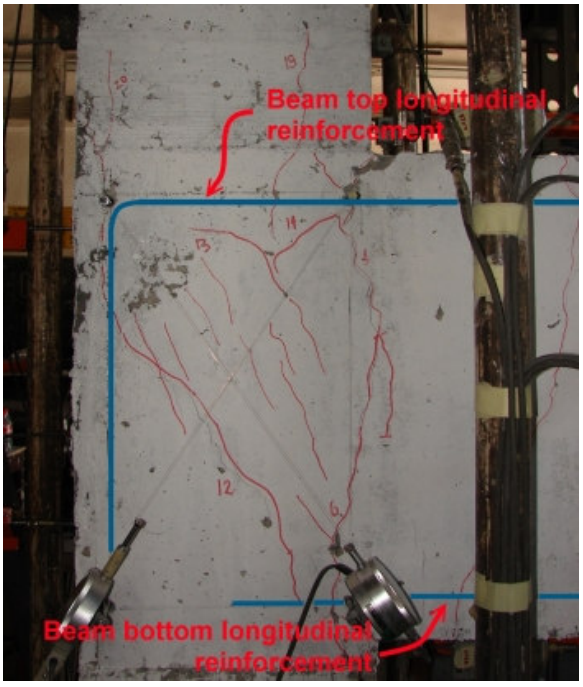

Figure 4.2. Joint shear cracks of US3-C-Control at the drift level of 1.75%

Not only the joint region but also north and south sides of the top column just above the joint region were damaged due to excessive shear demand. In pull direction of loading,

joint shear cracks started to extend upward to the top column at the drift level of 1.40%. Up to the end of the test, top column damaged significantly close to the joint region due to shear (Figure 4.3 (a)). Additionally, in the push direction of loading, cracks which occurred due to slippage, extended through bottom column and resulted with considerable damage at the bottom column close to the joint region. The concrete cover was crushed at the front face of the column, as it is shown in Figure 4.3 (b). The failure patterns of the subassembly in the push and pull directions of loading are given in Figure 4.4 (a) and (b), respectively.

(a) Top column shear cracks

(b) Bottom column damage due to slippage

Figure 4.3. Damages at the column

(a) Crack Pattern of US3-C-Control in pull direction of loading

(b) Crack Pattern of US3-C-Control in push direction of loading

Figure 4.4. Failure patterns of US3-C-Control

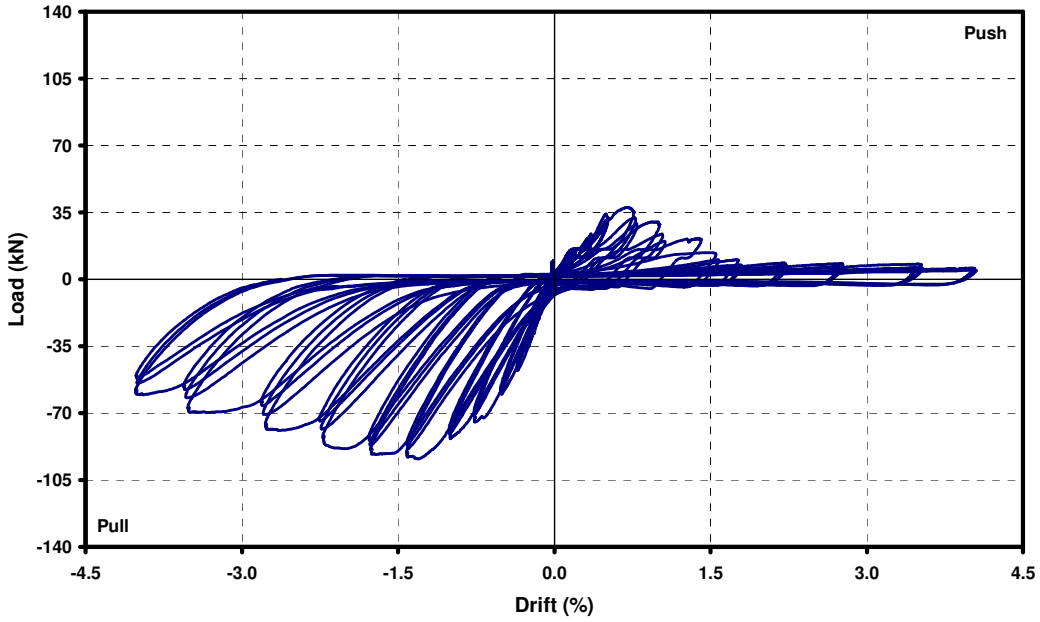

Figure 4.5.Load vs. story drift graph of US3-C-Control

As shown in Figure 4.5, brittle behavior (a sudden drop in load carrying capacity) was observed both in push and pull directions of loading due to the bond slip and joint shear failures, respectively. Because of the diagonal shear cracking of the joint region and bond-slip failure of the inadequately anchored beam bottom longitudinal reinforcement, the loops exhibited considerable pinching (the middle part of each hysteretic loop was relatively narrow). Also stiffness and strength degradations occurred during the repeated cycles of a drift level. Failure due to bond-slip was more brittle when it was compared to joint shear failure since it resulted with a higher rate of strength degradation.

4.3. US3-CS-Control

The only difference between US3-C-Control and US3-CS-Control was the presence of a slab. Comparison between the responses of these subassemblies was expected to reveal the effects of the slab contribution to the overall behavior. In general, under reversed cyclic loading, US3-CS-Control behaved in the same manner when it was compared to US3-C-Control. As also observed in US3-C-Control specimen, in the US3-CS-Control experiment, the first flexural cracks occurred at the longitudinal beam. In the push direction of loading after a drift level of 0.50%, beam-column interface was damaged

gradually due to the bond slip failure of the beam bottom longitudinal reinforcement. On the other hand, in the pull direction of loading after the drift level of 1.40% joint shear cracks occurred. Lateral load reached the maximum of 37 kN in the push direction and 109 kN in pull direction. When US3-C-Control and US3-CS-Control were compared, initiation of joint shear damage of the US3-CS-Control delayed from 0.75% drift level to 1.40% drift level. Moreover, in the pull direction of loading, load carrying capacity increased approximately 15%. On the other hand, in push direction of loading, observed maximum load level was the same with US3-C-Control. Column was again damaged close to the top and bottom of the joint because of the shear and bond slip failures, respectively.

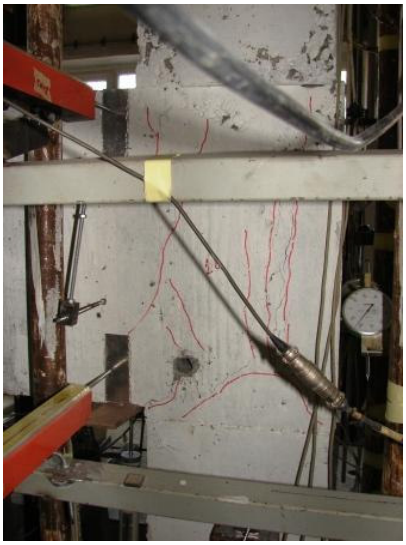

(a) Vertical cracks at the east side of the joint at 2.20% drift level (initiation of concrete spalling)

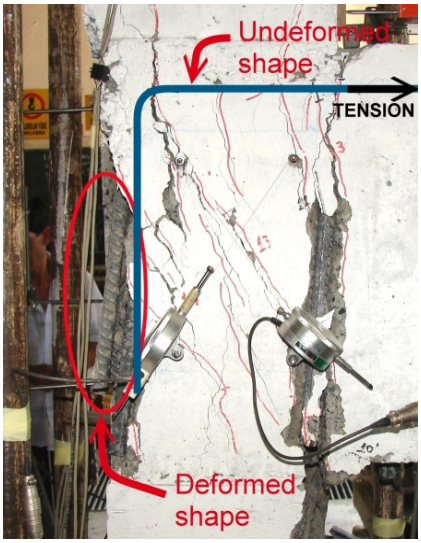

(b) Spalling due to longitudinal beam top bars slippage (3.50% drift level)

(c) Diagonal cracks at the backside of the transverse beam (2.75% drift level)

Figure 4.6. Crack pattern at the backside of the US3-CS-Control

The main difference observed during the tests of the control specimens was the deformations occurred at the east side of the joint and transverse beam regions in US3-CS-Control (Figure 4.6). Diagonal cracks occurred at the east side of the transverse beam and vertical cracks occurred at the back side of the column in the joint region. As shown in Figure 4.6 (b), due to the slippage of the longitudinal beam top reinforcements, 90 degree bent region of the same reinforcements were deformed such that the east side of the joint concrete was pushed out and the concrete at this region spalled.

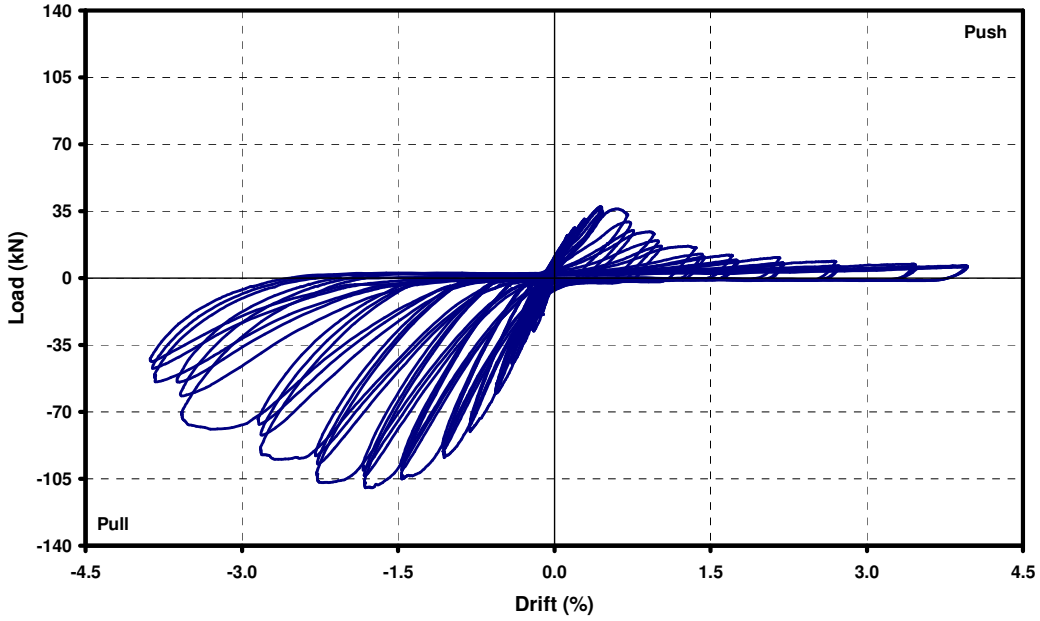

Figure 4.7.Load vs. top displacement graph of US3-CS-Control

The lateral load vs. story drift graph of US3-CS-Control subassembly is given above in Figure 4.7. The general shape of the graph is the same as the one of US3-C-Control. Brittle bond slip and joint shear failures governed the behavior again in push and pull directions of loading, respectively. In the same figure, pinching of the hysteresis loops, stiffness and strength degradation can also be observed. Failure pattern of US3-CS-Control is given below in Figure 4.8.

Figure 4.8. Failure pattern of US3-CS-Control

4.4. US3-CS-FRP1

Based on the US3-CS-Control test results and seismic design deficiencies, a proper FRP retrofitting orientation was developed in order to overcome these deficiencies. Detailed information about the orientation was given in the Chapter 3, under Experimental Study section. The retrofitted US3-CS-FRP1 had the same design and detailing as US3-CS-Control specimen.

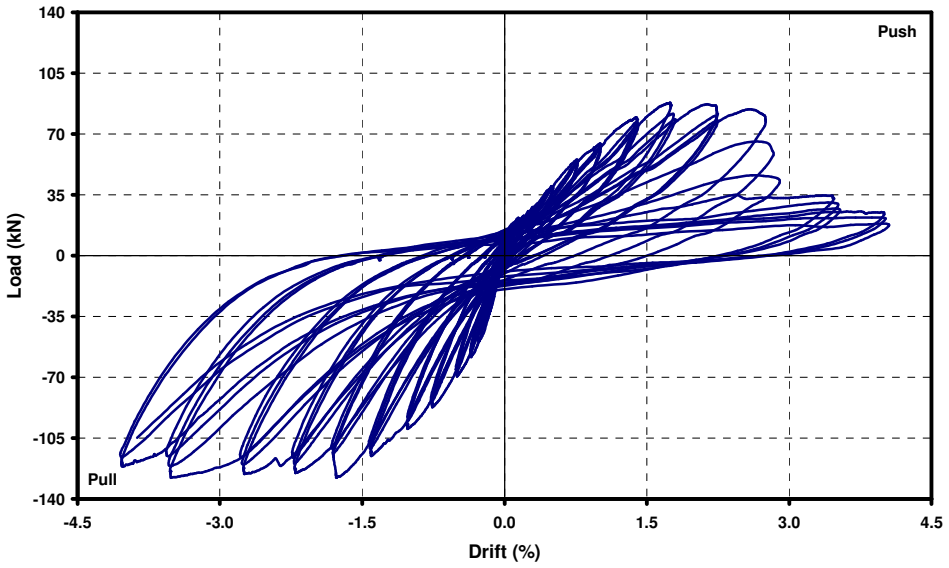

Figure 4.9.Load vs. story drift graph of US3-CS-FRP1

Lateral load vs. story drift response of US3-CS-FRP1 is shown in Figure 4.9. In this figure, it can easily be observed that lateral load increased gradually up to 1.75% drift level in push direction of loading and reached its maximum of 88 kN at that drift level. From the drift levels of 2.20% to 2.75%, maximum lateral load remained constant. However for the second and third cycles of 2.75% drift level, load decreased sharply because of the slippage of longitudinal beam bottom reinforcements. After that, decrease in the lateral load was continuous in the push direction of loading up to the end of the test. In the pull direction of loading, lateral load increased gradually until 1.75% drift level, which corresponded to a maximum lateral load of 128 kN. From that drift level on the lateral load remained constant.

Table 4.1. Failure patterns of FRP sheets

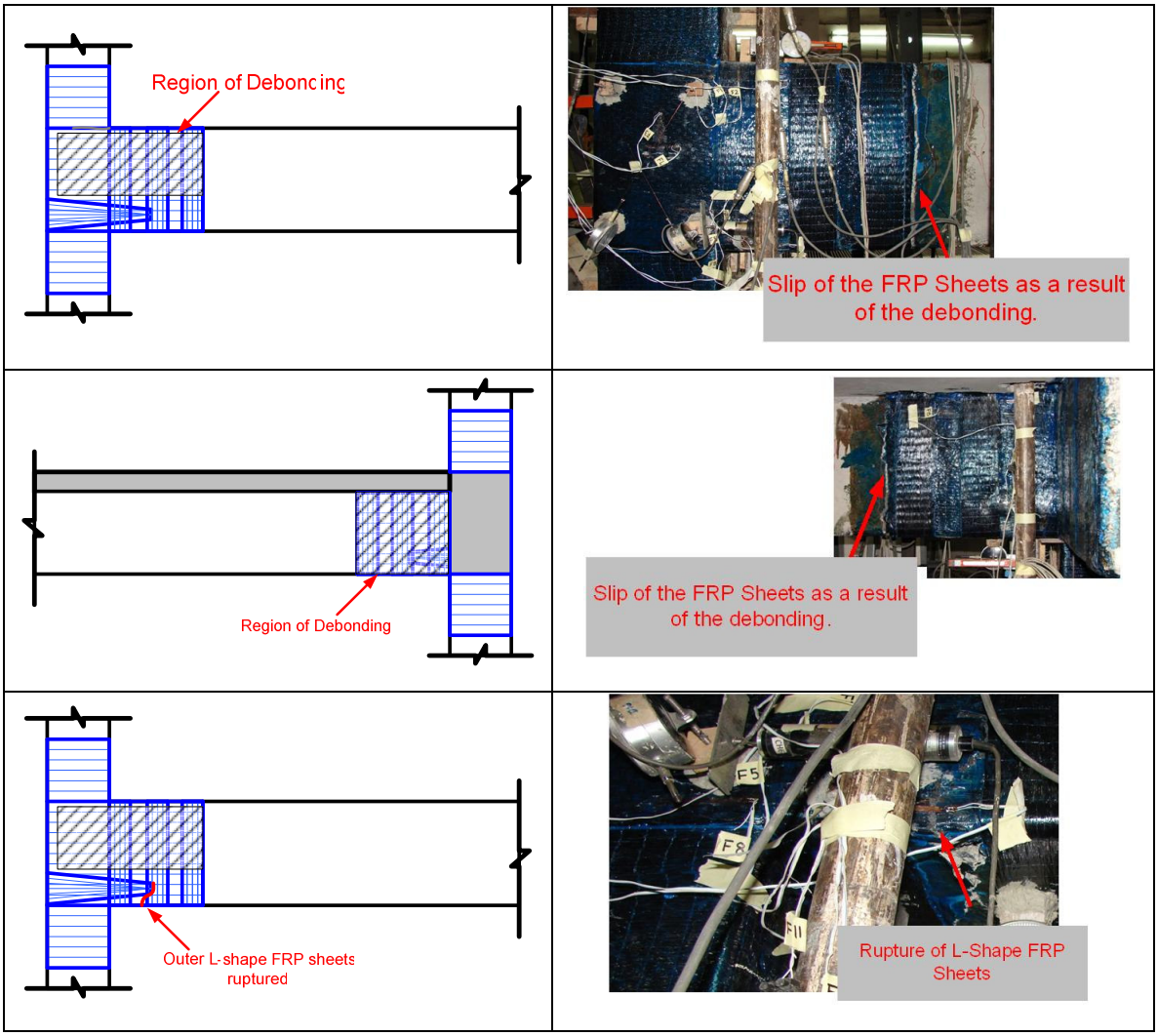

In the push direction of loading, the first flexural crack occurred at the bottom of the longitudinal beam when the lateral load was 39.5 kN and the drift level was 0.50%. It was located at 520 mm away from the column. In the pull direction of loading, the first crack was also flexural and occurred at 0.25% drift level, 500 mm away from the column face at the top of the longitudinal beam. At the next drift levels, debonding and rupture of FRP sheets were also observed while additional flexural cracks occurred at the longitudinal beam. L-shape FRP sheets and FRP anchorage strips at the north side of the longitudinal beam debonded in the pull direction. The maximum lateral load that caused debonding was 126 kN at the corresponding drift level of 1.75%. After that, L-shape FRP sheets and FRP anchorage strips at the south side also debonded at the drift level of 2.75% when the lateral load was 125.5 kN. In the push direction of loading, at 2.20% drift level, a flexural crack (crack #11) occurred at the bottom of the longitudinal beam between 1st and 2nd FRP anchorage strips. At the 3.50% drift level when the lateral load was 35 kN, this crack caused the rupture of outer L-shape FRP sheets at the bottom of longitudinal beam close to the anchorage hole of FRP belts (Table 4.1). However, rupture did not affect the behavior significantly because the lateral load was already reduced significantly due to the bond-slip failure.

Finally, it can be concluded that the main reason of the failure in push direction of loading was again the slippage of longitudinal beam bottom reinforcements which caused a sudden failure. On the other hand, it can easily be observed by considering lateral load vs. column top displacement response (Figure 4.9) that the failure was ductile in pull direction of loading.

In order to inspect the damage visually for a more comprehensive explanation on the behavior of the specimen, FRP wraps were removed after the experiment. Crack patterns at the longitudinal beam and joint region under the FRP wraps are shown in Figure 4.10 and Figure 4.11. Crack #11 was the most significant crack which is shown in Figure 4.10. It occurred in push direction of loading at the bottom of the longitudinal beam at 2.20% drift level as a result of the slippage of longitudinal beam positive reinforcements when the moment at that cross-section was 106 kNm. At the following drift levels, because slippage increased dramatically, crack #11 widened too much that not only concrete cover but also

the concrete core spalled. Figure 4.11 shows the damage at the joint region under the FRP wraps. The joint shear deformation was critical for control specimens which caused the brittle failure of specimens in pull direction of loading. Therefore, one of the main objectives of CFRP retrofitting was to limit joint shear deformations. As it is shown in Figure 4.11, some diagonal shear cracks occurred at the joint region but they were not so remarkable.

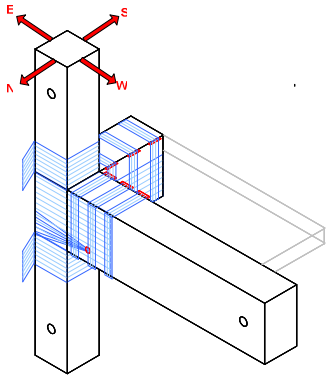

a) 3D View

b) South View

c) North View

Figure 4.10. Views of crack #11 under FRP wraps

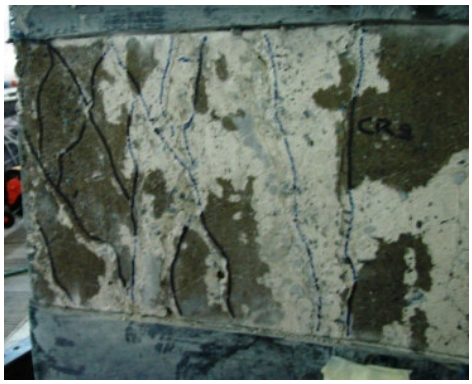

Figure 4.11. Image of the joint after the removal of FRP wraps

4.5. US3-CS-FRP2

The second retrofitted subassembly, namely US3-CS-FRP2, was tested at last. Its retrofitting scheme is given in Figure 3.14. The only difference between second and first retrofitting schemes was the length of the FRP belt. The test results of US3-CS-FRP1 showed that joint shear failure was prevented in pull direction of loading and hence, a desired ductile behavior was observed. When the behavior in push direction of loading was discussed, the improvement achieved by FRP belt application was obvious as mentioned above. However, slippage of the longitudinal beam bottom bars could not be stopped and accordingly rapid strength and stiffness degradation again occurred. Therefore, length of the FRP belt was increased in US3-CS-FRP2 in order to stop slippage.

Figure 4.12. Crack pattern of US3-CS-FRP2 at the drift level of 1.40%

During the test of US3-CS-FRP2, up to the drift level of 1.40%, only flexural and diagonal shear cracks were observed at the longitudinal beam and slab as shown in Figure 4.12. After that drift level, not only cracking of concrete but also debonding and rupture of FRP sheets at different locations of FRP application were observed. At the drift level of 1.40%, outer L-shape FRP sheets debonded at the north side of the longitudinal beam. Debonding occurred in pull direction of loading when the maximum lateral load was 130 kN. At the next drift level, 1.75%, FRP belt debonded at the north side of the longitudinal

beam, from the face of the column to the anchorage hole of the belt. Although FRP belt and outer L-shape FRP sheets debonded, lateral load increased until the drift level of 2.20%. However, at the drift level of 2.75%, maximum lateral load decreased in push direction of loading as a result of the debonding of inner L-shape FRP sheets at the longitudinal beam-column interface. When debonding occurred, the lateral load decreased sharply from 97 kN to 77 kN since the contribution of inner L-shape FRP sheets to prevent slippage disappeared. At the drift level of 3.50%, outer L-shape FRP sheets debonded at the joint region in push direction of loading, due to the buckling under compression (Table 4.2 (c)). In pull direction of loading, it was observed that the flexural crack at the longitudinal beam-column interface propagated diagonally through the joint region. Rotation of the column just above the joint region increased as a result of this crack which caused the debonding of column wraps at the east side, due to the buckling. Finally, at the drift level of 4.00%, outer L-shape FRP sheets and FRP belt ruptured at the north side of longitudinal beam-column interface. Failure patterns of FRP sheets are given in Table 4.2.

Table 4.2. Failure patterns of FRP sheets in US3-CS-FRP2

<table>
<tr>
<td> 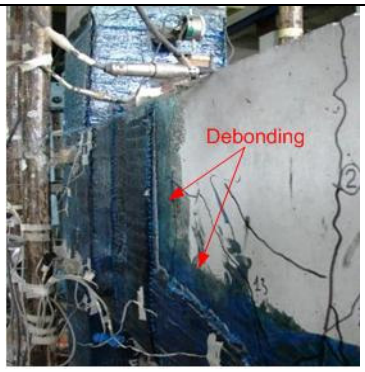

(a) Debonding of the FRP belt and outer L-shape FRP sheets</td>
<td> 
(b) Debonding of the inner L-Shape FRP sheets</td>
</tr>
<tr>
<td> 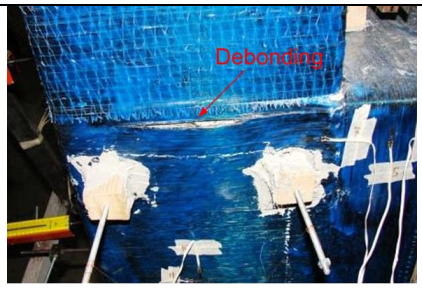

(c) Debonding of outer L-shape FRP sheets at the joint region</td>
<td> 
(d) Rupture of outer L-shape FRP sheets and FRP belt</td>
</tr>
</table>

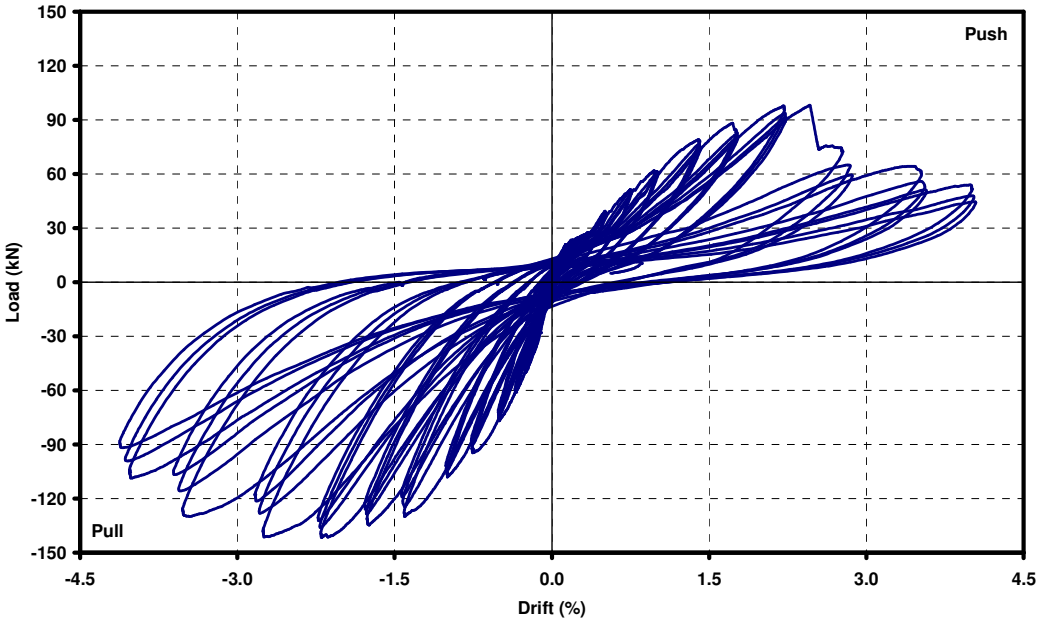

Figure 4.13.Load vs. story drift graph of US3-CS-FRP2

Lateral load vs. story drift response of US3-CS-FRP2 is shown in Figure 4.13. In this figure, it can easily be observed that lateral load increased gradually up to 2.20% drift level in each direction of loading and reached the maximum of 99 kN in push and 141 kN in pull direction of loading. At the drift level of 2.75%, lateral load decreased sharply in push direction of loading as mentioned above. After that, decrease in the lateral load was gradual up to the end of the test. At the drift level of 4.00%, maximum lateral load was 54 kN in push direction of loading. In pull direction of loading, debonding of outer L-shape FRP sheets caused joint shear failure and thus, lateral load decreased gradually after the drift level of 2.75%. In general, it can be concluded that, rapid strength and stiffness degradation due to bond-slip failure was limited in US3-CS-FRP2 when it was compared with other subassemblies. However, in the pull direction of loading, the desired ductile failure observed in US3-CS-FRP1 could not be occurred in this subassembly.

In order to inspect the damage under the FRP wraps visually, they were removed after the experiment. Figure 4.14 shows the crack pattern under the FRP wraps at the longitudinal beam and joint region. There was a main flexural crack at the longitudinal beam-column interface which occurred due to the slippage of longitudinal beam bottom reinforcements. Not only bond-slip but also joint shear failure was ocular under the FRP

wraps. At the joint region, there were significant diagonal shear cracks and besides, the cover concrete was crushed. The damage at the joint region was more remarkable when it was compared with US3-CS-FRP1, as it can be seen in Figure 4.14.

Figure 4.14. Image of the joint after the removal of FRP wraps

4.6. Summary of the Test Observations

The test results showed that joint shear deformations and slippage of longitudinal beam bottom reinforcements are the main reasons of undesired non-ductile behavior of control specimens. CFRP retrofitting delayed and/or prevented both of them and hence improved the overall seismic response in retrofitted specimens. Failure modes are summarized in Table 4.3 below for all specimens.

Table 4.3. Summary of the Test Observations

	Push direction of loading			**Pull Direction of Loading**	
Specimen Name	**Mode of Failure**	**%Drift Level**	**Location of the hinging**	**Mode of Failure**	**%Drift Level**
US3-C-Control	Bond-Slip	0.75	Longitudinal beam-column	Joint shear	1.40
US3-CS-Control	Bond-Slip	0.75	Longitudinal beam-column	Joint shear	1.75
US3-CS-FRP1	Bond-Slip	2.75	200 mm away from the column	Ductile behavior	1.75-4.00
US3-CS-FRP2	Bond-Slip	2.75	Longitudinal beam-column	Joint shear	3.50

5. DISCUSSION OF TEST RESULTS

5.1. General

This chapter includes discussion and comparison among experimental results of the subassemblies. Seismic performance of the subassemblies was evaluated in terms of lateral load versus column top displacement response, stiffness and energy dissipation characteristics. The behavior of joint region was discussed in terms of joint shear deformations and bond slip effects. In addition, effects of the presence of a slab on the seismic behavior of beam-column joint subassemblies are discussed.

5.2. Lateral Load versus Story Drift Response

Lateral load vs. column top displacement graphs were given in Test Observations chapter for each subassembly. The envelopes of these hysteretic loops are shown below in Figure 5.1.

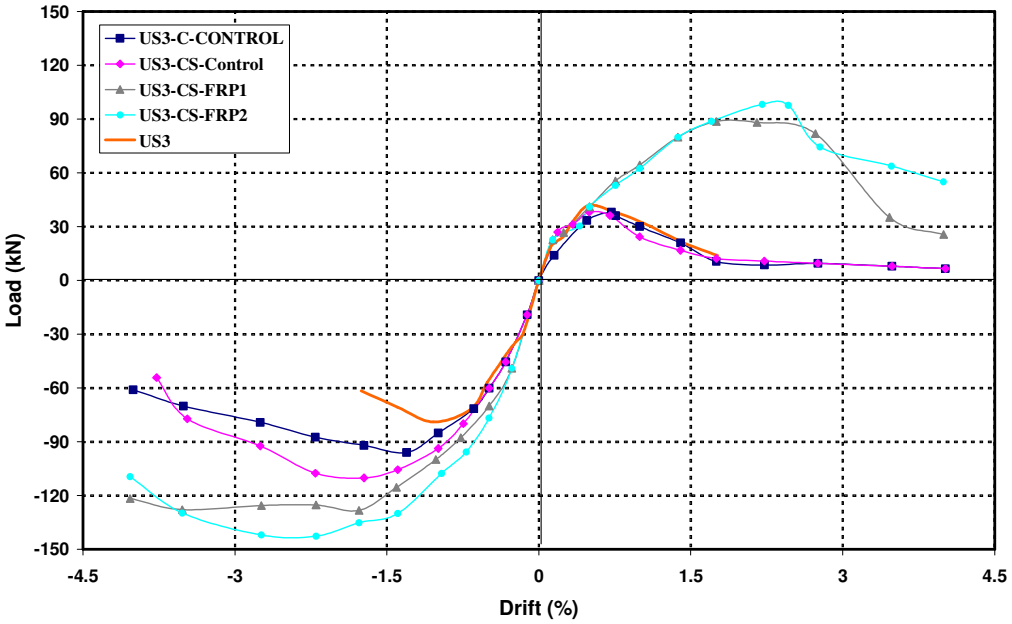

Figure 5.1. Hysteretic loop envelopes of test subassemblies

Sudden decrease in the lateral load carrying capacities of subassemblies confirmed that brittle failure occurred in both push and pull directions of loading of US3-C-Control and US3-CS-Control specimens. As it was also mentioned in previous chapter, joint shear and bond slip failures were main reasons of brittle behavior for both specimens in pull and push directions of loading, respectively. The only difference between these subassemblies was the presence of slab which increased maximum lateral load reached in pull direction of loading approximately 10%. Hence, it can be concluded that slab contributed to flexural strength of longitudinal beam in pull direction of loading when the slab bars were in tension. While the failure was due to joint shear deteriorations in pull direction of loading and the presence of slab does not increase joint shear strength, it may be concluded that joint shear demand was reached at higher lateral load level in US3-CS-Control when it was compared with US3-C-Control. The presence of slab seems inconsequential for seismic behavior in push direction of loading since the shapes of envelopes of these subassemblies were nearly the same.

Limiting the bond-slip and overcoming joint shear failure were main goals of retrofitting technique applied in US3-CS-FRP1 in order to move plastic hinge formation to the longitudinal beam for a desired ductile failure. Retrofitting scheme developed to serve these goals was given in previous chapter. As it can easily be observed from Figure 5.1, US3-CS-FRP1 behaved quite better than control specimens. In push direction of loading, bond slip failure was detained until the drift level of 2.75 % and the maximum lateral load increased 2.5 times when it was compared with US3-CS-Control. However, brittle failure again occurred at that drift level as a result of the significant slippage. On the other hand, US3-CS-FRP1 executed a desired performance in pull direction of loading. Ductile failure was achieved that joint shear deformations were limited and could not govern the behavior before beam hinging formed. In addition to that, maximum lateral load also increased 16%.

In order to overcome significant strength and stiffness degradation after the occurrence of bond-slip failure, length of the FRP belt was increased in the retrofitting scheme of US3-CS-FRP2. This improved the behavior in push direction of loading with respect to the behavior of US3-CS-FRP1. Maximum lateral load increased 10% and besides, strength degradation after the occurrence of bond-slip failure was more gradual.

US3-CS-FRP2 maintained more than 50% of its maximum lateral load capacity at the end of the test while lateral load decreased approximately 70% in US3-CS-FRP1 after the occurrence of bond-slip failure. In pull direction of loading, the behaviors of two retrofitted specimens were similar. Maximum lateral load increased approximately 10% in US3-CS-FRP2. However, the overall behavior was more brittle with respect to the behavior of US3-CS-FRP1, since significant joint shear deteriorations occurred after the debonding of L-shape FRP sheets. The overall response of specimen was still acceptable.

As it was mentioned in the Experimental Study chapter, this study is a part of ongoing NSF (grant no: OISE-0535294) and TUBITAK (grant no: İÇTAG-1597-NSF (103I026)) funded research conducted at Bogazici University Structures Laboratory. In Figure 5.1, US3 stands for 2D specimen tested in this research program by Selcuk Altay (Phd. Candidate). This specimen consisted of only column and longitudinal beam with the same geometric and reinforcement detailing. Here, overall behaviors of US3-C-Control and US3 were compared in order to investigate the effects of transverse beam which was one of the main objectives of this study. At first, it can be seen in this figure, the behaviors of two specimens were totally same in push direction of loading. Therefore, it can be concluded that transverse beam does not affect the bond-slip characteristic of the anchorage deficient joints. However, there were two main differences in overall behavior in pull direction of loading; (1) maximum lateral load increased approximately 20%, and (2) the drift level where brittle joint shear failure observed was delayed from 1.00% to 1.40%. Therefore, it can be concluded that transverse beam increased joint shear capacity. These results are also matching with the conclusions of similar studies in the literature. Two reasons were given in the literature in order to reveal these outcomes; (1) transverse beam increases effective joint width and hence joint shear capacity, and (2) it confines the joint region and facilitates to sustain joint shear failure (Ehsani and Wight, 1985a).

5.3. Stiffness Degradation

Seismic performance of a beam-column joint may be evaluated by investigating the stiffness degradation characteristic throughout the test. Stiffness degradation during seismic loading is caused by various factors such as flexural and shear cracking, bond slip effects, joint shear deterioration, cover crushing and spalling. The contribution of each

factor on the stiffness degradation is different. Therefore, for all specimens, stiffness was computed for each cycle in push and pull directions of loading separately since the failure modes were different for two directions of loading in control specimens. It was aimed to investigate the effect of joint shear and bond slip failures on stiffness degradation individually. Figure 5.2 (a) through (d) show the stiffness vs. drift response of all specimens in push and pull directions of loading. In this figure, it can easily be seen that the stiffness values of all specimens in pull direction of loading were higher when it was compared to those in push direction of loading. The reason was that flexural capacity of longitudinal beam was higher in pull direction of loading due to higher reinforcement area at the top. Besides, rate of stiffness degradation in push direction of loading was higher which means that bond slip failure is more critical than the joint shear failure in terms of stiffness degradation. Furthermore, once bond slip effect became significant in push direction of loading, stiffness decreased rapidly to zero in the consecutive cycles. Hence, it can be concluded that beam-column joints with bond-slip deficiencies can not resist any lateral loading after significant slippage. According to the Figure 5.2 (c) and (d), gradual stiffness degradation was observed in retrofitted specimens in both push and pull directions of loading. At the end of the test, US3-CS-FRP1 still maintained approximately 15% of its initial stiffness in pull direction of loading and 5% of its initial stiffness in push direction of loading. In US3-CS-FRP2, 12% of initial stiffness was maintained at the end of the test in both push and pull directions of loading.

In order to compare the stiffness degradation characteristics of specimens, Figure 5.2 (a) through (d) were joined in Figure 5.3 (a) and (b). As it is seen in Figure 5.3 (b), stiffness degradation rate was nearly same for control specimens in pull direction of loading. However, as a result of the contribution of slab to flexural strength of the longitudinal beam, stiffness values for US3-CS-Control were rather higher. In push direction of loading, in spite of higher initial stiffness of US3-CS-Control, its stiffness values were nearly same with US3-C-Control after bond slip failure governed the behavior of specimens. Stiffness vs. drift response of retrofitted specimens was quite better than that of control specimens. Not only initial stiffness of retrofitted specimens but also stiffness values in consecutive cycles throughout the test were higher. Stiffness values of US3-CS-FRP2 were higher initially in pull direction of loading and were higher at the end of the

test in push direction of loading when it was compared with those of US3-CS-FRP1. Higher stiffness value at the end of the test illustrated lower strength degradation after the occurrence of bond-slip failure. Therefore, it can be concluded that, second retrofitting scheme improved the behavior in push direction of loading as it was aimed. The failure was not as brittle as it was in US3-CS-FRP1. Causes of the improvement achieved in retrofitted specimens can be summarized as follow;

- Behavior of retrofitted specimens was more ductile in both push and pull directions of loading since joint shear and bond-slip failures were limited and/or delayed.
- Retrofitting increased the capacity of subassemblies in both pull and push directions of loading since CFRP sheets acted as additional reinforcement.
- Additional confinement provided by CFRP wraps improved ductility of subassemblies.

Finally, peak to peak secant stiffness vs. drift response of subassemblies was given in Figure 5.4. Improvement in the overall stiffness vs. drift responses of retrofitted specimens can also be observed in that figure. Overall stiffness values per cycle were also summarized in Table 5.1.

Table 5.1. Overall stiffness for each cycle (kN/mm)

Cycle #	**1**	**2**	**3**	**4**	**5**	**6**	**7**	**8**	**9**	**10**
Drift (%)	**0.35**	**0.35**	**0.35**	**0.50**	**0.50**	**0.50**	**0.75**	**0.75**	**0.75**	**1.00**
US3-C-Control	5.16	5.11	4.99	4.55	4.52	4.37	3.65	3.43	3.23	2.86
US3-CS-Control	5.54	5.42	5.58	4.92	4.75	4.57	3.83	3.54	3.31	2.93
US3-CS-FRP1	6.23	6.33	5.95	5.51	5.44	5.34	4.85	4.69	4.61	4.12
US3-CS-FRP2	6.44	6.48	6.44	5.80	5.73	5.52	4.92	4.87	4.67	4.36
Cycle #	**11**	**12**	**13**	**14**	**15**	**16**	**17**	**18**	**19**	**20**
Drift (%)	**1.00**	**1.00**	**1.40**	**1.40**	**1.40**	**1.75**	**1.75**	**1.75**	**2.20**	**2.20**
US3-C-Control	2.62	2.46	2.04	1.78	1.66	1.45	1.36	1.28	1.06	0.99
US3-CS-Control	2.72	2.55	2.17	2.03	1.94	1.73	1.64	1.54	1.32	1.22
US3-CS-FRP1	4.00	3.92	3.53	3.47	3.36	2.92	2.82	2.70	2.37	2.31
US3-CS-FRP2	4.30	4.14	3.83	3.64	3.50	3.16	3.08	2.99	2.75	2.68
Cycle #	**21**	**22**	**23**	**24**	**25**	**26**	**27**	**28**	**29**	**30**
Drift (%)	**2.20**	**2.75**	**2.75**	**2.75**	**3.50**	**3.50**	**3.50**	**4.00**	**4.00**	**4.00**
US3-C-Control	0.92	0.78	0.72	0.65	0.56	0.50	0.45	0.41	0.38	0.36
US3-CS-Control	1.14	0.92	0.83	0.74	0.57	0.49	0.43	0.38	0.35	0.32
US3-CS-FRP1	2.21	1.88	1.64	1.43	1.16	1.11	1.01	0.91	0.87	0.45
US3-CS-FRP2	2.59	1.98	1.76	1.61	1.37	1.23	1.12	1.01	0.94	0.85

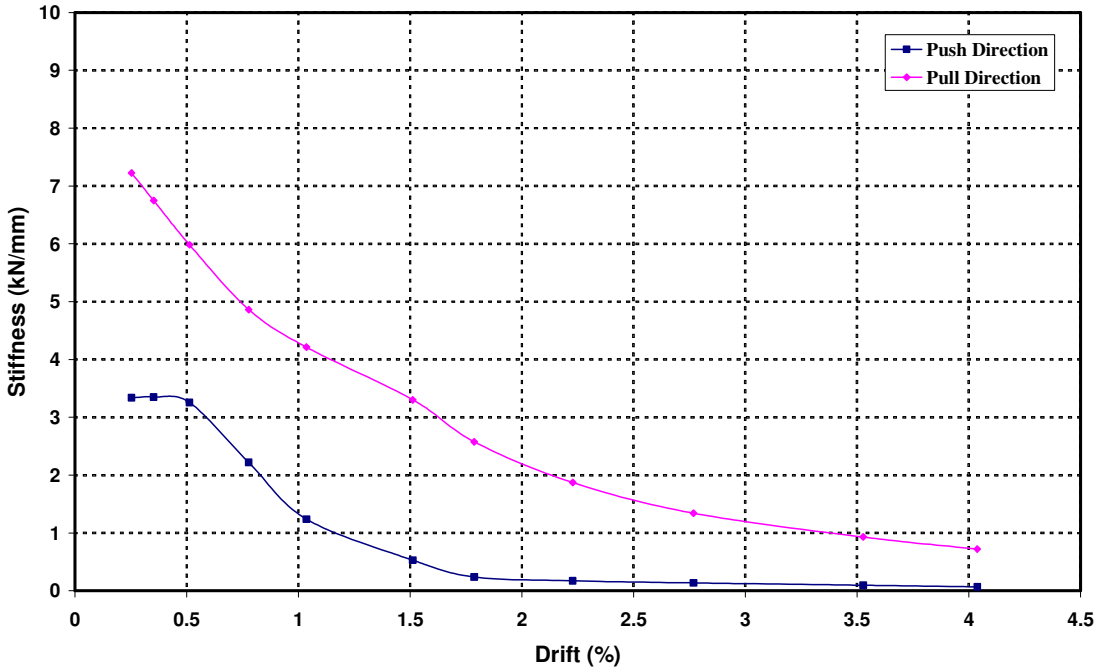

(a) US3-C-Control

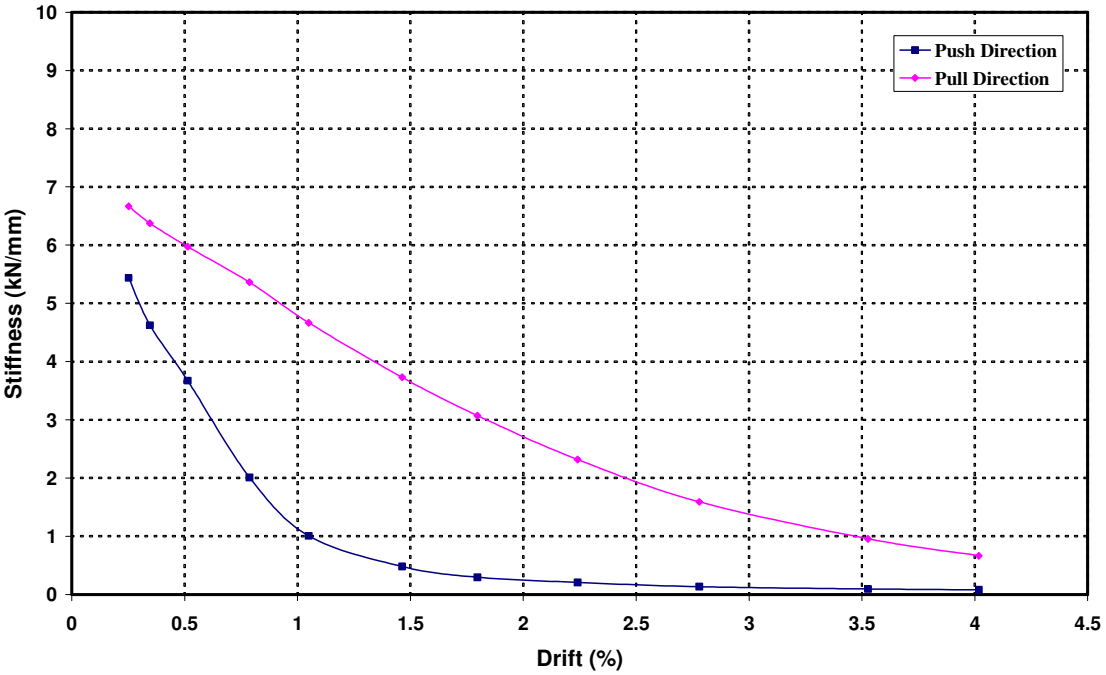

(b) US3-CS-Control

Figure 5.2. Stiffness degradation in pull and push directions of loading for all specimens

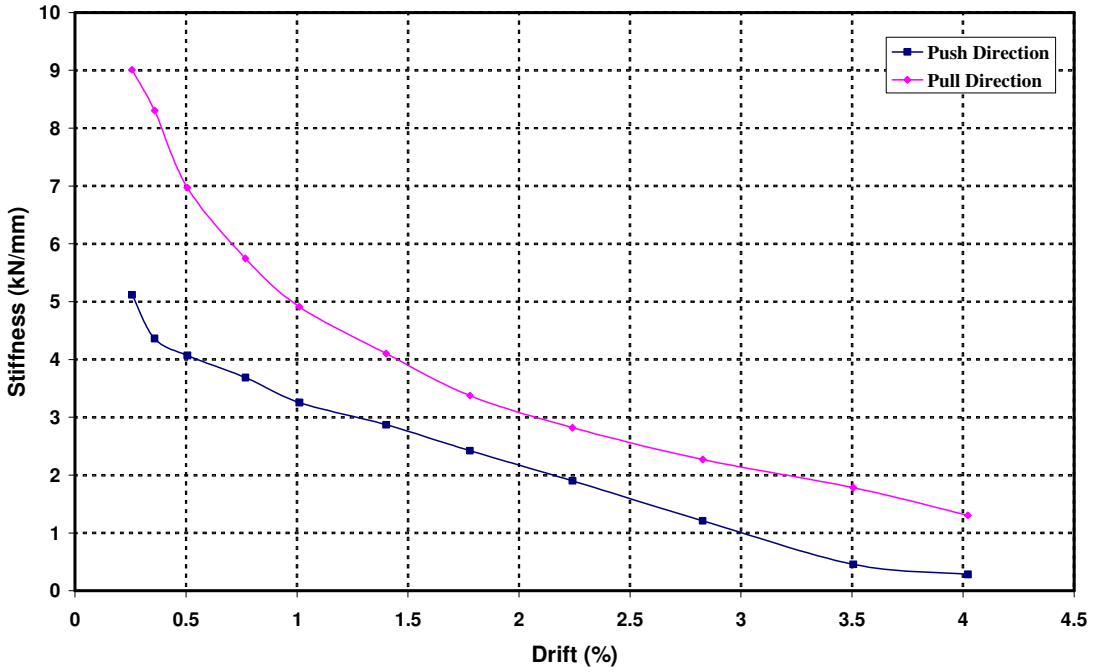

(c) US3-CS-FRP1

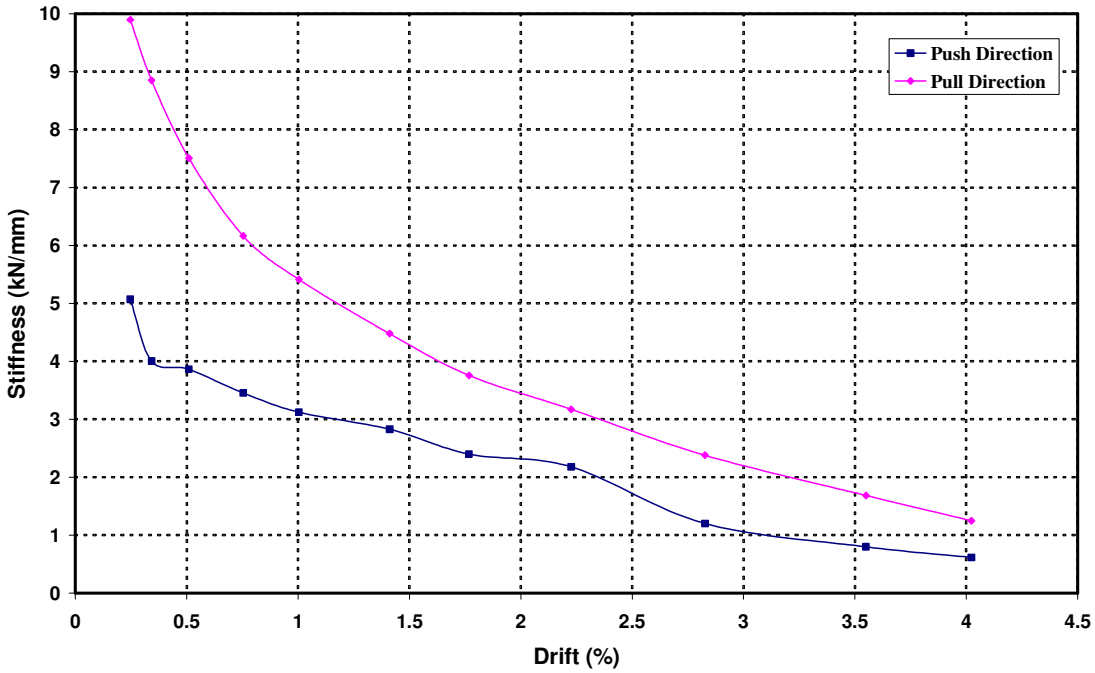

(d) US3-CS-FRP2

Figure 5.2. Stiffness degradation in pull and push directions of loading for all specimens

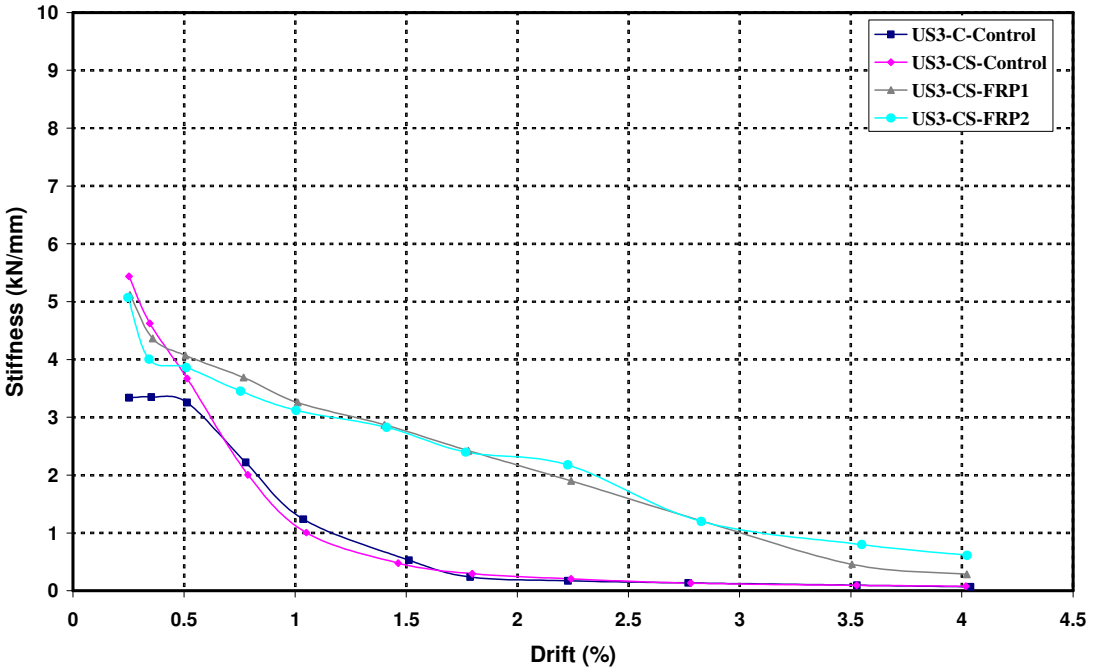

(a) Push Direction

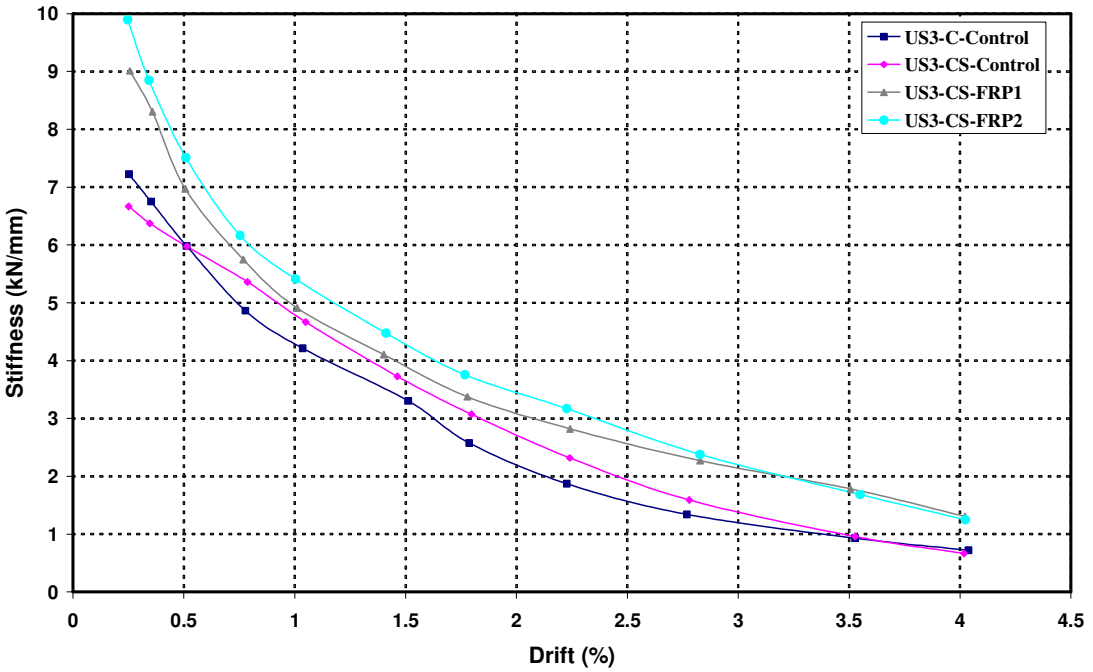

(b) Pull Direction

Figure 5.3. Comparison of stiffness vs. drift response of specimens

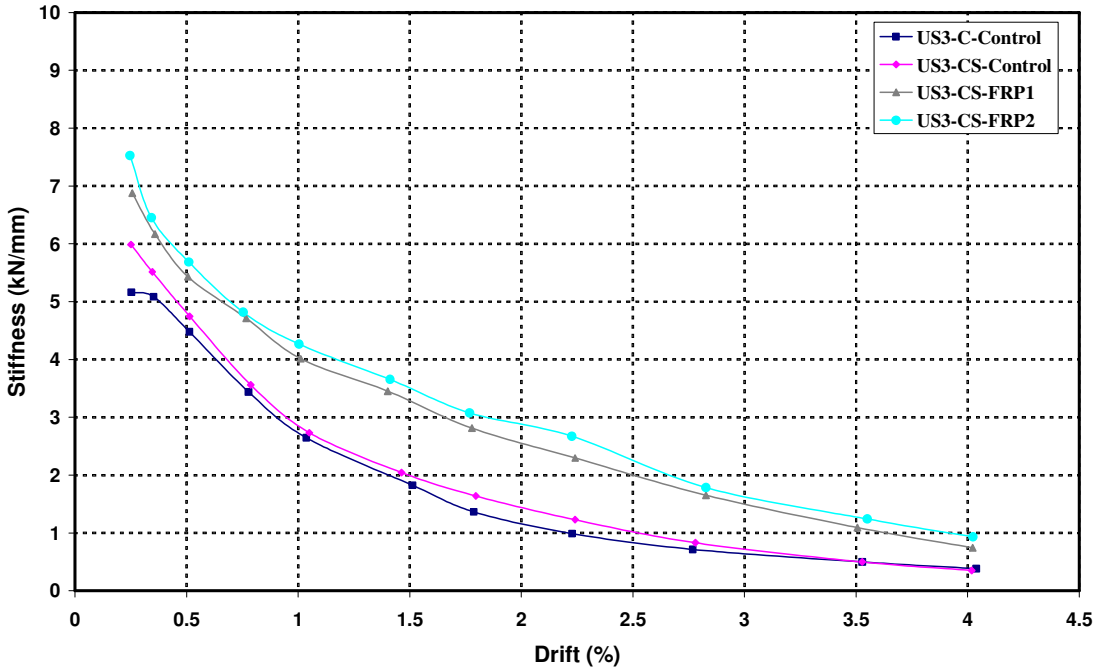

Figure 5.4. Comparison of peak to peak stiffness vs. drift response of specimens

5.4. Energy Dissipation

The capability of a structure to dissipate energy has a strong influence on its response to an earthquake loading. Therefore, ductile behavior of beam-column joints in RC structures is significant since it is correlated with desired energy dissipation potential of structure. Beam-to-column joint may be characterized as desired in terms of energy dissipation potential, if the energy dissipated per cycle increases while the drift increases. If the energy dissipated per cycle becomes constant or decreases while the drift increases, beam-to-column joint is assumed to have a poor response.

Energy dissipated per cycle is the area enclosed by the hysteretic loop of the cycle, as it is shown in Figure 5.5. The cumulative energy dissipated was then calculated by summing up the energy dissipated in consecutive loops throughout the test. Figure 5.6 shows the cumulative energy dissipation with drift for all subassemblies. At a glance, it may be concluded from the figure that retrofitted specimens dissipated approximately 150% more energy than control specimens which was the sign of improvement achieved by retrofitting. Initially, energy dissipation potential of retrofitted specimens was similar

with that of the control specimens but improved energy dissipation potential started to be observed after the drift level of 1.00%. While bond-slip failure and joint shear deteriorations started to be observed in control specimens before this drift level, the behavior was more ductile in retrofitted specimens since bond slip failure was delayed up to 2.75% drift level and joint shear failure was limited and/or stopped. Additionally, energy dissipation characteristics of control specimens were similar since the presence of slab did not change the overall behavior significantly.

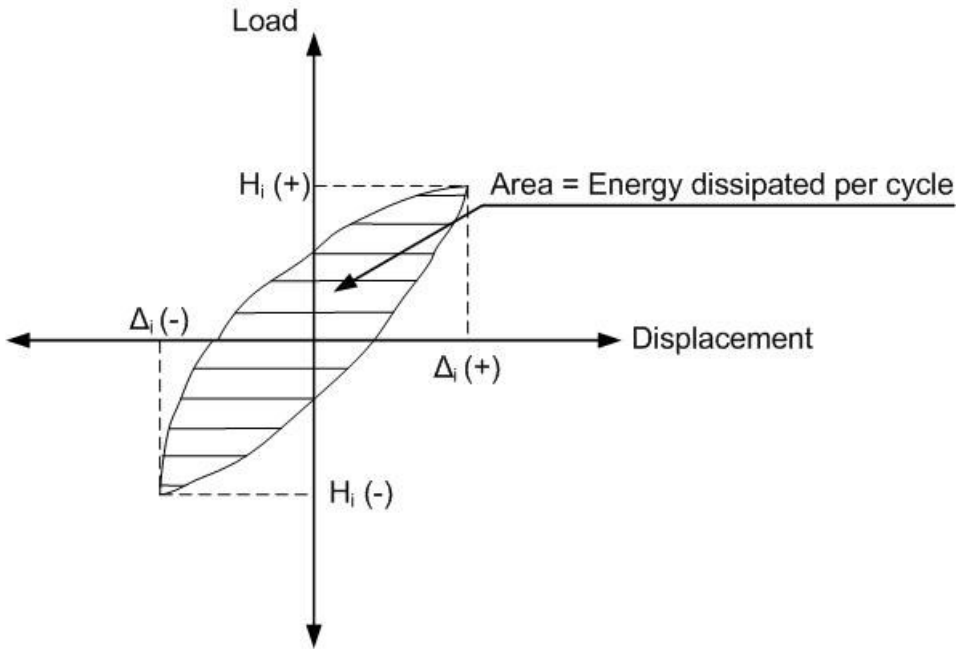

Figure 5.5. Energy dissipation

Figure 5.7 (a) through (d) show the energy dissipated per cycle for all specimens. Energy dissipated per cycle values were also summarized in Table 5.2. In this figure, energy dissipation per cycle was approximately zero up to the drift level of 0.50% for all specimens. Test results showed that, only few cracks occurred up to that drift level during experiments. Since energy dissipation consists of (1) energy dissipated by the steel reinforcement; (2) energy dissipated by friction along existing cracks in concrete; and (3) energy dissipated during the formation of new cracks; observation of low energy dissipation was reasonable in the first drift levels. In control specimens, energy dissipated per cycle became nearly constant as the drift increased while it improved gradually in retrofitted specimens. For all specimens, energy dissipation was smaller at the repeat

cycles of each drift level when they were compared with their corresponding first cycles as a result of the stiffness and strength degradation during the repeated cycles.

Table 5.2. Energy dissipated per cycle (kN.m)

Cycle #	**1**	**2**	**3**	**4**	**5**	**6**	**7**	**8**	**9**	**10**
Drift (%)	**0.35**	**0.35**	**0.35**	**0.5**	**0.5**	**0.5**	**0.75**	**0.75**	**0.75**	**1**
US3-C-Control	0.08	0.06	0.05	0.15	0.11	0.11	0.44	0.30	0.26	0.56
US3-CS-Control	0.08	0.05	0.04	0.16	0.12	0.07	0.45	0.31	0.27	0.60
US3-CS-FRP1	0.12	0.08	0.08	0.21	0.15	0.14	0.44	0.30	0.27	0.64
US3-CS-FRP2	0.11	0.09	0.06	0.23	0.17	0.14	0.50	0.32	0.28	0.63
Cycle #	**11**	**12**	**13**	**14**	**15**	**16**	**17**	**18**	**19**	**20**
Drift (%)	**1**	**1**	**1.4**	**1.4**	**1.4**	**1.75**	**1.75**	**1.75**	**2.2**	**2.2**
US3-C-Control	0.42	0.39	1.00	0.70	0.51	0.99	0.55	0.50	1.19	0.69
US3-CS-Control	0.43	0.39	0.89	0.51	0.48	0.95	0.59	0.56	1.28	0.72
US3-CS-FRP1	0.44	0.41	1.15	0.81	0.74	1.80	1.26	1.14	2.46	1.77
US3-CS-FRP2	0.47	0.44	1.24	0.91	0.81	1.61	1.18	1.13	2.21	1.79
Cycle #	**21**	**22**	**23**	**24**	**25**	**26**	**27**	**28**	**29**	
Drift (%)	**2.2**	**2.75**	**2.75**	**2.75**	**3.5**	**3.5**	**3.5**	**4**	**4**	
US3-C-Control	0.63	1.36	0.95	0.79	1.66	1.00	0.88	1.32	0.92	
US3-CS-Control	0.70	1.59	0.87	0.78	1.86	1.06	0.86	1.07	0.86	
US3-CS-FRP1	1.67	3.61	3.26	3.06	5.09	3.83	3.38	4.38	3.51	
US3-CS-FRP2	1.70	4.24	2.91	2.55	4.58	3.50	3.20	4.14	3.63	

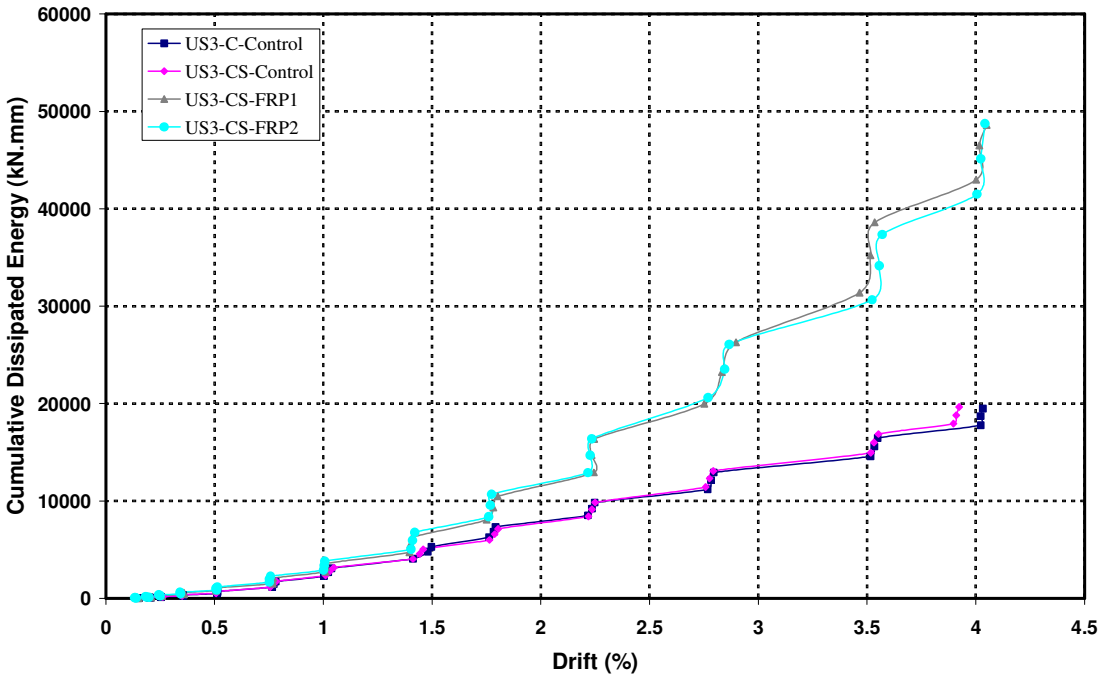

Figure 5.6. Comparison of cumulative energy dissipation characteristics of specimens

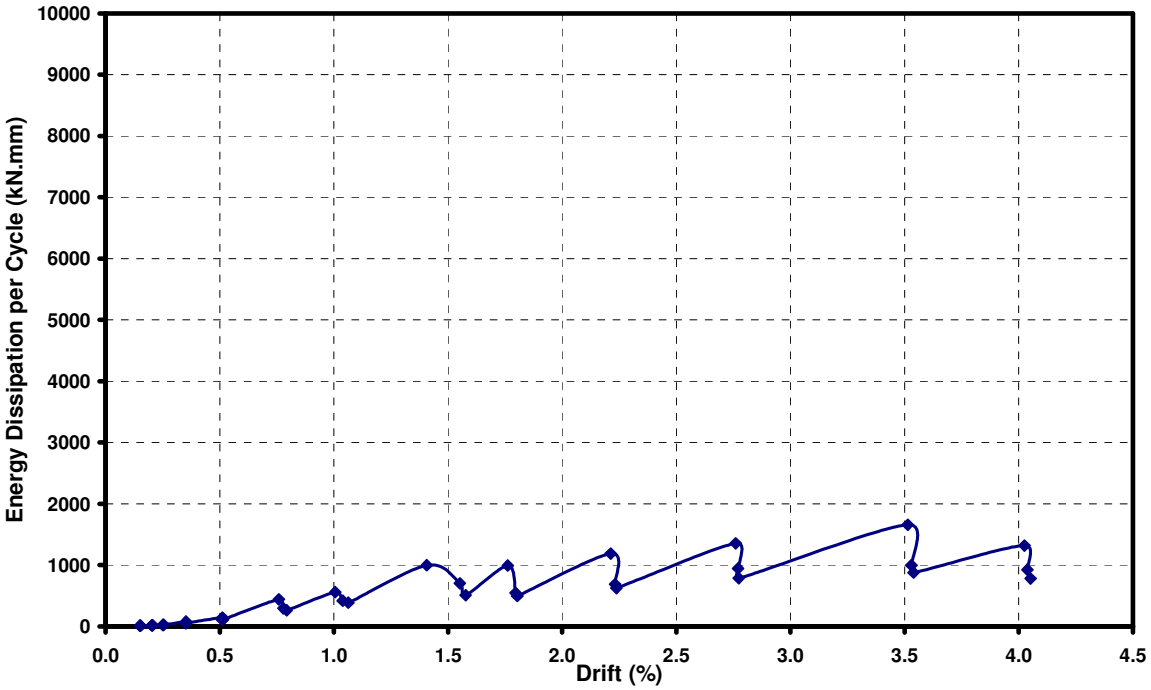

(a) US3-C-Control

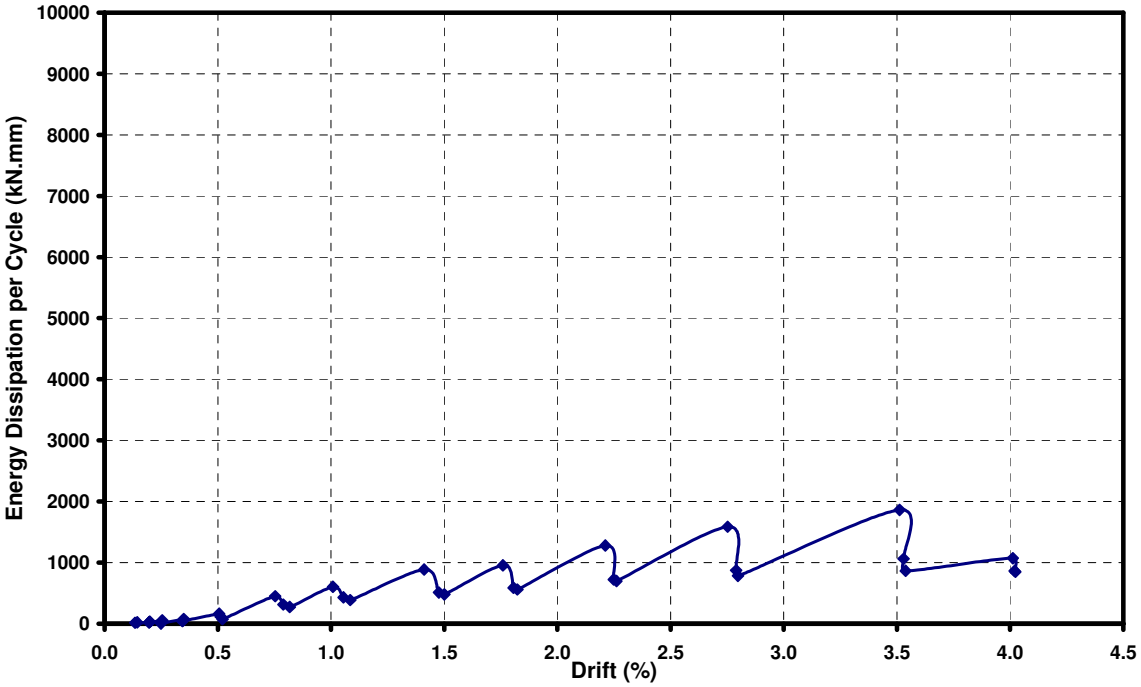

(b) US3-CS-Control

Figure 5.7. Energy dissipated per cycle versus drift graph of all specimens

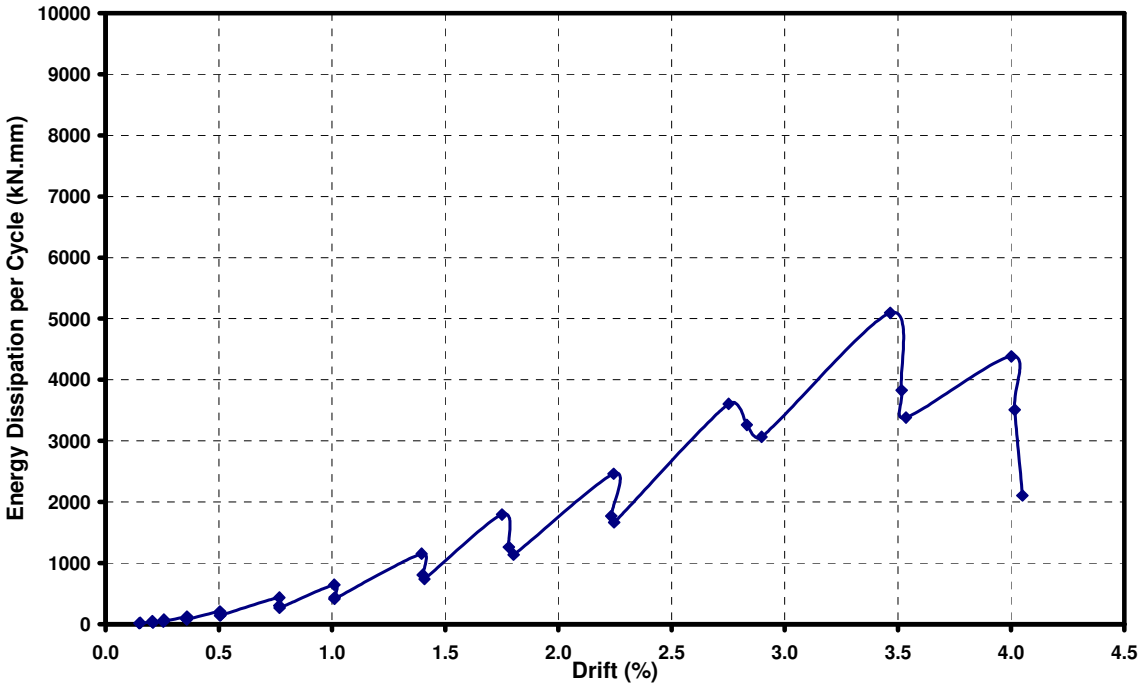

(c) US3-CS-FRP1

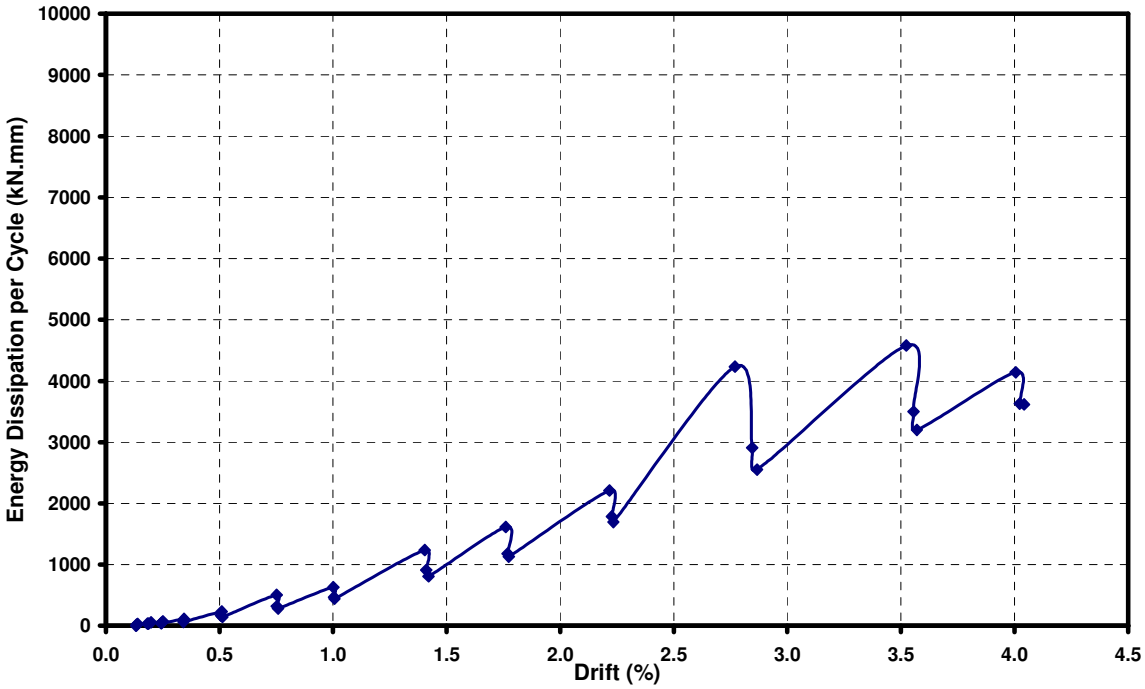

(d) US3-CS-FRP2

Figure 5.7. Energy dissipated per cycle versus drift graph of all specimens

5.5. Joint Shear

One of the main deficiencies of subassemblies was the lack of transverse reinforcement in the joint region. As it is mentioned above, joint shear failure governed the behavior of control specimens in pull direction of loading as a result of this deficiency. That was easily observed by diagonal shear deformations in the joint region during the tests as shown in Test Observations chapter with related photographs. Besides, as it is discussed in lateral load versus story drift response of specimens, excessive shear deformations in the joint region caused brittle modes of failure in pull direction of loading of these specimens. On the other hand, the failure of US3-CS-FRP1 was ductile in pull direction of loading since plastic hinge formed at the longitudinal beam and joint shear deformations were limited by the FRP application. When the FRP wraps were removed from the concrete surface for visual inspection after the test, it was observed that diagonal shear cracks were not so remarkable in joint region of US3-CS-FRP1. In US3-CS-FRP2, remarkable joint shear deformations again observed at the joint region after the removal of FRP wraps. Brittle joint shear failure was again occurred, but was delayed until the drift level of 2.75% which is acceptable.

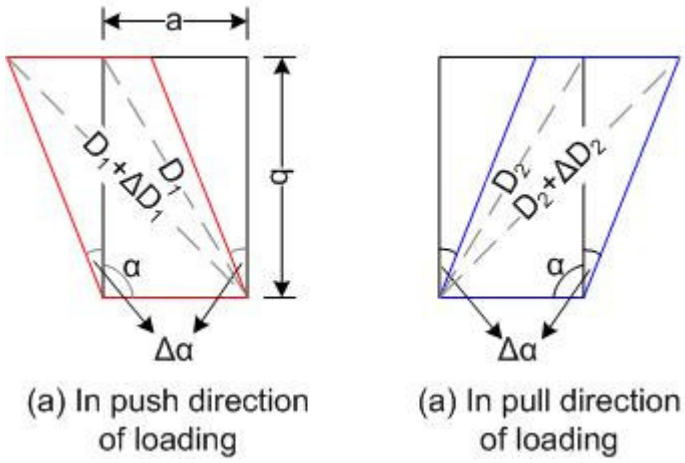

Figure 5.8. Deformed shape of the joint during cyclic loading

In order to compare the behavior of joint region more precisely, two LVDTs were used to measure joint shear deformation levels of subassemblies. Joint shear deformations were calculated by assuming that pure shear damage occurred in the joint region (Figure 5.8). These LVDTs were placed diagonally as it is shown in Figure 5.9 to be able to

measure diagonal deformations during the tests. As a result, joint shear deformation, which was defined as the change in α angle (Δα), was calculated by the formula given below;

(a) In push direction of loading;

$$\Delta\alpha = \arctan((\sqrt{((D_1+\Delta D_1)^2-b^2)}-\sqrt{((D_2-\Delta D_2)^2-b^2)})/(2xb)) \quad (1)$$

(b) In pull direction of loading;

$$\Delta\alpha = \arctan((\sqrt{((D_2+\Delta D_2)^2-b^2)}-\sqrt{((D_1-\Delta D_1)^2-b^2)})/(2xb)) \quad (2)$$

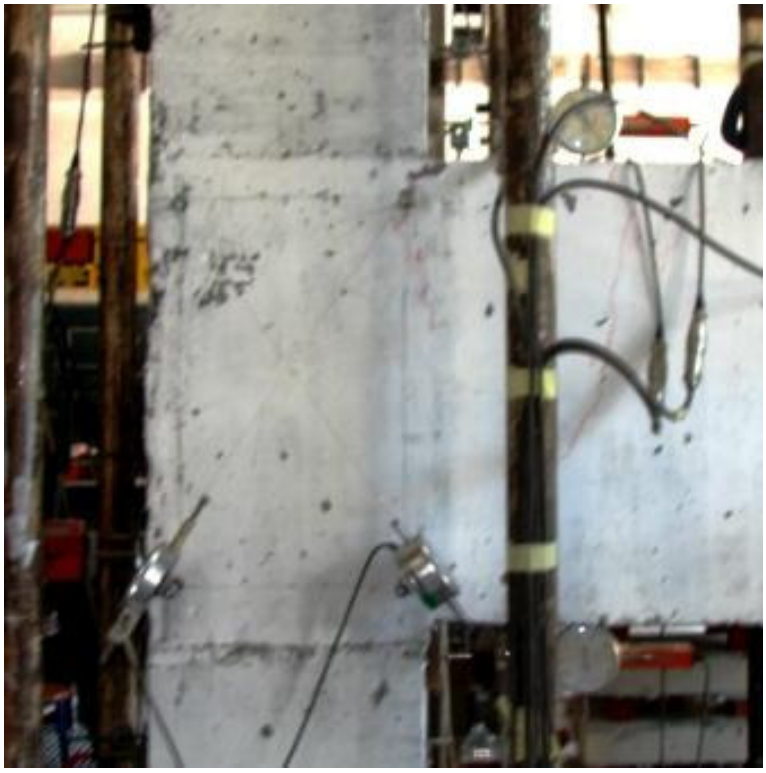

Figure 5.9. Joint shear deformation LVDTs

For all specimens, joint shear deformations with drift graphs were given in Figure 5.10 (a) through (d) and lateral load versus joint shear deformation response were given in 5.11 (a) through (d). According to these figures, joint shear deformations occurred only in pull direction of loading of control specimens. They failed at low lateral load level due to bond-slip in push direction of loading whereby maximum shear capacity of the joint region

could not be achieved. Conversely, as it can easily be observed in Figure 5.10 (c), joint shear deformations were around the same amplitudes in pull and push directions of loading of US3-CS-FRP1. Maximum lateral load reached in push direction of loading was extremely higher than that in control specimens as it was mentioned. Therefore, it was meaningful to observe joint shear deformations in push direction of loading of US3-CS-FRP1 since maximum joint shear capacity may not be achieved. However, after the drift level of 2.75 % (where bond slip failure occurred), joint shear deformations declined in push direction of loading because lateral load decreased dramatically. In US3-CS-FRP2, joint shear deformations were again observed in both push and pull directions of loading. In push direction of loading, after the occurrence of bond-slip failure, joint shear deformations decreased with decreasing lateral load. In pull direction of loading, joint shear deformation level was nearly same with control specimens at the end of the test. However, significant shear deformations occurred after the drift level of 2.75% and thus the behavior of joint region was more acceptable.

Wrapping orientation was same for two retrofitted specimens except the length of the FRP belt. However, significant joint shear deterioration occurred in US3-CS-FRP2 while joint shear failure was prevented in US3-CS-FRP1. The difference in joint behavior of these specimens was caused by debonding of outer L-shape FRP sheets at the joint region in US3-CS-FRP2. This resulted in disappearing of additional confinement provided by FRP wrapping which prevented joint region against shear failure in US3-CS-FRP1.

After joint shear failure governed the behavior, shear deformations were inelastic in control specimens and in US3-CS-FRP2. Diagonal shear cracks in the joint region were not closed not only during release of the lateral load in pull direction of loading but also during loading in the reversed direction. However, since inelastic deformations occurred at the beam plastic hinge in US3-CS-FRP1, diagonal shear cracks in the joint region were closed during the release of lateral load in both pull and push directions of loading which means the joint shear damage was in elastic range.

One of the main aims of retrofitting technique applied was to be able to limit joint shear deformations in order to have ductile behavior. While the joint shear deformations

were around 0.05 radians in control specimens, it was reduced to approximately 0.015 radians in US3-CS-FRP1. Hence, joint shear deformations were reduced 70% by the applied retrofitting technique. As it is evidenced above, FRP application improved the behavior of joint region against shear deficiency. In US3-CS-FRP2, while joint shear deformation level was nearly same with control specimens, the occurrence of joint shear failure was delayed until 2.75% drift level. The improvement achieved by FRP application may also be seen in Figure 5.12 and Figure 5.13.

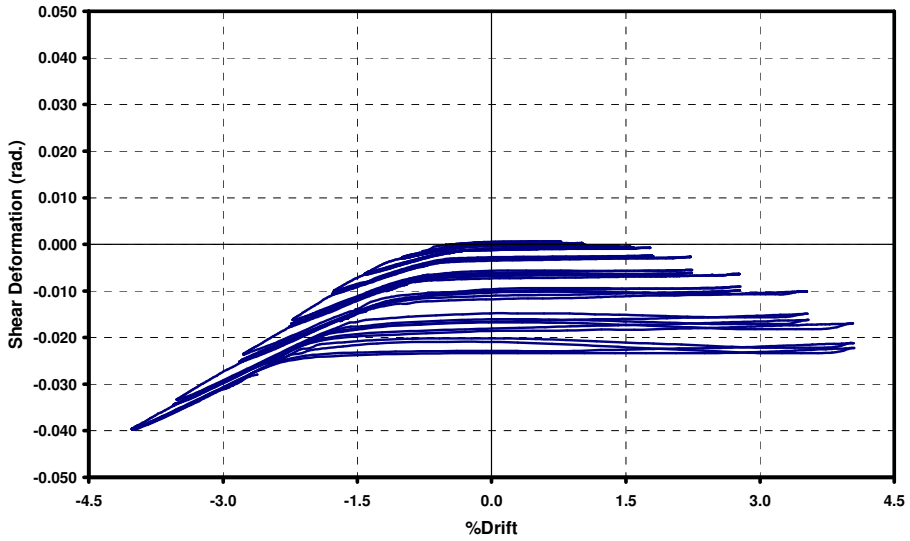

(a) US3-C-Control

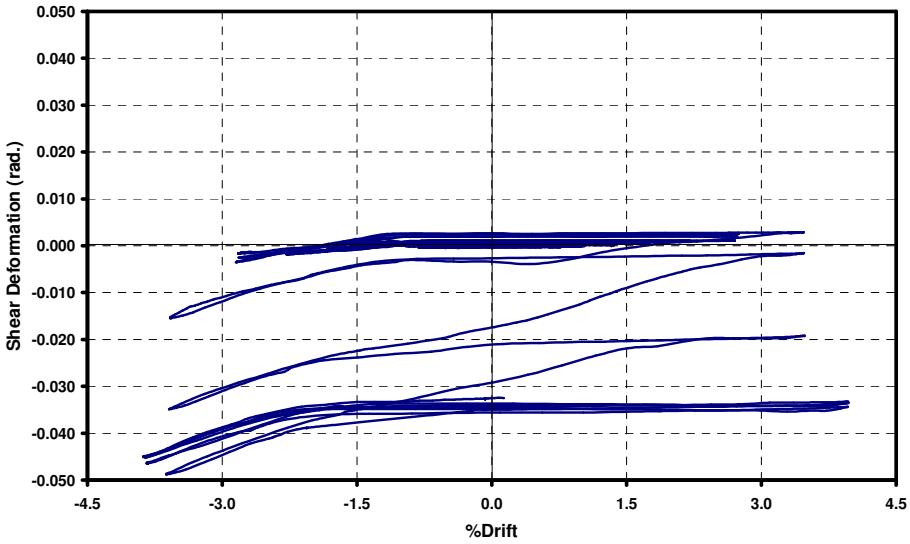

(b) US3-CS-Control

Figure 5.10. Shear deformation versus drift response of specimens

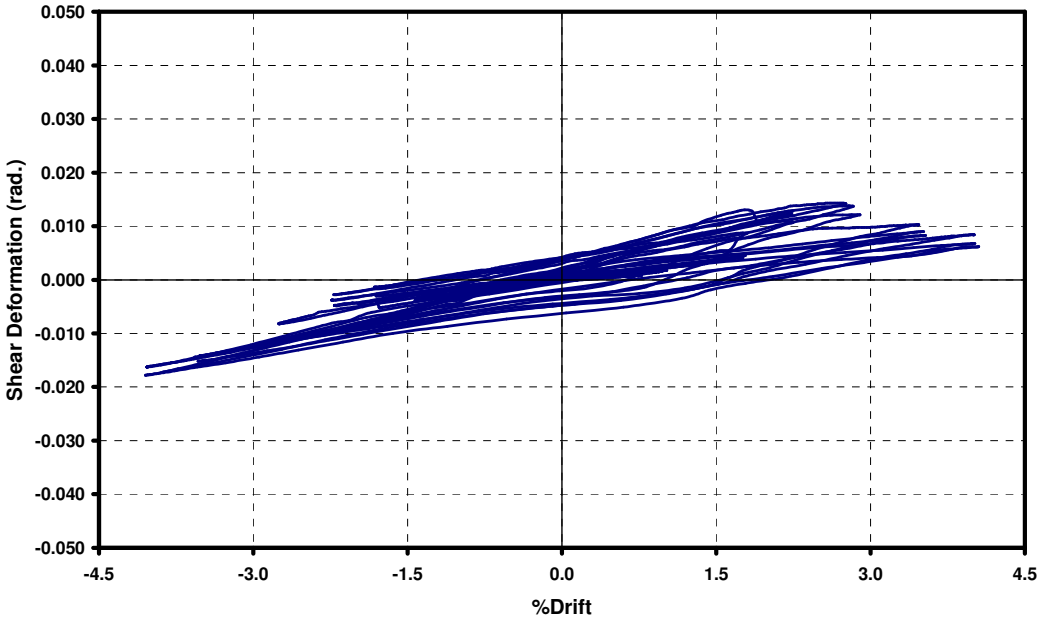

(c) US3-CS-FRP1

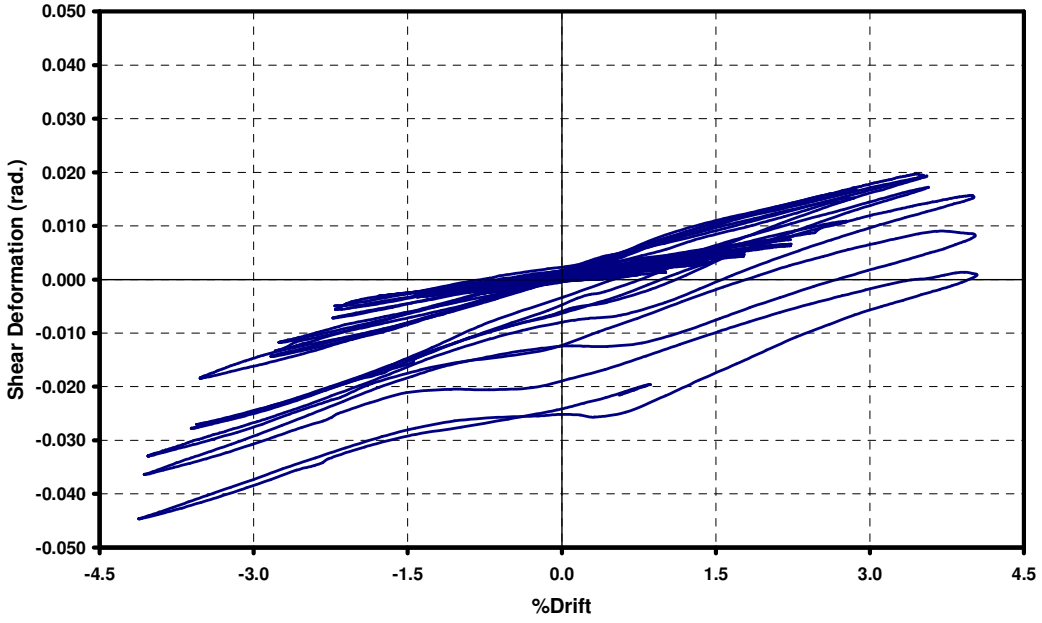

(d) US3-CS-FRP2

Figure 5.10. Shear deformation versus drift response of specimens

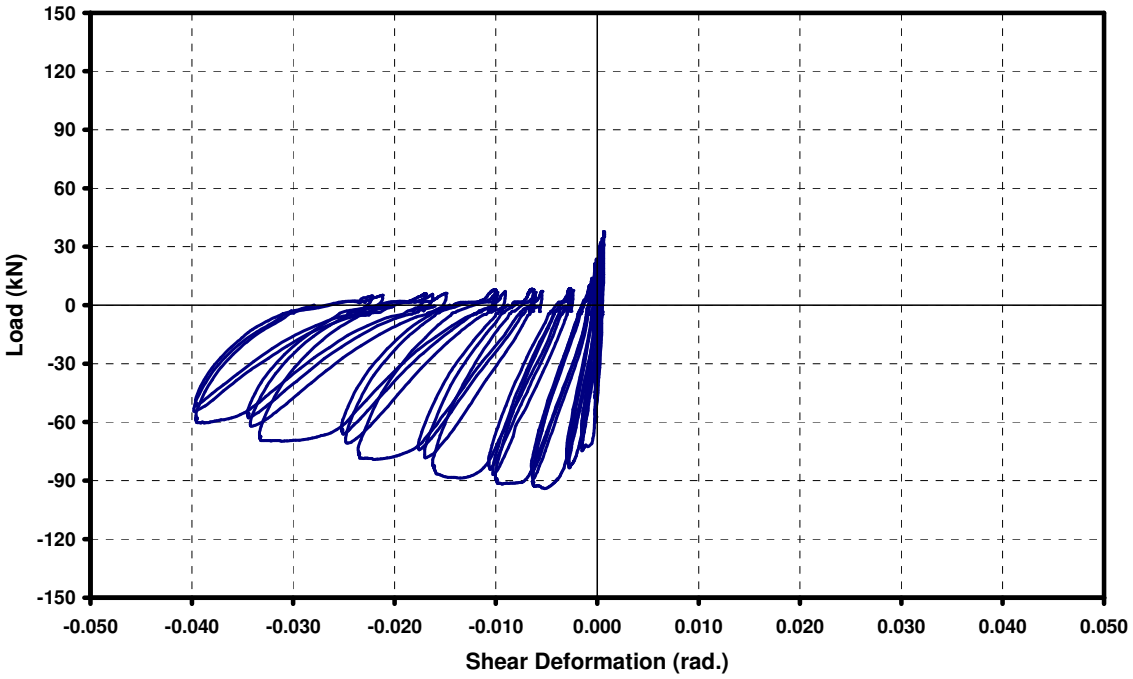

(a) US3-C-Control

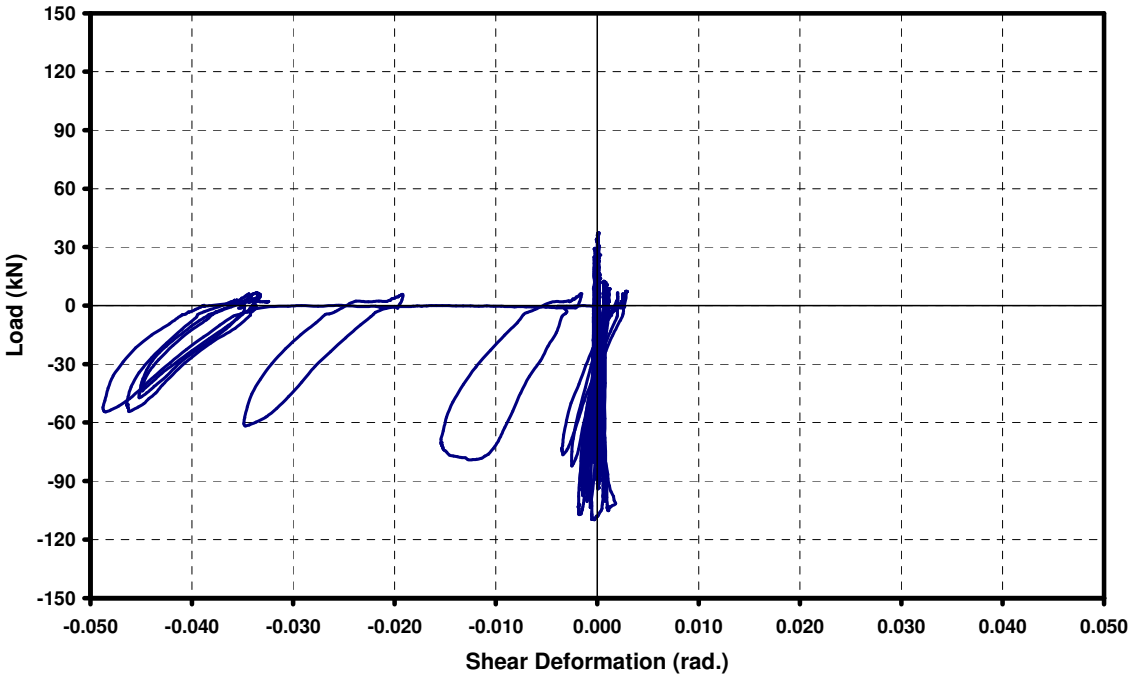

(b) US3-CS-Control

Figure 5.11. Lateral load versus shear deformation response of specimens

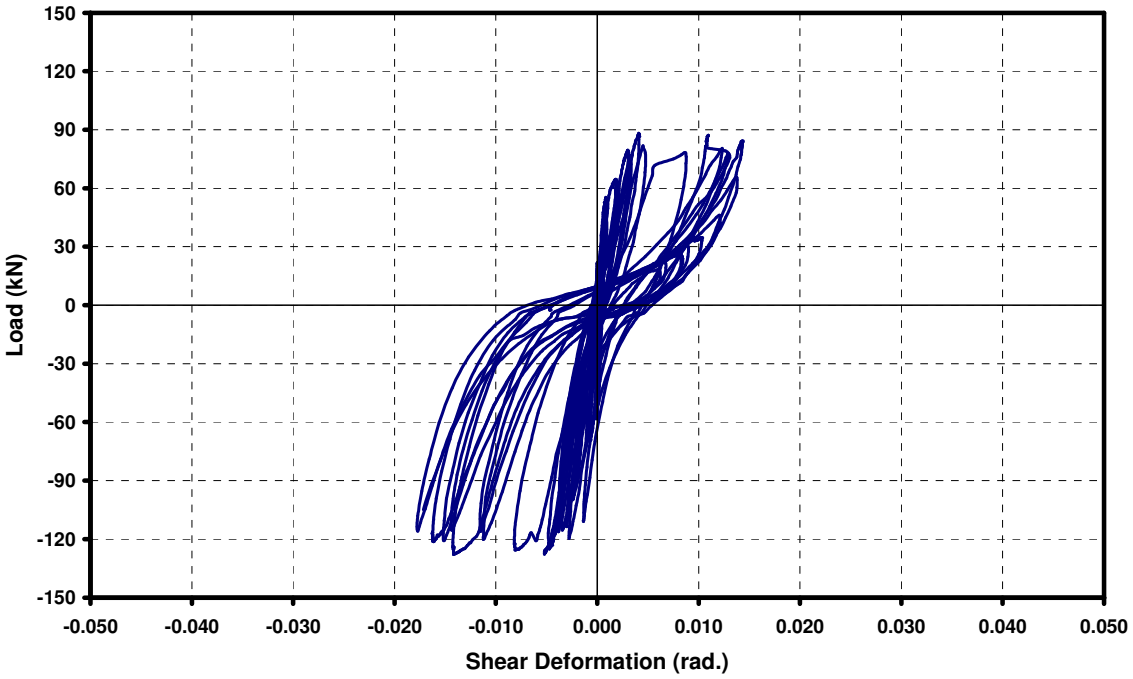

(c) US3-CS-FRP1

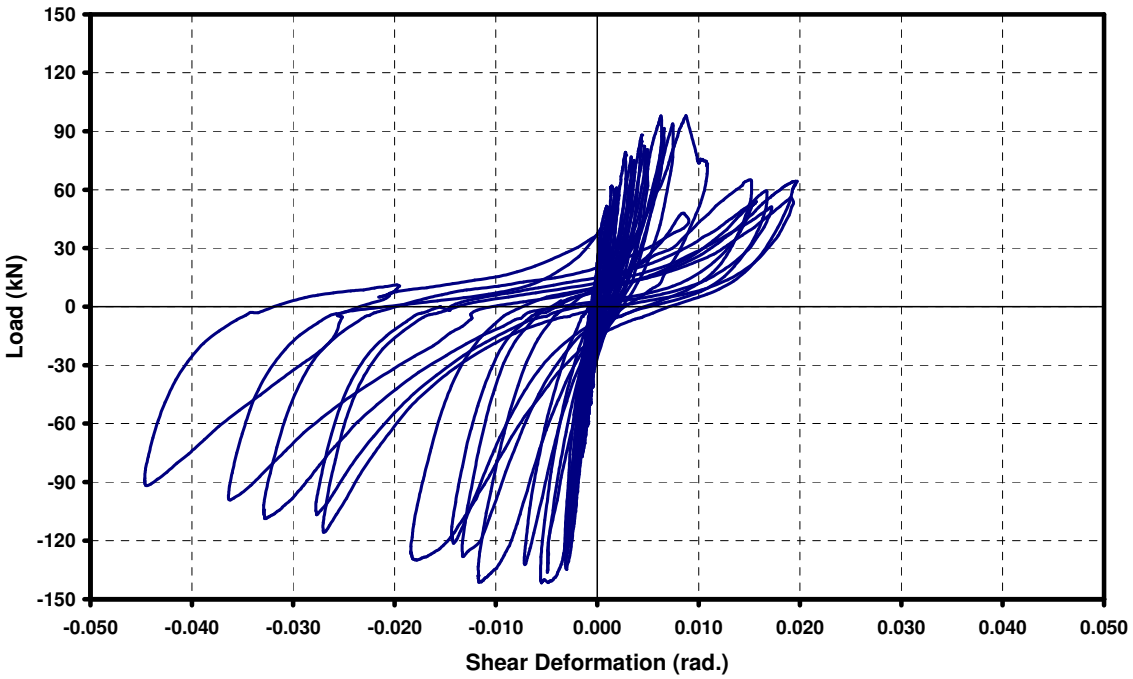

(d) US3-CS-FRP2

Figure 5.11. Lateral load versus shear deformation response of specimens

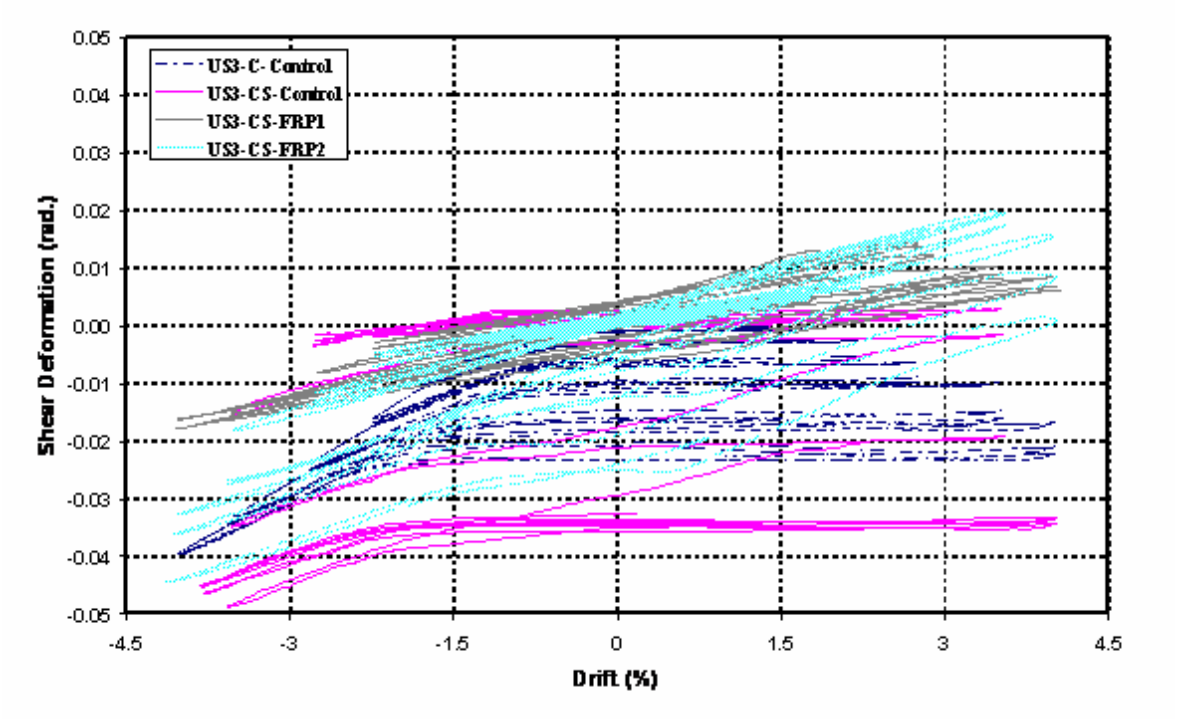

Figure 5.12. Comparison of shear deformation versus drift graphs

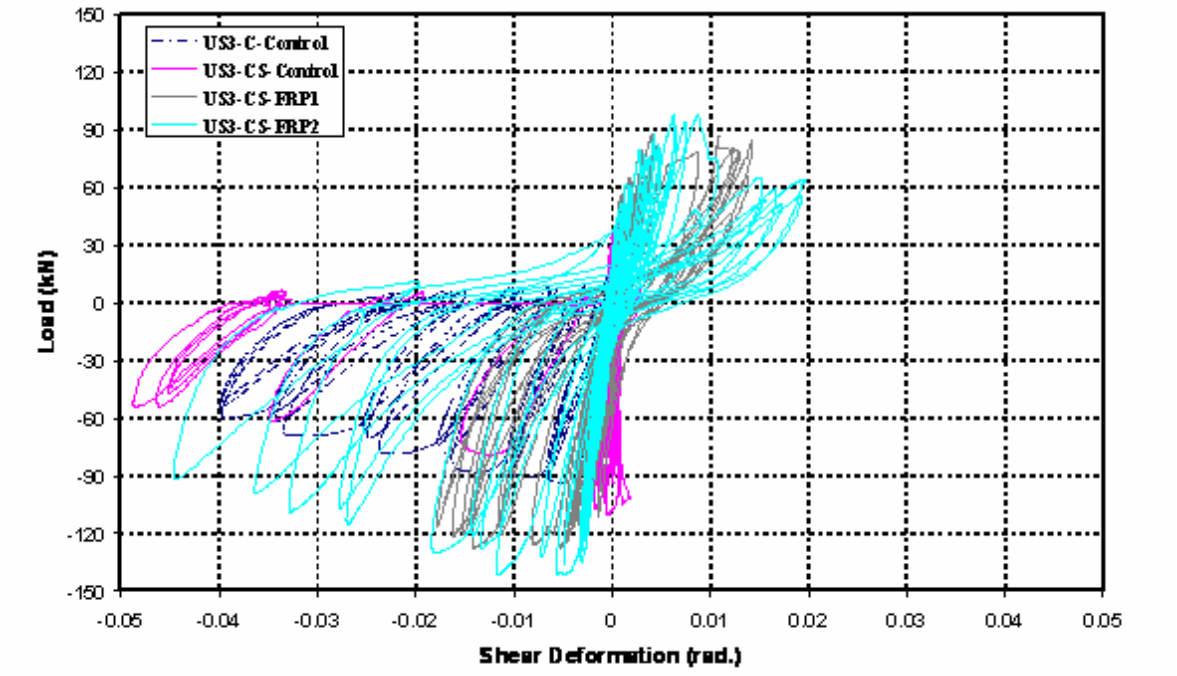

Figure 5.13. Comparison of lateral load versus shear deformation graphs

5.6. Bond Slip

Inadequate anchorage of longitudinal bars is a significant deficiency of existing RC structures because it causes slippage of bars during reversed cyclic loading in a moderate earthquake. In this study, longitudinal beam bottom reinforcements were anchored only 150 mm. into the joint region of subassemblies in order to investigate effects of this typical detailing deficiency on seismic behavior (Figure 5.14). In gravity load designed RC structures, longitudinal beam bottom reinforcements are under compression only at the joint region. However, because of the seismic forces, moment reversals are expected at that region of RC frames which also result in stress reversals on these reinforcements. Therefore, sufficient bond strength was required to restrain resultant tensile stresses of negative seismic moments, which is impossible while the anchorage lengths of reinforcements are inadequate.

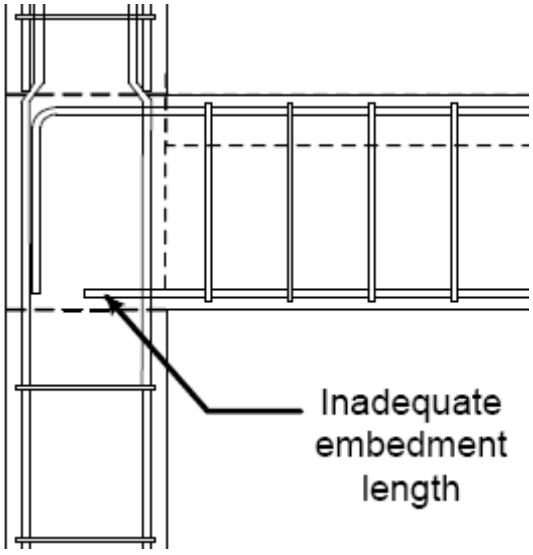

Figure 5.14. Detailing of longitudinal beam bottom reinforcements

The test results showed that brittle failure occurred due to slippage of longitudinal beam bottom reinforcements in push direction of loading of all specimens while the maximum lateral load was lower than the required value for a ductile beam hinging. Slippage was measured directly by using an LVDT that was placed at the backside of the column throughout a small hole which was drilled to the end of the longitudinal beam bottom bar (Figure 5.15). The data of this LVDT was plotted with drift and with strain of

the corresponding bar. These graphs are given below for all specimens from Figure 5.16 to Figure 5.19.

Figure 5.15. LVDT layout for slippage reading

Figure 5.16 (a) and 5.17 (a) show that first significant slippage occurred at the drift level of 0.50% in push direction of loading of control specimens. Slippage increased in consecutive cycles throughout the test and reached 25 mm at the end of the test. On the other hand, in US3-CS-FRP1, significant slippage was delayed up to the drift level of 2.75% as shown in Figure 5.18 (a). FRP belt was applied in US3-CS-FRP1 with the aim of stopping or delaying bond slip failure. This result illustrates the improvement achieved by this FRP retrofitting technique. Although, retrofitting improved the behavior in push direction of loading by delaying the bond-slip failure, the behavior was still brittle with significant strength degradation. FRP belt could not work efficiently after the drift level of 2.75%, since the main flexural crack, where slippage occurred, was at the section of the FRP belt anchorage hole. Therefore, in US3-CS-FRP2, it was aimed to stop slippage up to the end of the test by increasing the length of the FRP belt. However, as shown in Figure 5.19 (a), significant slippage was again observed at the drift level of 2.75% as a result of the debonding of inner L-shape FRP sheets. Alternatively, hinging due to bond-slip failure occurred at the longitudinal beam-column interface and thus, FRP belt worked efficiently up to the end of the test. It limited the slippage and strength degradation after the occurrence of bond-slip failure.

Slippage occurred in all specimens when strain value in the bars was rather above of 1000 μЄ. In control specimens, strain of the longitudinal beam bottom bars decrease rapidly after slippage occurred. In US3-CS-FRP1, strain could not be measured because of the fail of strain gauges after the drift level of 2.75%. Since lateral load decreased after slippage occurred in push direction of loading of this specimen, it can be concluded that strain of the longitudinal beam bottom bars also decreased. However, the pattern and the strain level at the end of the test could not be determined. In US3-CS-FRP2, rate of the strain degradation was more gradual when it was compared with control specimens. While strain decreased nearly to zero with increasing slippage in control specimens, it was approximately 750 μЄ in US3-CS-FRP2 at the end of the test.

In conclusion, FRP belt application improved the behavior in push direction of loading by delaying the bond slip failure to the drift level of 2.75%. As it is mentioned above, maximum lateral load of retrofitted specimens were higher in push direction of loading and stiffness degradation characteristics were also better. Besides, while bond slip failure caused excessive deformations at the longitudinal beam-column interface and at bottom column close to the joint region in control specimens, neither the interface nor the column was damaged due to bond slip failure in US3-CS-FRP1. In US3-CS-FRP2, hinging due to bond-slip failure was again observed at the longitudinal beam-column interface but column did not damage.

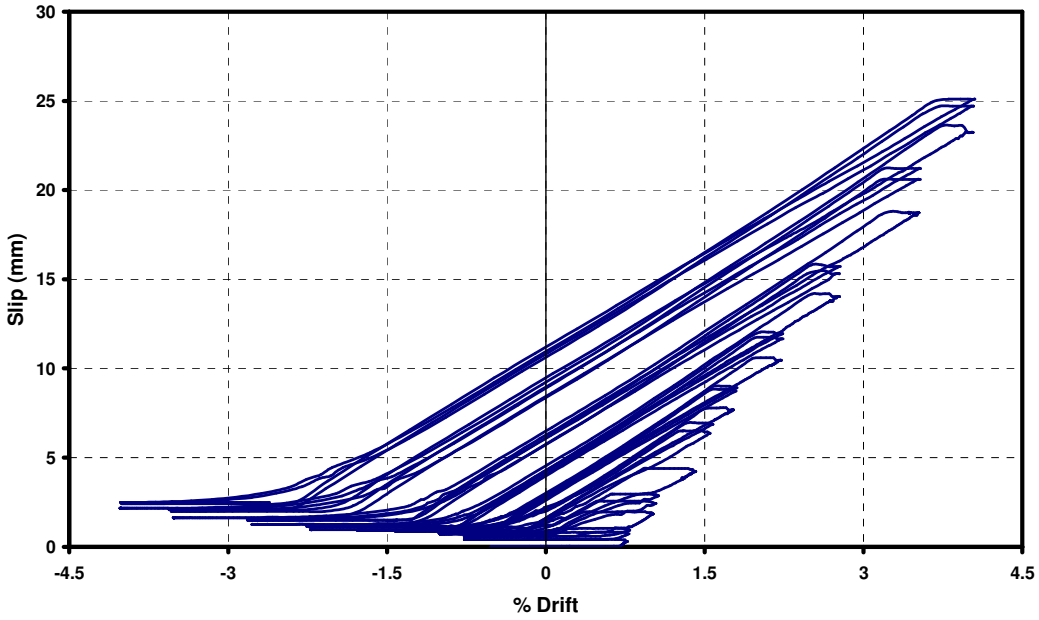

(a) Slip versus drift response

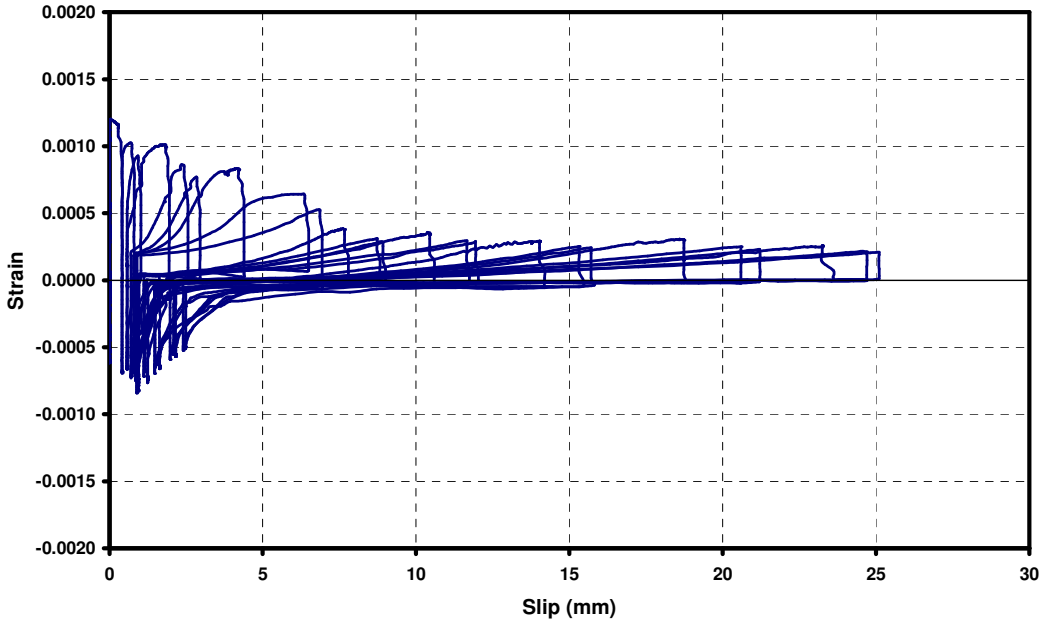

(b) Strain versus slip response

Figure 5.16 Bond-slip response of US3-C-Control

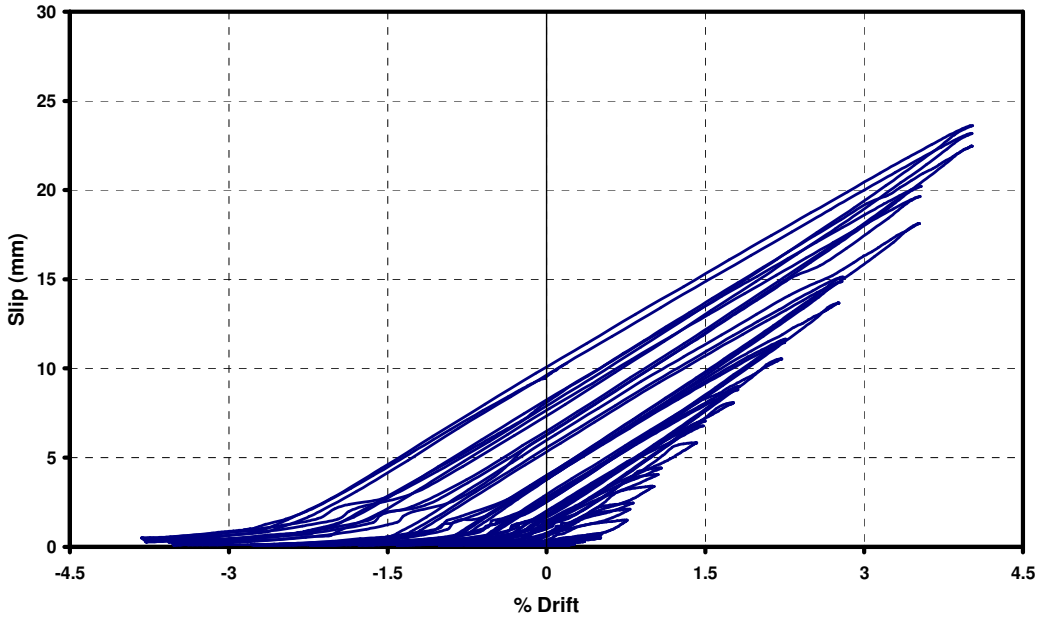

(a) Slip versus drift response

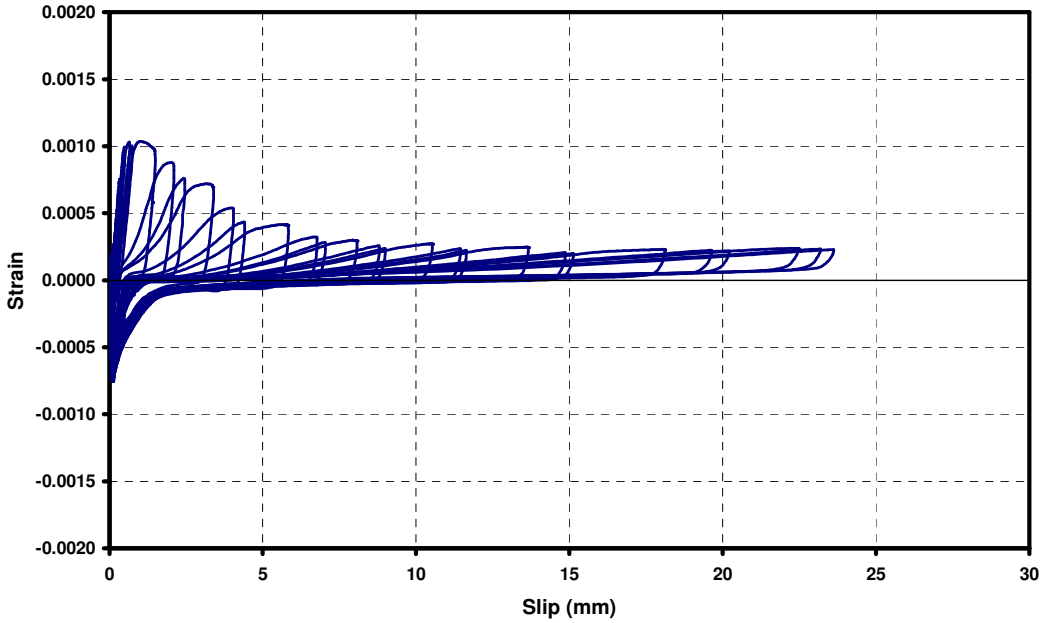

(b) Strain versus slip response

Figure 5.17. Bond-slip response of US3-CS-Control

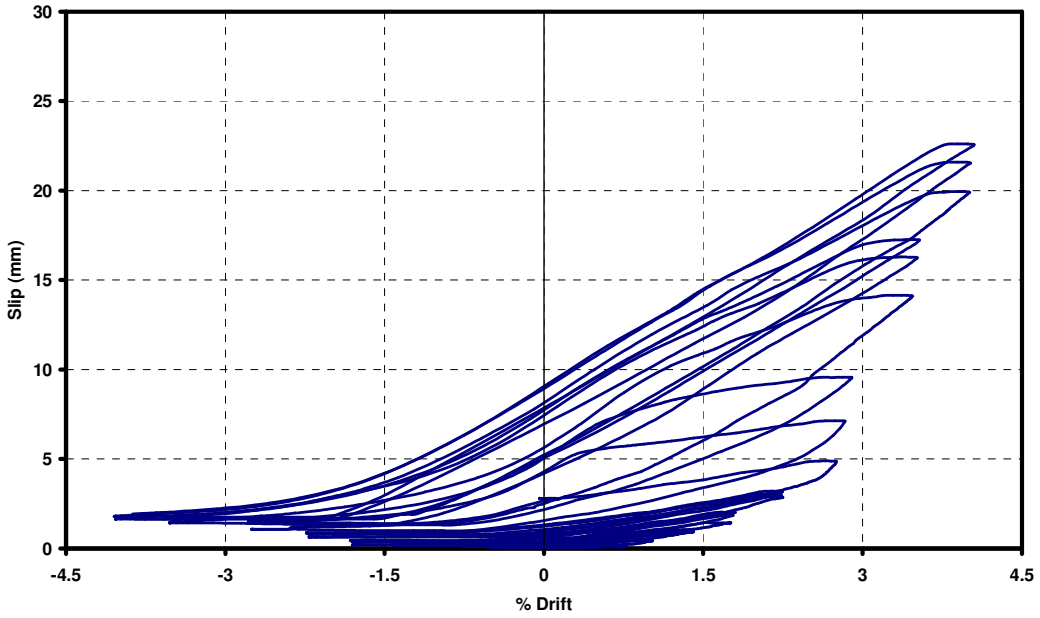

(a) Slip versus drift response

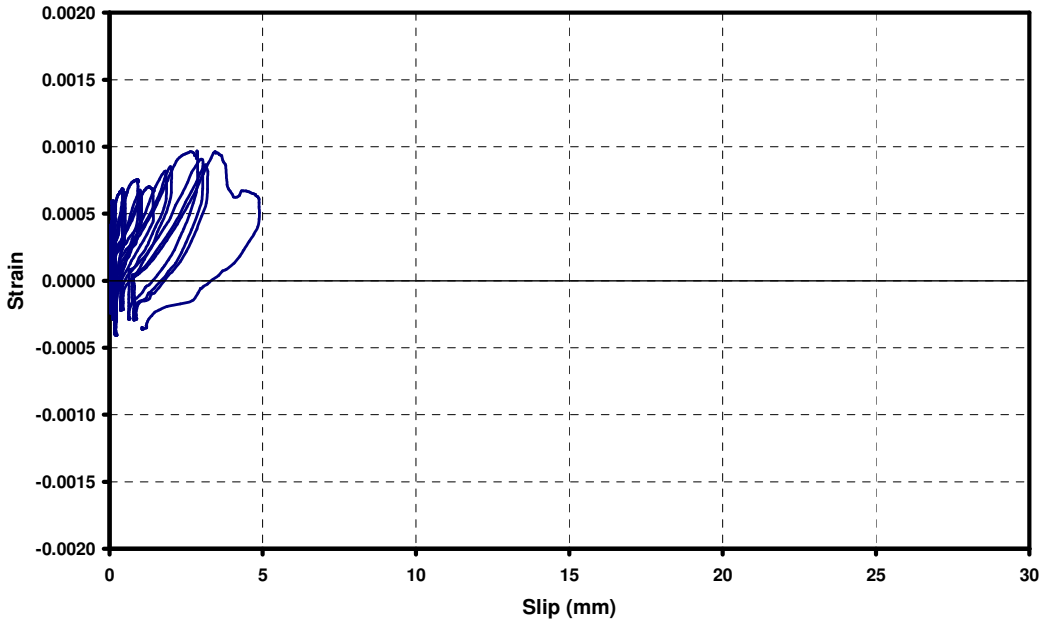

(b) Strain versus slip response

Figure 5.18. Bond-slip response of US3-CS-FRP1

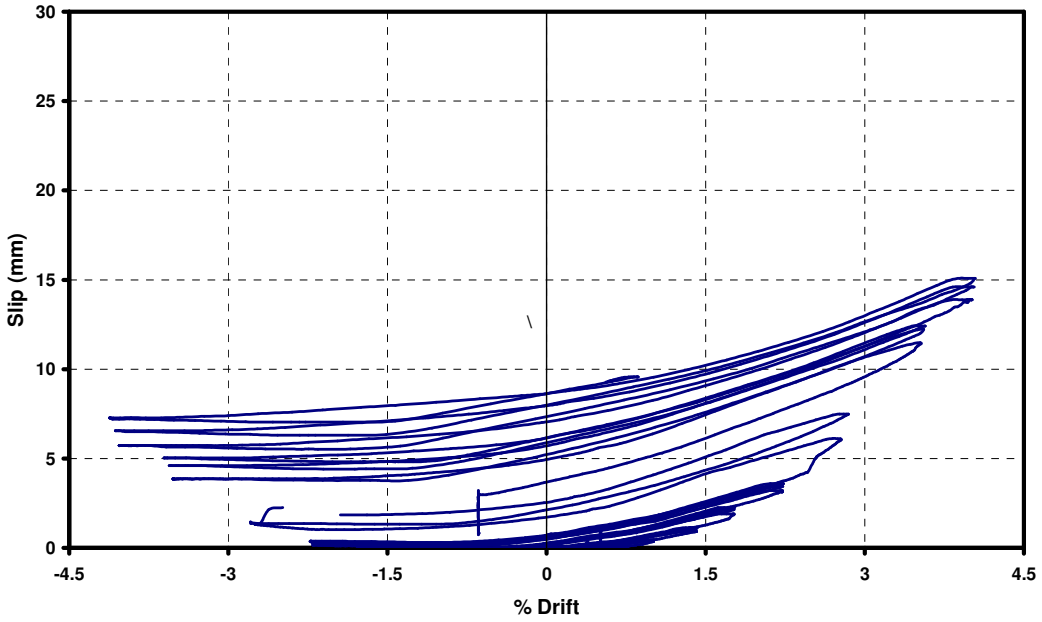

(a) Slip versus drift response

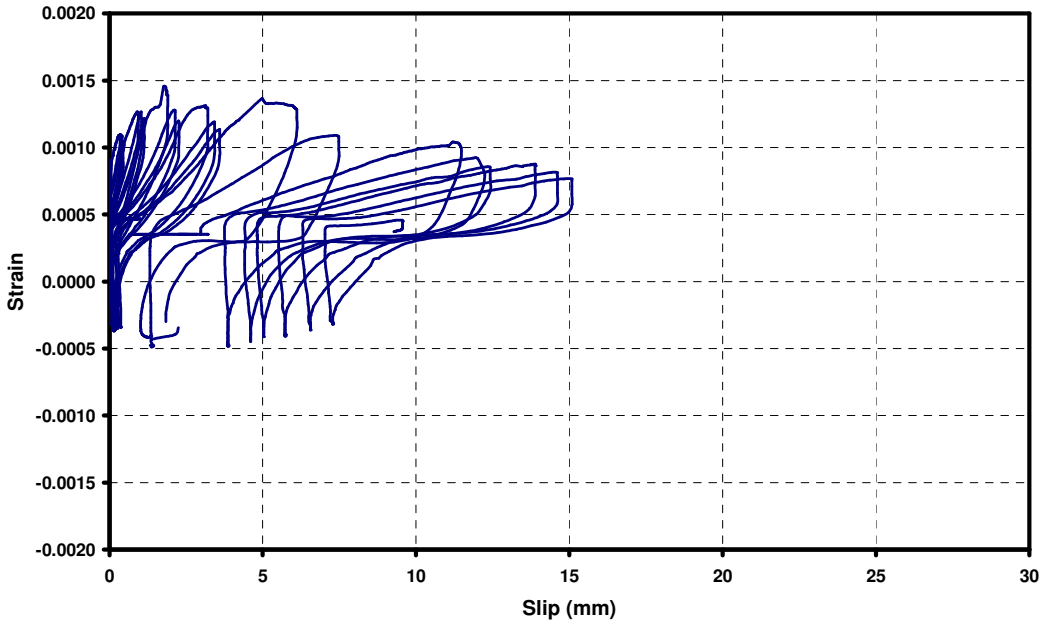

(b) Strain versus slip response

Figure 5.19. Bond-slip response of US3-CS-FRP2

5.7. Slab Contribution

Previous studies have proved that the presence of slab influences the behavior of RC frames under lateral loading. Two control specimens were tested in this study in order to investigate effects of the presence of slab on seismic behavior of deficient beam-column joints. One of them (US3-C-Control) included only transverse beam while the other one (US3-CS-Control) included both transverse beam and slab. Lateral load versus column top displacement envelopes of these specimens showed that the presence of slab increased the lateral load capacity of the specimen in pull direction of loading, as it was mentioned above. However, it was not effective on the behavior in push direction of loading as a result of the failure mode. In push direction of loading, compressive stresses occur at the top portion of longitudinal beam due to positive moment. Longitudinal beam top bars were subjected to low compressive stresses since bond slip failure initiated at early drift levels while the lateral load level was rather below the required level corresponding to beam hinging. Therefore, the contribution of slab bars to the longitudinal beam top bars was not required (Figure 5.20).

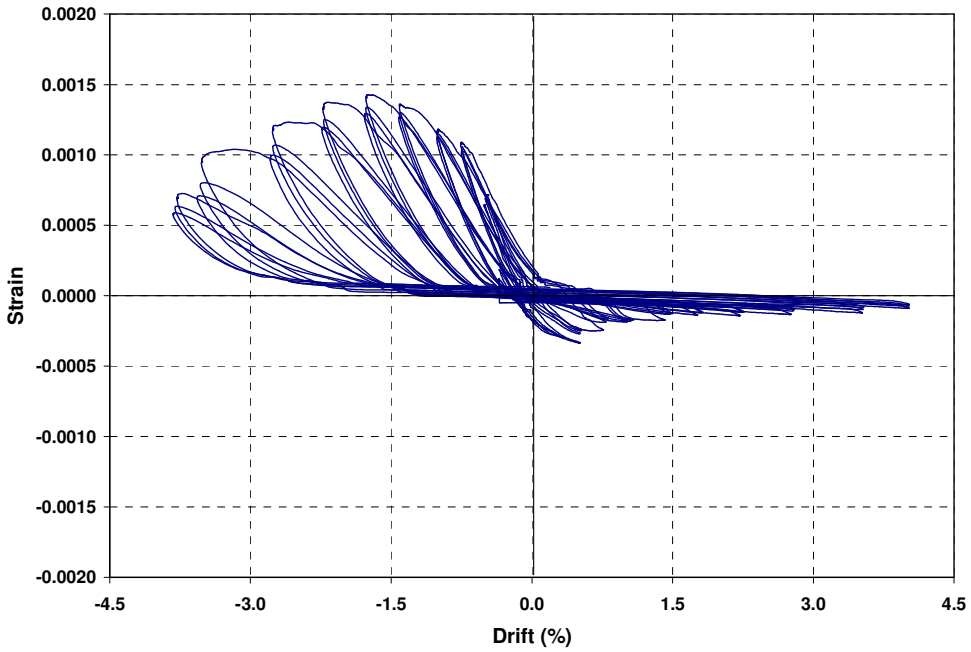

Figure 5.20. Slab bar strain versus drift graph (gage #18 in US3-CS-Control)

Total of 15 strain gauges were mounted on the longitudinal slab bars of US3-CS-Control in order to investigate strain profile on the slab during the test (Figure 3.18). Strain contribution with the drift level was determined by using data of these strain gauges and plotted in Figure 5.21. Strain value of each strain gauge corresponding to the maximum lateral load at each drift level was determined and strain distribution surfaces on the slab was plotted by joining these values. It can easily be seen in that figure that, slab contribution got larger as the specimen was subjected to larger drift levels. All of the longitudinal slab reinforcements have experienced continuous strain increase until the drift level of 1.75%. Since joint shear failure governed the behavior after that drift level lateral load decreased gradually and hence slab bar strains also decreased gradually up to the drift level of 4.00%.

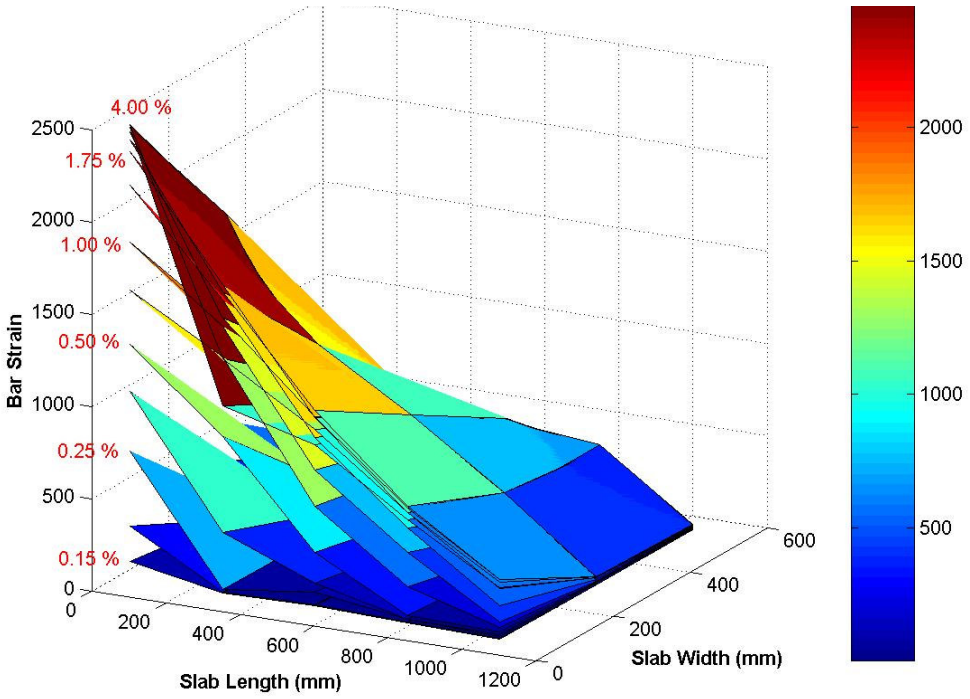

Figure 5.21. Slab contribution versus drift level

In this figure, intersection of slab length and bar strain axis illustrates the placement of joint in terms of strain gauge locations on the slab. Therefore, it is obvious that slab bar nearest the longitudinal beam has underwent most rapid strain increase and has yielded. Besides, first strain gauge array parallel to the transverse beam have exhibited higher strain

values when it is compared with arrays closer to the end of the longitudinal beam since moment is higher at sections of the slab closer to the joint.

Slab contribution affects the behavior of transverse beam under seismic action. Slab longitudinal bars were adequately anchored to the transverse beam. As a result of this, while slab contributes to the flexural strength of the longitudinal beam, transverse beam was subjected to torsional moments due to the eccentricity of slab as it is shown in the free body diagram in Figure 5.22. In US3-CS-Control specimen, diagonal cracks occurred at the back side of the transverse beam close to the joint region because of torsion. When retrofitting scheme was determined for US3-CS-FRP1, this was also considered and L-shape FRP sheets and FRP anchorage strips were applied in order to overcome this problem.

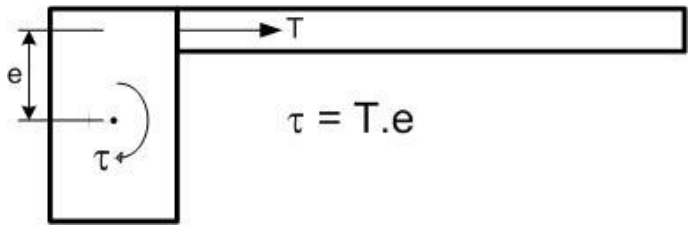

Figure 5.22. Torsion on the transverse beam due to slab contribution

Finally, slab contribution did not affect significantly the behavior of US3-CS-Control when it is compared to US3-C-Control except 10% lateral load increase in pull direction of loading. Failure mode was still same for both directions of loading of US3-CS-Control. Neither energy dissipation nor stiffness degradation characteristics were influenced significantly by the presence of slab.

5.8. Strain Gauge Data

5.8.1. Longitudinal Beam Bottom Longitudinal Bars

Strain gauges were placed on longitudinal beam bottom bars 150 mm away from the column face as it was shown in Figure 3.17. These bars were inadequately anchored into

the joint region, and hence bond-slip failure occurred during the experiments. Therefore, strain gauges were used to investigate the bond slip versus strain relation which was given above for all specimens.

In US3-C-Control, longitudinal beam bottom bars were not yielded in both direction of loading because the strain gauges readings throughout the test gave a value much less than 2000 μЄ (Figure 5.23 (a)). They were subjected to tensile stresses in push direction of loading which could not be restrained due to inadequate anchorage. After bond slip failure occurred, strain values decreased rapidly from 0.50% to 1.75% drift level because the bond between concrete and bars was deteriorated. After the drift level of 1.75%, rate of bar strain decrease declined and bar strain was nearly constant up to the end of the test. In pull direction of loading, bar strains increased until joint shear failure occurred. As a result of the gradual decrease of lateral load after the joint shear failure, bar strains decreased gradually as well. The strain vs. drift response of US3-CS-Control was similar as it can easily be seen in Figure 5.23 (b).

Since FRP sheets acted as additional reinforcement and contributed to the bars in retrofitted specimens, bar strains increased more gradually. In US3-CS-FRP1, strain data could not be collected after the drift level of 2.75% due to the fail of strain gauges. Therefore, strain profile could not be determined after the occurrence of bond-slip failure. In US3-CS-FRP2, after slippage was observed, strain was kept constant from 1.40% to 2.75% drift level. At the drift level of 2.75%, due to significant slippage bar strain decreased in repeat cycles. However, after that drift level, rate of the strain decrease was more gradual when it was compared with control specimens.

Finally, longitudinal beam bottom bars of all specimens started to slip when strain reached the value of 1000 μЄ approximately. Since FRP belt acted as additional reinforcement and contributed to the bars, longitudinal beam bottom bars of retrofitted specimens reached that strain value at later drift level and the aim of FRP application was succeeded.

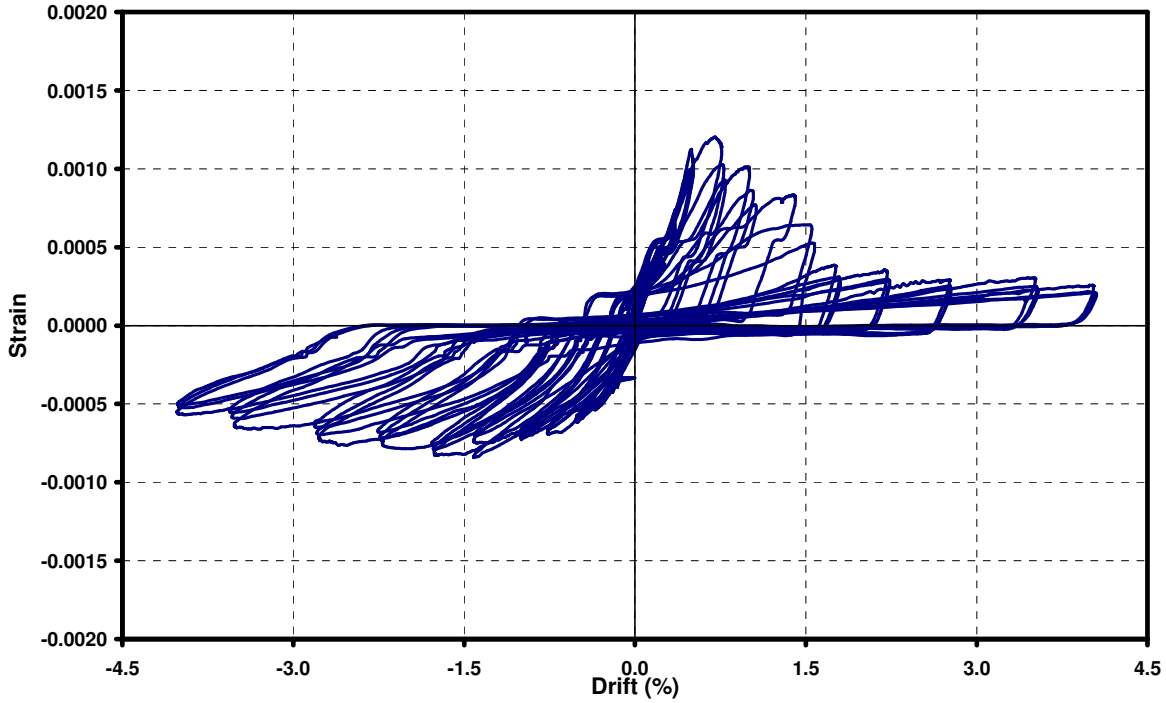

(a) US3-C-Control

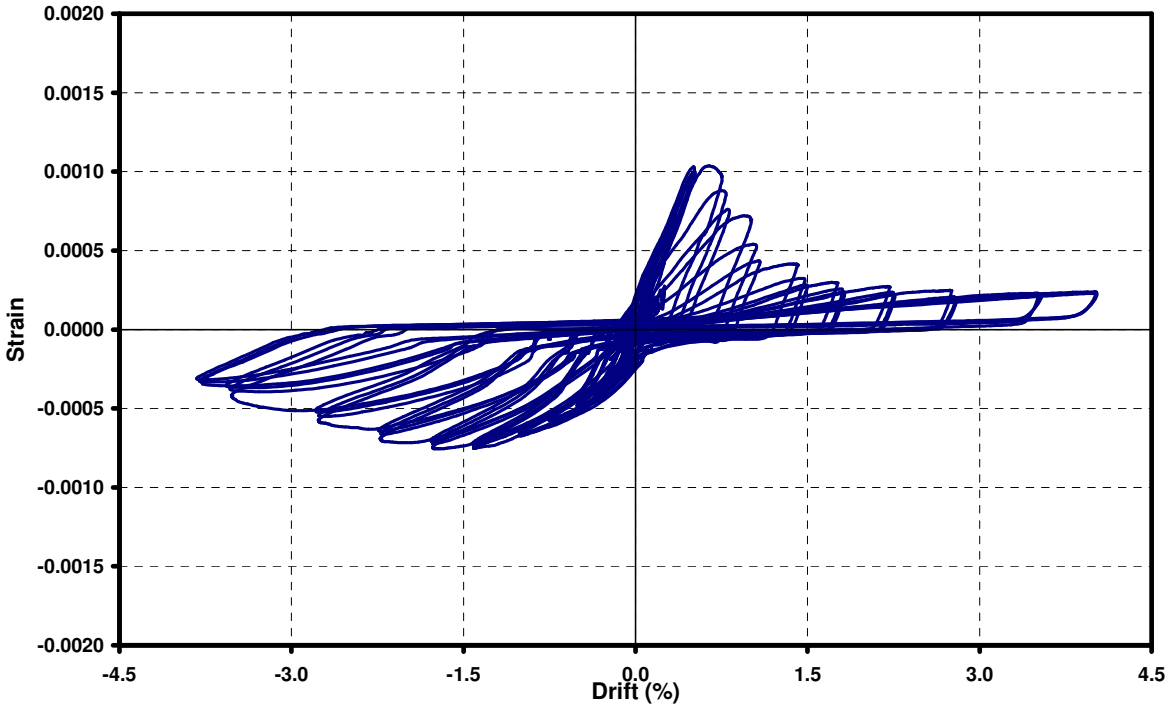

(b) US3-CS-Control

Figure 5.23. Strain versus drift response of longitudinal beam bottom bars (Gage #8)

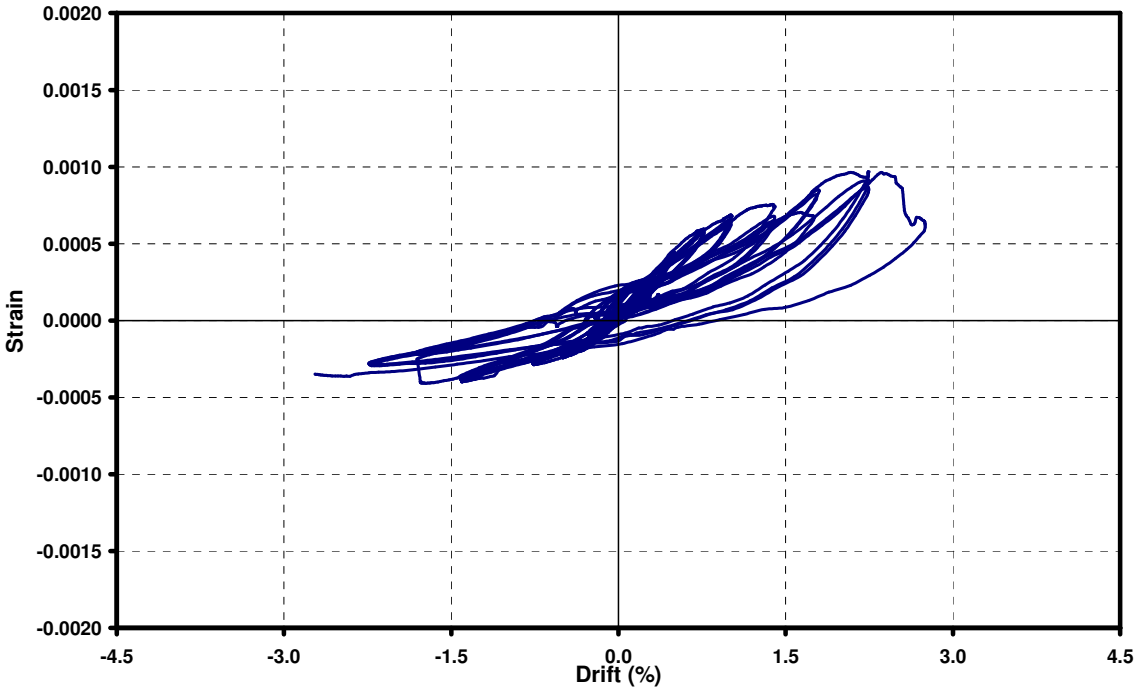

(c) US3-CS-FRP1

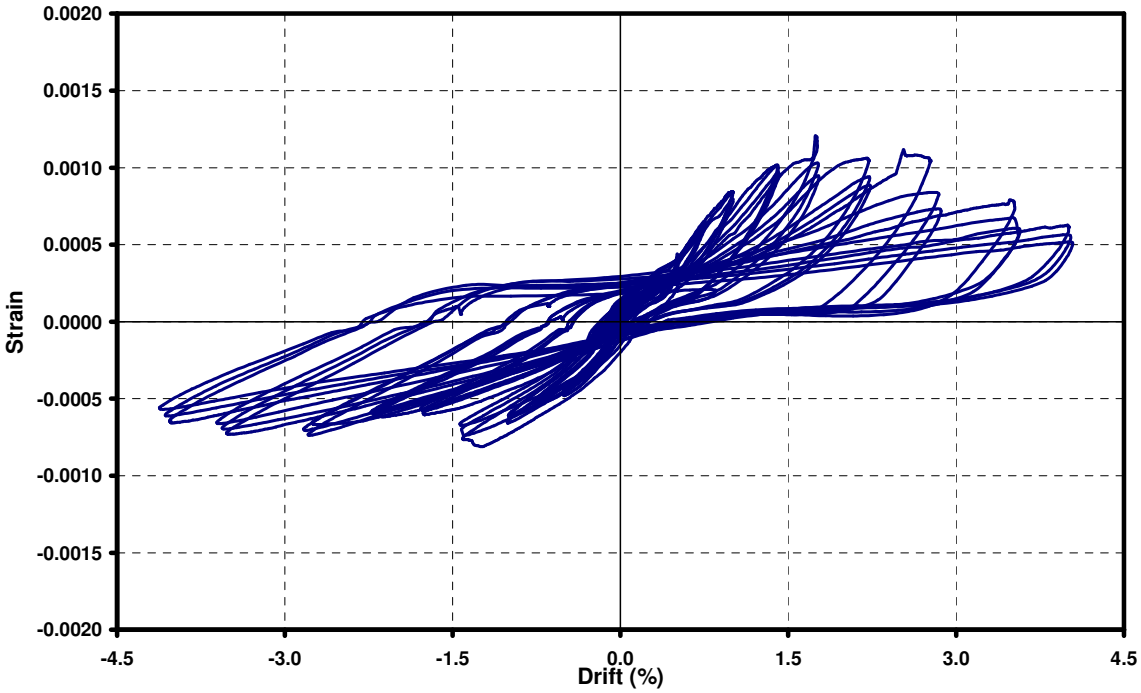

(d) US3-CS-FRP2

Figure 5.23. Strain versus drift response of longitudinal beam bottom bars (Gage #8)

5.8.2. Column Longitudinal Bars

One of the deficiencies investigated in this study was lapped splices of column longitudinal bars at the maximum moment region just above the joint. Inadequate lapped splice length may cause slippage of column longitudinal bars and hence undesired mode of failure under seismic action. Therefore, it is important to determine strain profile of lapped splice region during cyclic loading in order to investigate the behavior of beam-column joint precisely. Two strain gauges were placed on column longitudinal bars at the splice region because of that, as it is shown in Figure 3.17. The data collected by gauge #2 in US3-C-Control test was plotted with drift in Figure 5.24. As it can easily be seen in that figure, strain levels were so low in both directions of loading which means there is no risk of column failure. Form of the strain profile was same with the lateral load versus drift response of the specimen. Strain increased with increasing lateral load until the failure of specimen and afterwards decreased in both direction of loading in accordance with the failure mode. There is not a sign of slippage according to these results.

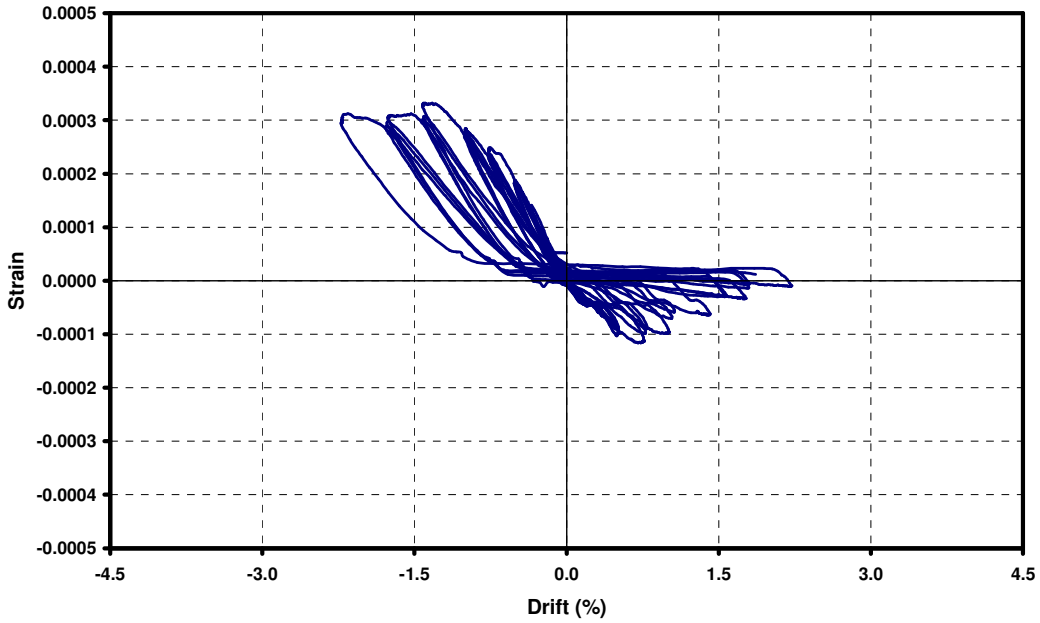

Figure 5.24. Column longitudinal bar strain in US3-C-Control (Gauge #2)

Strain versus drift graphs of longitudinal bars at the bottom portion of the column in US3-CS-Control and US3-CS-FRP1 were also given in Figure 5.25 (a) and (b),

respectively. These graphs confirm the above mentioned conclusions since the response was similar. When it was compared with US3-CS-Control, strain level of column longitudinal bars in US3-CS-FRP1 was higher as a result of the higher lateral load.

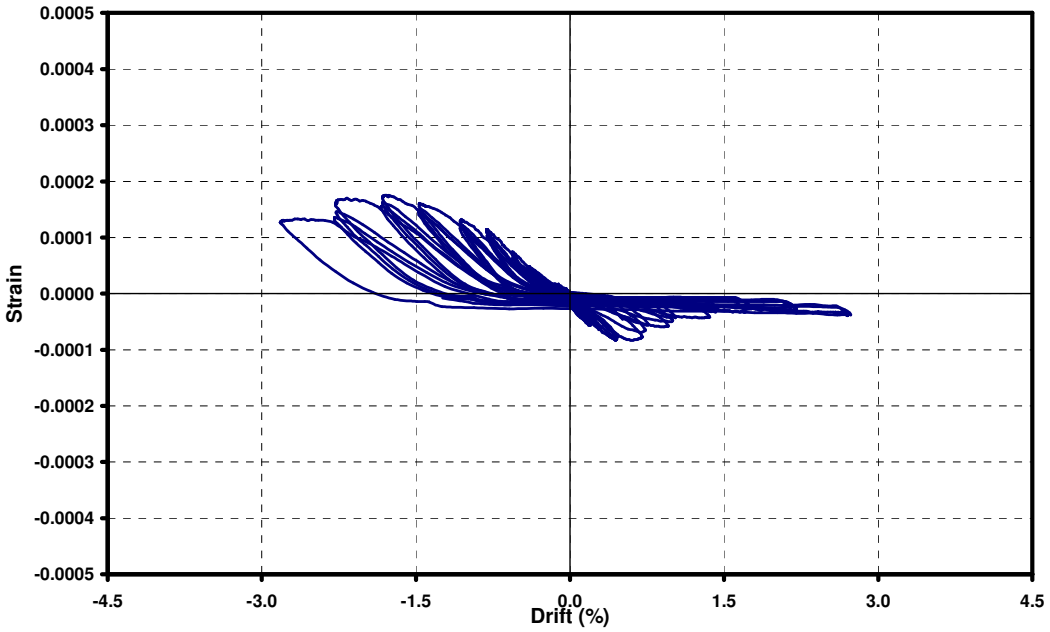

(a) US3-CS-Control

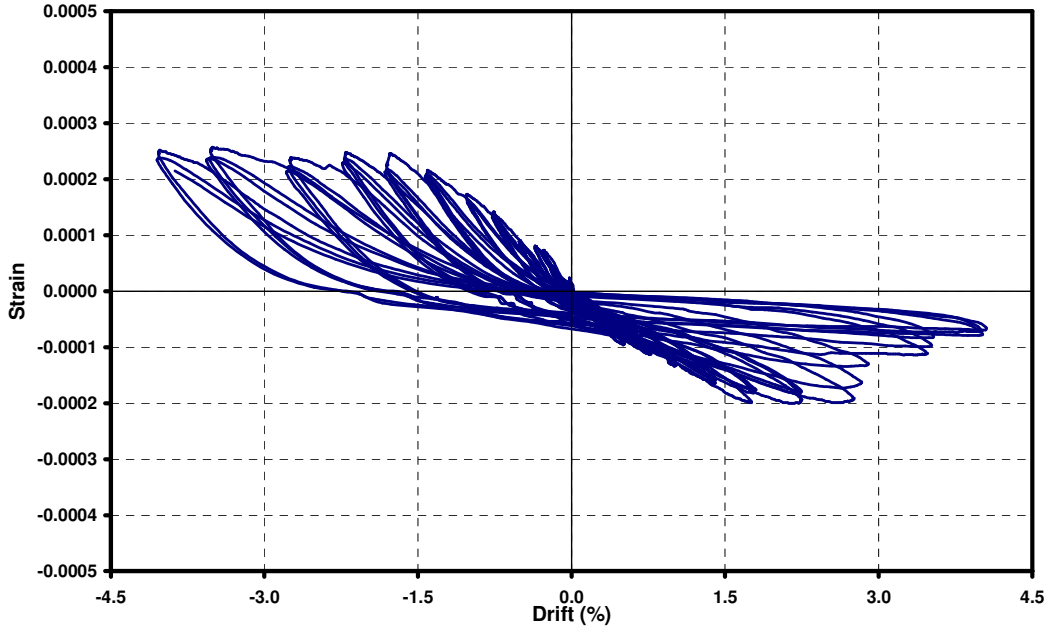

(b) US3-CS-FRP1

Figure 5.25. Bottom column longitudinal bar strain (Gauge #12)

5.8.3. Transverse Reinforcements

Strain gauges were placed on transverse reinforcements of column and beams as it was shown in Figure 3.17 in previous chapter in order to investigate shear stress levels of these members. In all specimens, stirrup strain was far from yielding strain and besides shear failure was not observed in members during the experiments. However, some diagonal shear cracks were observed which were not so remarkable.

Column transverse reinforcement strain versus drift relation is shown in Figure 5.26 for all specimens. Strain levels of control specimens were nearly same. In retrofitted specimens, additional confinement of column FRP wraps resulted in lower column stirrup strain. Stirrup strains of longitudinal beam were lower than stirrup strains of column in control specimens (Figure 5.27). Since shear forces were restrained not only by transverse reinforcements but also by concrete, cross-sectional area of member also affected the level of stirrup strain. Because the cross sectional area of longitudinal beam was higher than that of column, the lower stirrup strain of longitudinal beam was reasonable. In US3-CS-FRP1, longitudinal beam transverse reinforcement strains were higher than those of control specimens as a result of the increase in lateral load but level of strains was still far from yielding. FRP sheets wrapped around longitudinal beam for anchorage of L-shape FRP sheets and FRP belt also supplied additional confinement to the longitudinal beam and served as stirrup that is why the stirrup strain level was so low.

Transverse beam was not loaded directly during the tests as a result of the boundary conditions. Therefore, transverse beam stirrup strains were approximately zero in US3-C-Control. However, as it was mentioned above, because of the contribution of slab to the flexural capacity of longitudinal beam, transverse beam were subjected to torsional forces. Test results showed that transverse beam stirrup strain of US3-CS-Control reached the strain value of 1000μЄ due to torsion. Diagonal shear cracks were also observed at the back side of the transverse beam in US3-CS-Control. In order to stop cracking of transverse beam, FRP wraps were applied in retrofitted specimens. It can easily be seen in Figure 5.28 (c) and (d) that retrofitting improved torsional resistance of transverse beam and stirrup strain level was kept nearly at zero as it was in US3-C-Control.

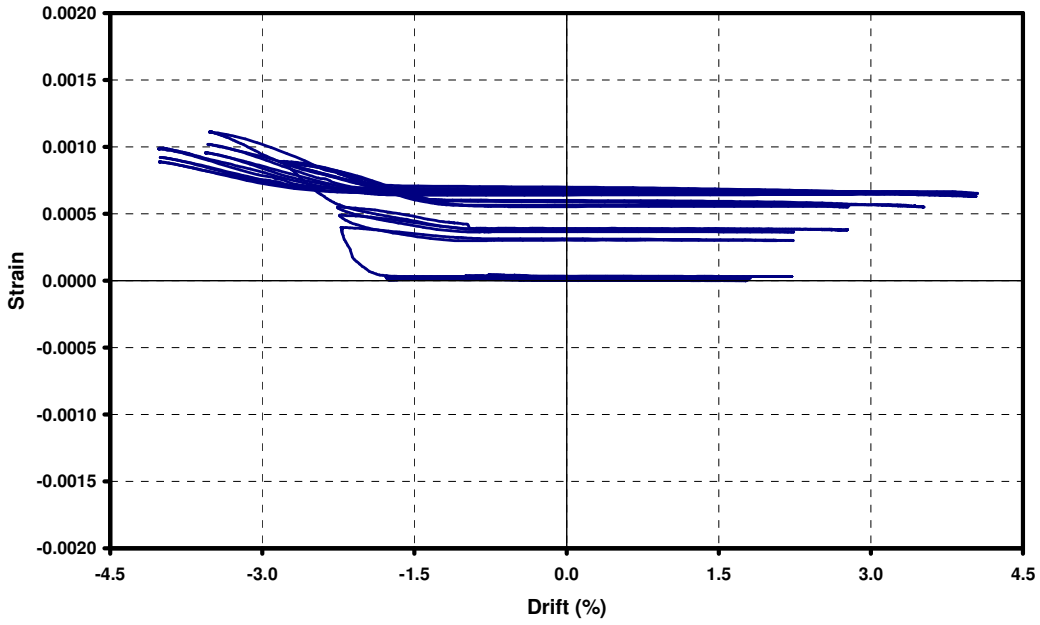

(a) US3-C-Control

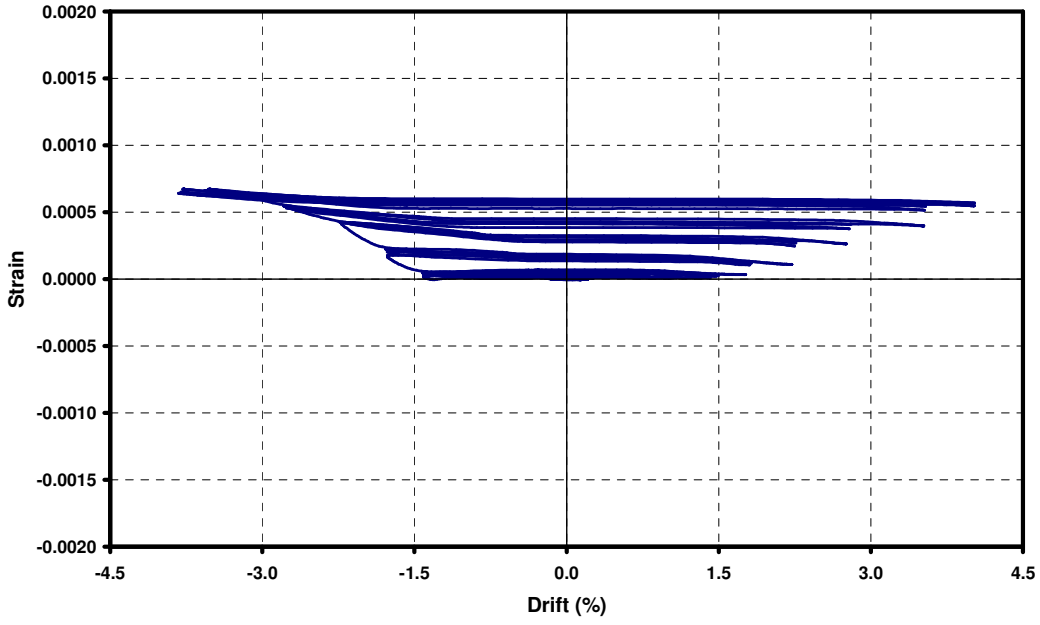

(b) US3-CS-Control

Figure 5.26. Strain versus drift response of column transverse reinforcement (Gage #3)

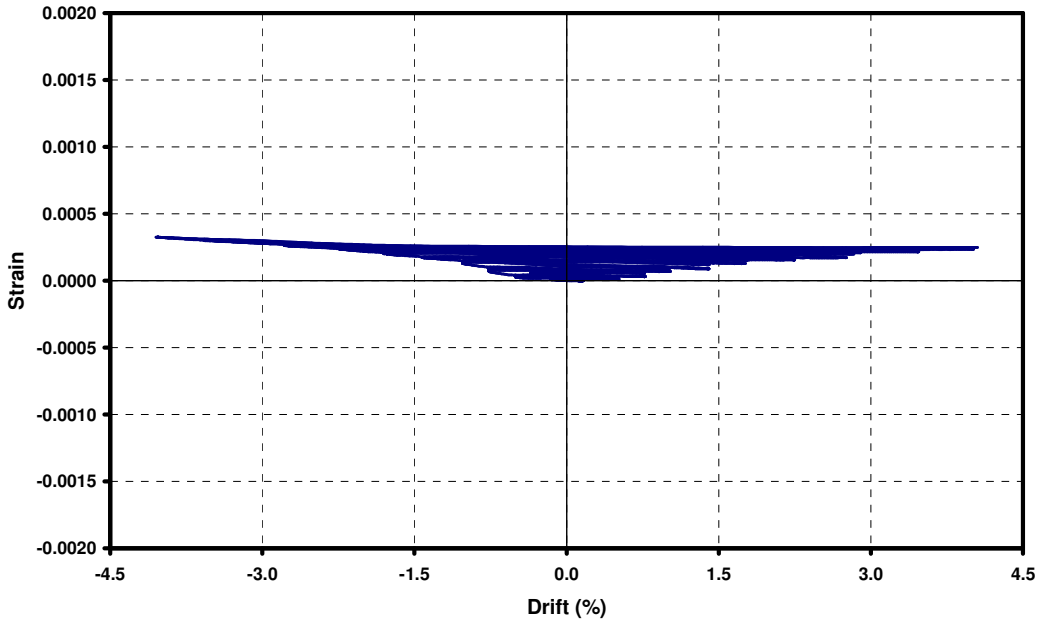

(c) US3-CS-FRP1

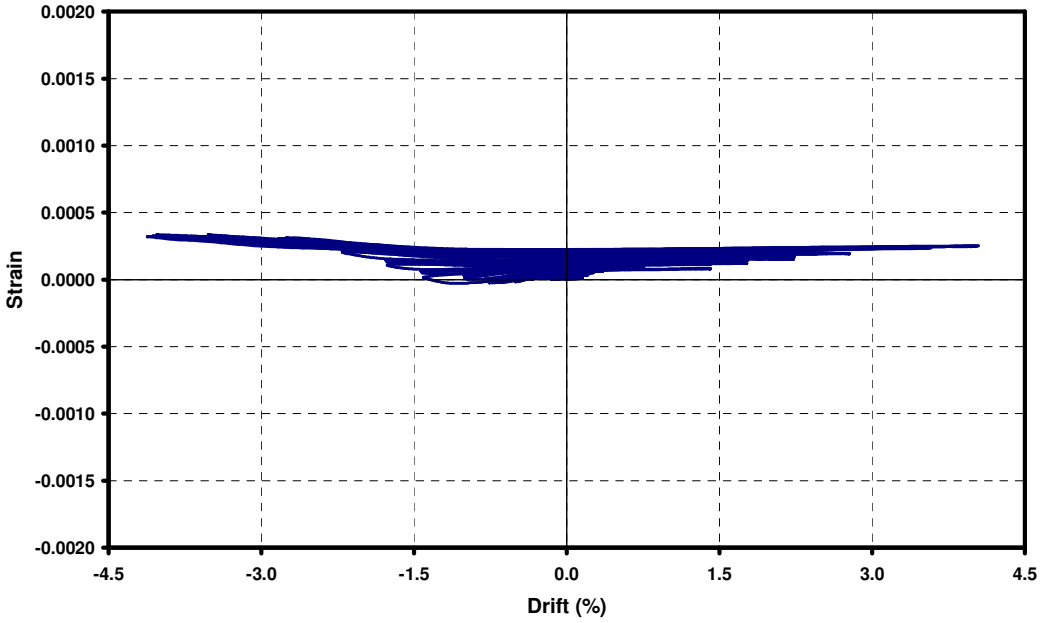

(d) US3-CS-FRP2

Figure 5.26. Strain versus drift response of column transverse reinforcement (Gage #3)

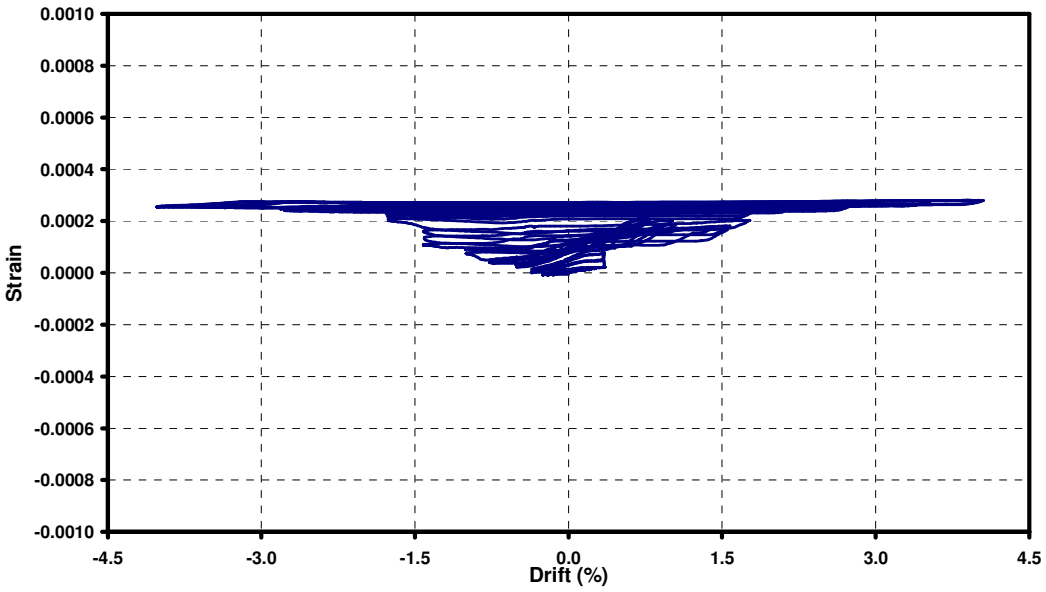

(a) US3-C-Control

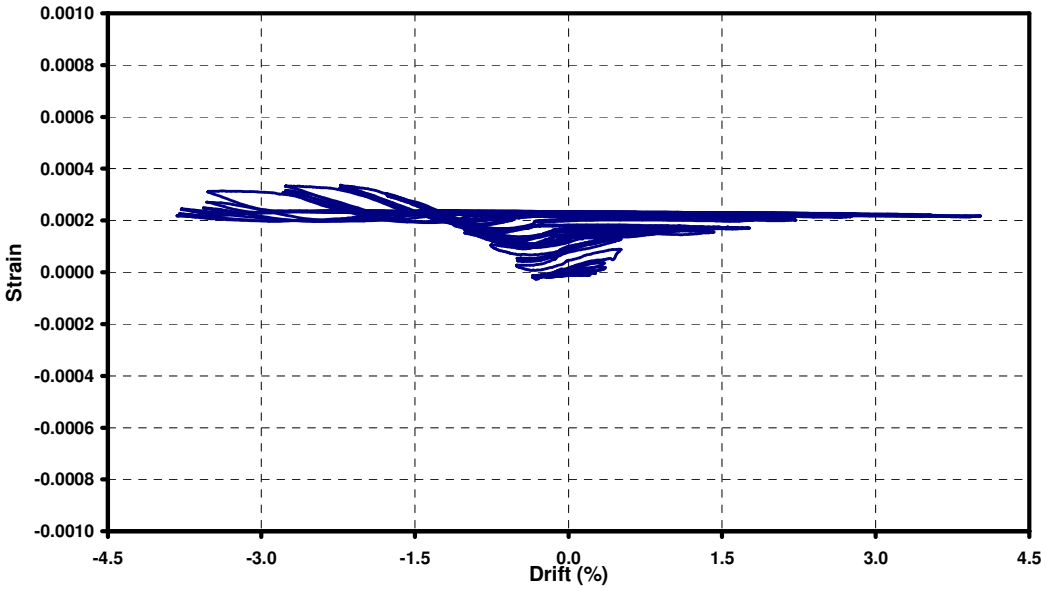

(b) US3-CS-Control

Figure 5.27. Strain versus drift response of longitudinal beam strirrup(Gage #10)

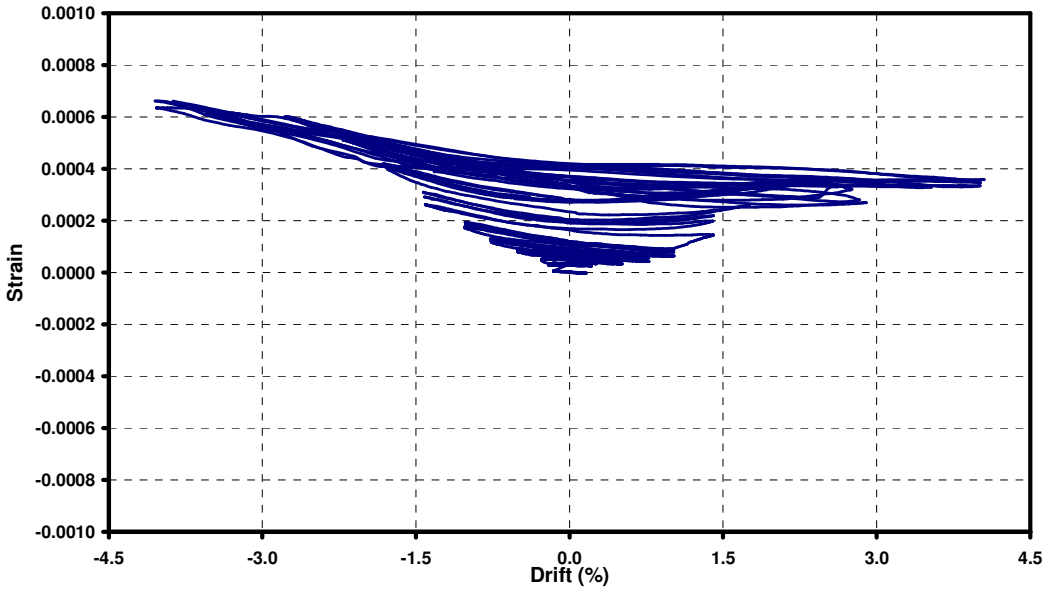

(c) US3-CS-FRP1

Figure 5.27. Strain versus drift response of longitudinal beam stirrup (Gauge #10)

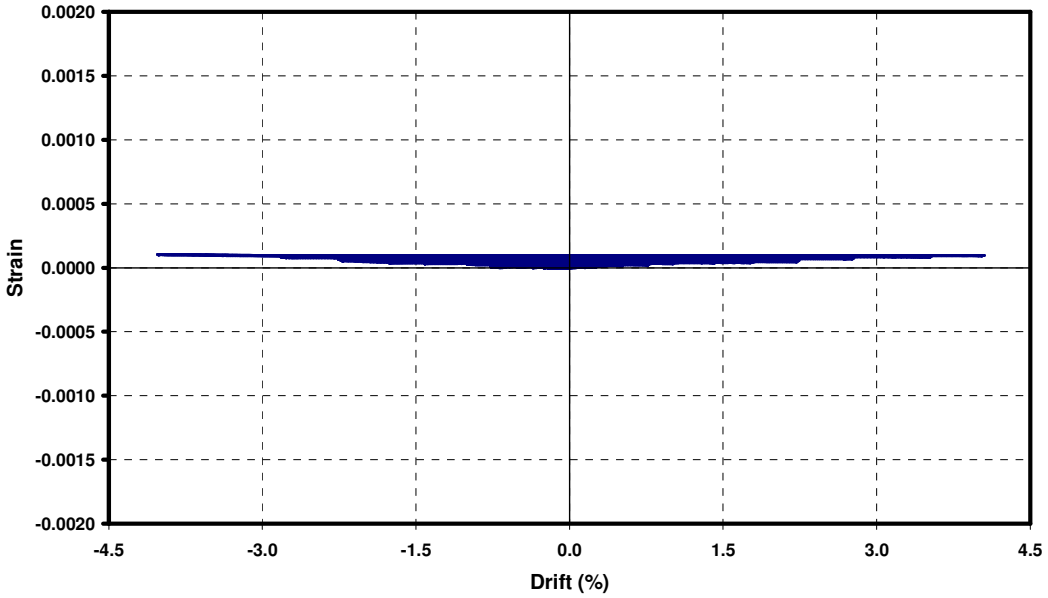

(a) US3-C-Control

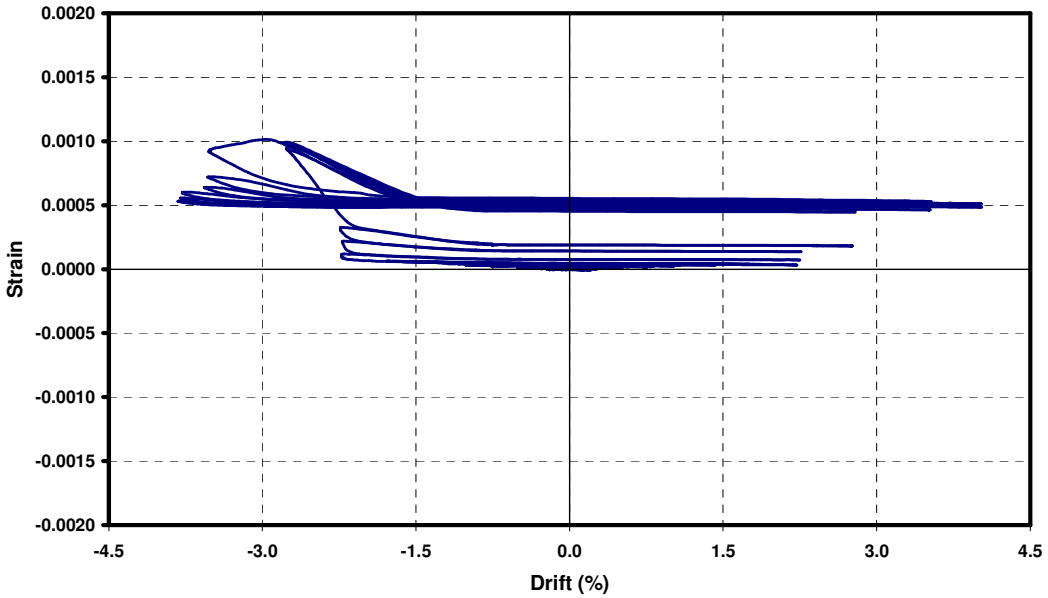

(b) US3-CS-Control

Figure 5.28. Strain versus drift response of transverse beam stirrup (Gauge #13)

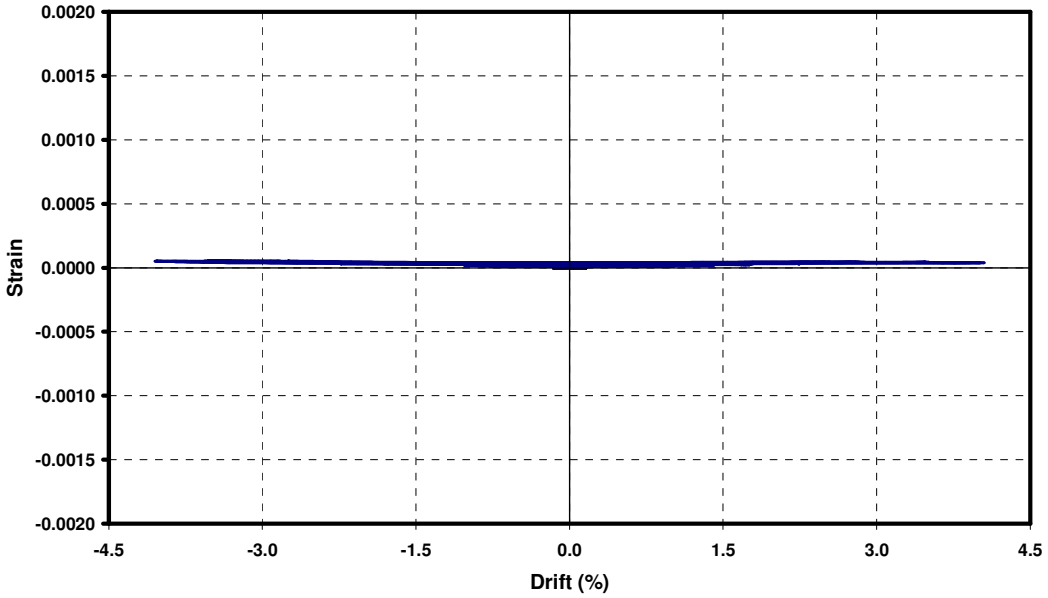

(c) US3-CS-FRP1

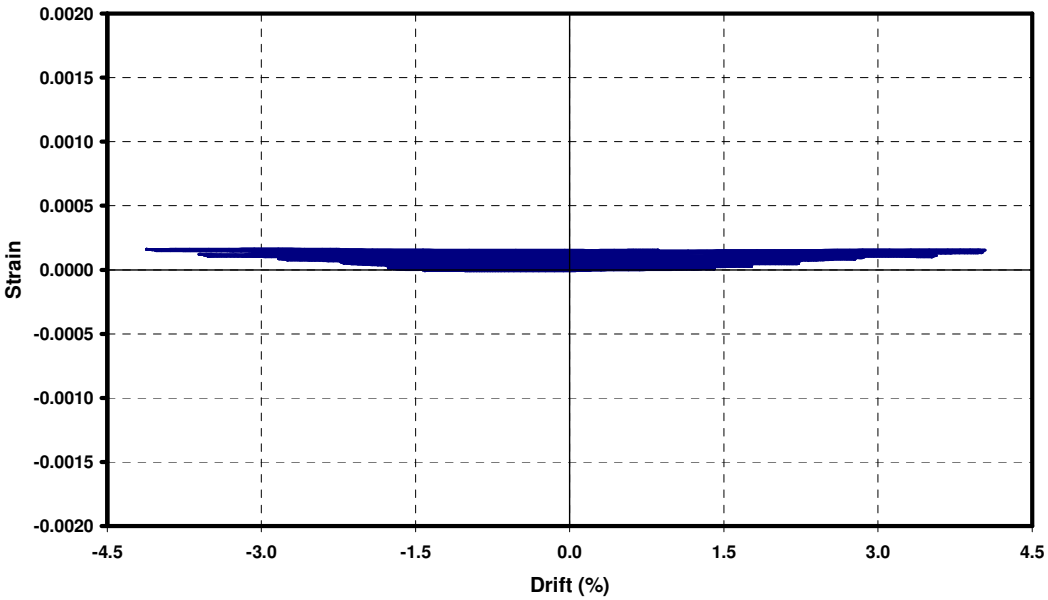

(d) US3-CS-FRP2

Figure 5.28. Strain versus drift response of transverse beam stirrup (Gauge #13)

5.8.4. FRP Strains

- **US3-CS-FRP1**

In US3-CS-FRP1, 18 strain gages were placed on FRP sheets in order to evaluate performance of retrofitting technique (Figure 3.19). Figures 5.29 and 5.30 show strain versus drift responses of inner and outer L-shape FRP sheets. As it was mentioned in test observations, these FRP sheets debonded during the experiment. It can easily be seen in these figures that, strain increases in both direction of loading until debonding occur. However, it was obvious in Figure 5.29 that strain decreased rapidly at the corresponding drift level of debonding. These FRP sheets were also ruptured at the bottom of longitudinal beam close to the anchorage hole of FRP belt at the drift level of 3.50%. As constant strain after that drift level confirms in Figure 5.30, they did not carry stress after the occurrence of rupture.

Column confinement FRP wraps were applied in US3-CS-FRP1 in order to stop damages occurred at the top and bottom columns close to the joint region in control specimens. The test results showed that these FRP wraps worked properly since these damages totally stopped in US3-CS-FRP1. According to Figure 5.31, FRP wrap strains increased in consecutive cycles throughout the test and reached approximately the maximum of 1300 μЄ.

One of the most important concerns in FRP application is proper anchorage which is required to furnish effectiveness of FRP application. Therefore, anchorage strips were applied in US3-CS-FRP1 in order to prevent debonding of L-shape FRP sheets but they were still debonded during the experiment. However, debonding did not affect the behavior significantly; ductile failure was maintained in pull direction of loading and bond slip failure was delayed to the drift level of 2.75%. Figures 5.32 and 5.33 show strain versus drift responses of anchorage strips wrapped around longitudinal and transverse beams, respectively. Maximum strain of anchorage strip at the longitudinal beam was around 6500 μЄ which was the highest strain among the measured FRP sheet strains. The strain of this anchorage strip in push direction of loading was approximately twice the strain in pull

direction as a result of the contribution of FRP belt in push direction of loading. Anchorage strips wrapped around transverse beam were applied in order to prevent not only debonding of L-shape FRP sheets but also to prevent diagonal shear cracks occurred due to torsion at the backside of transverse beam in US3-CS-Control. In US3-CS-FRP1, strain of transverse reinforcement in transverse beam was nearly zero while it was around 1000 μЄ in control specimen. That result shows the contribution of anchorage strips to torsional resistance of transverse beam. It may be concluded that, these strips carried the resultant torsional stresses in addition to the stresses grew out of resistance to the debonding of L-shape FRP sheets. Maximum strain of first strip was around 1500 μЄ as it is shown in Figure 5.33 below.

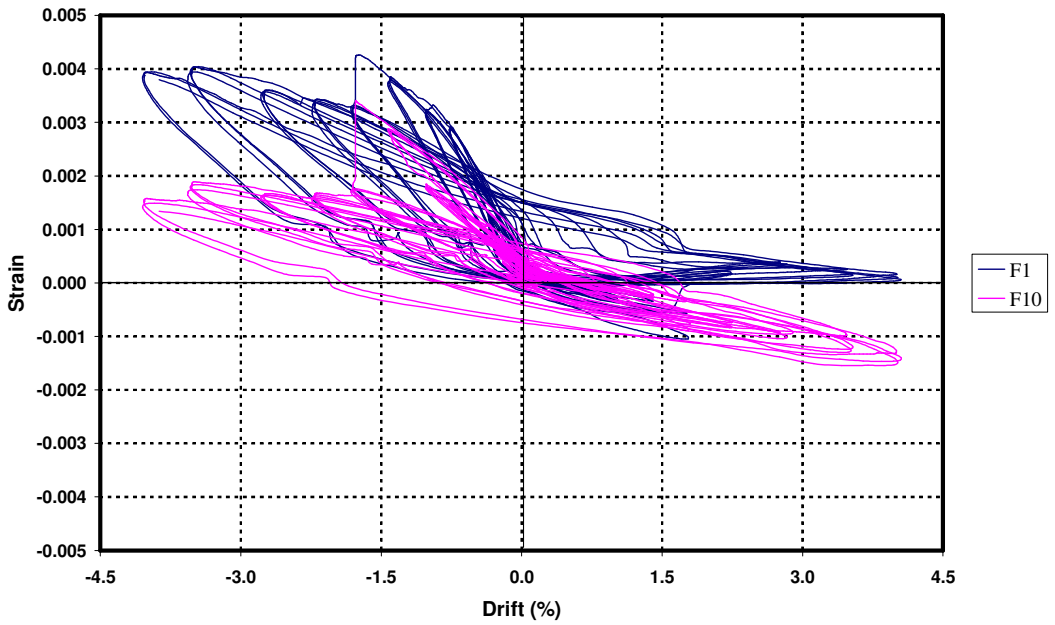

Figure 5.29. Strain versus drift response of L-shape FRP sheets (gage #F1 and #F10)

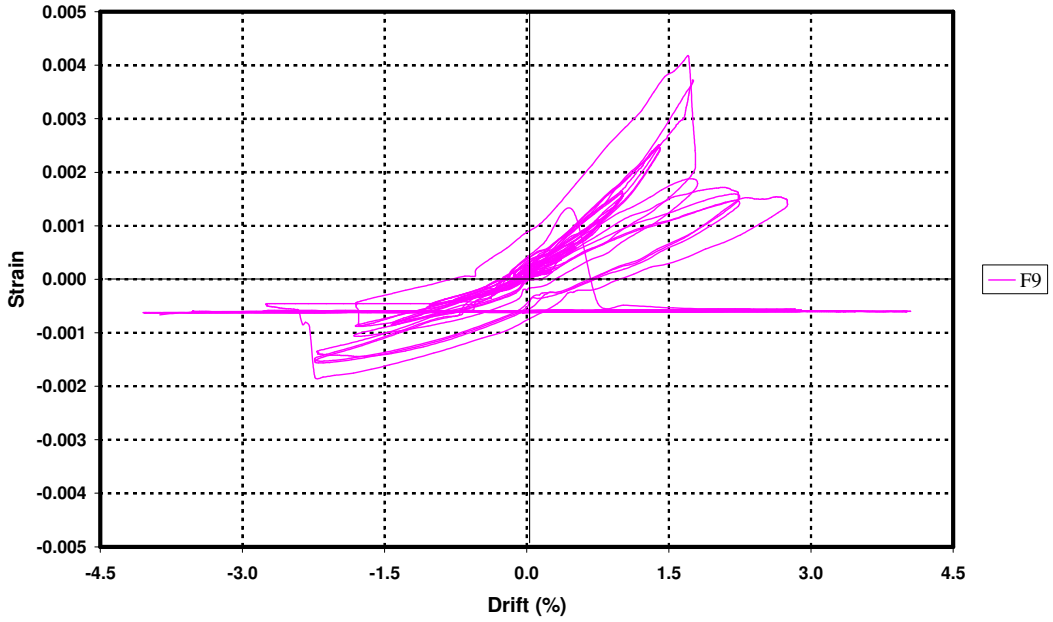

Figure 5.30. Strain versus drift response of L-shape FRP sheets (gage #F9)

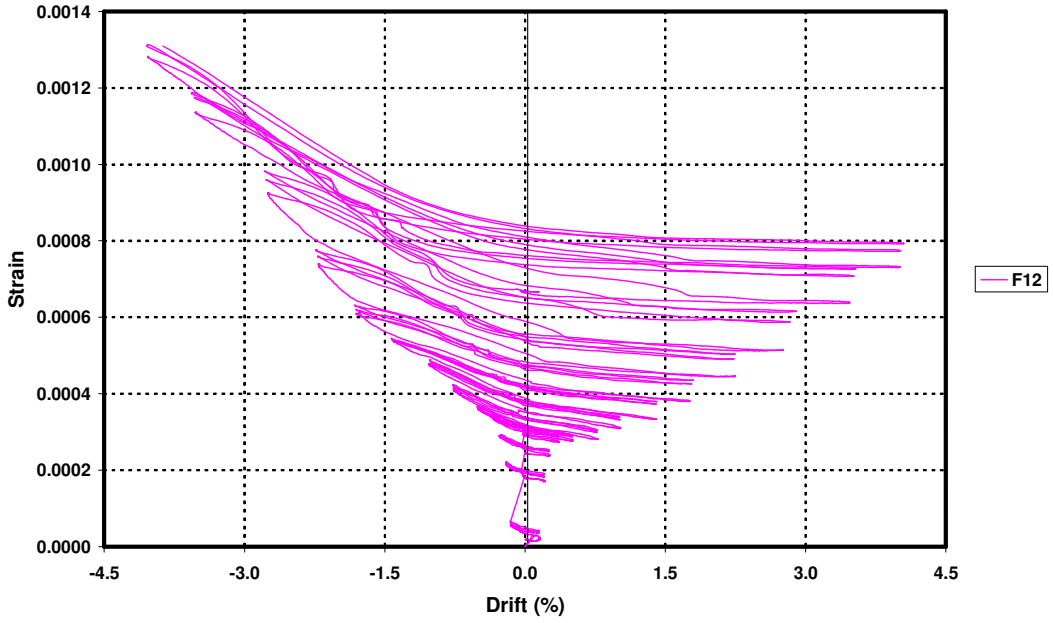

Figure 5.31. Strain versus drift response of column FRP wraps

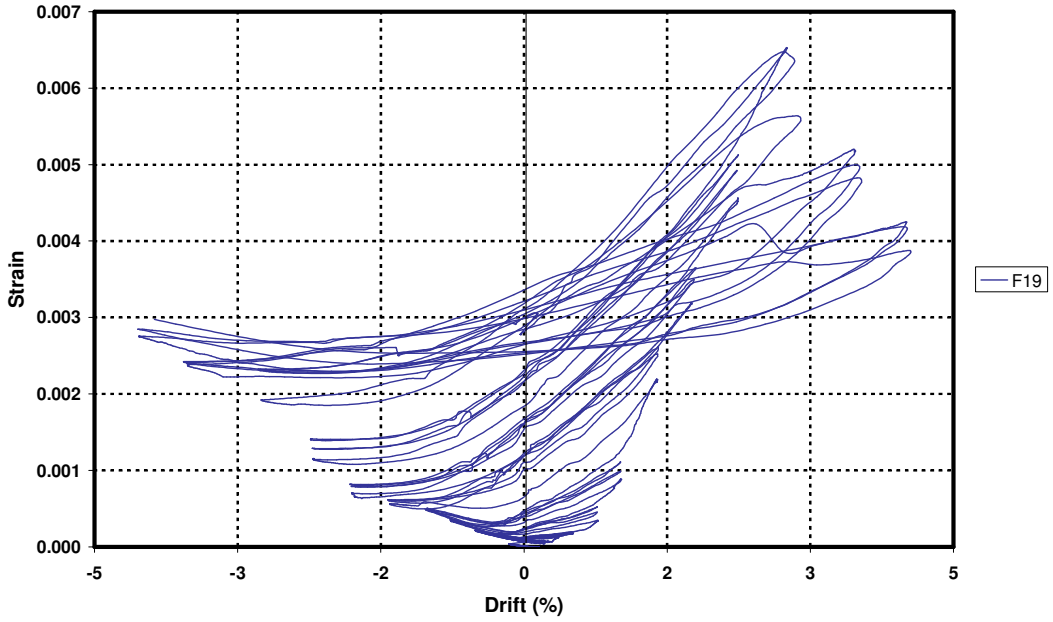

Figure 5.32. Strain versus drift response of longitudinal beam first anchorage strip

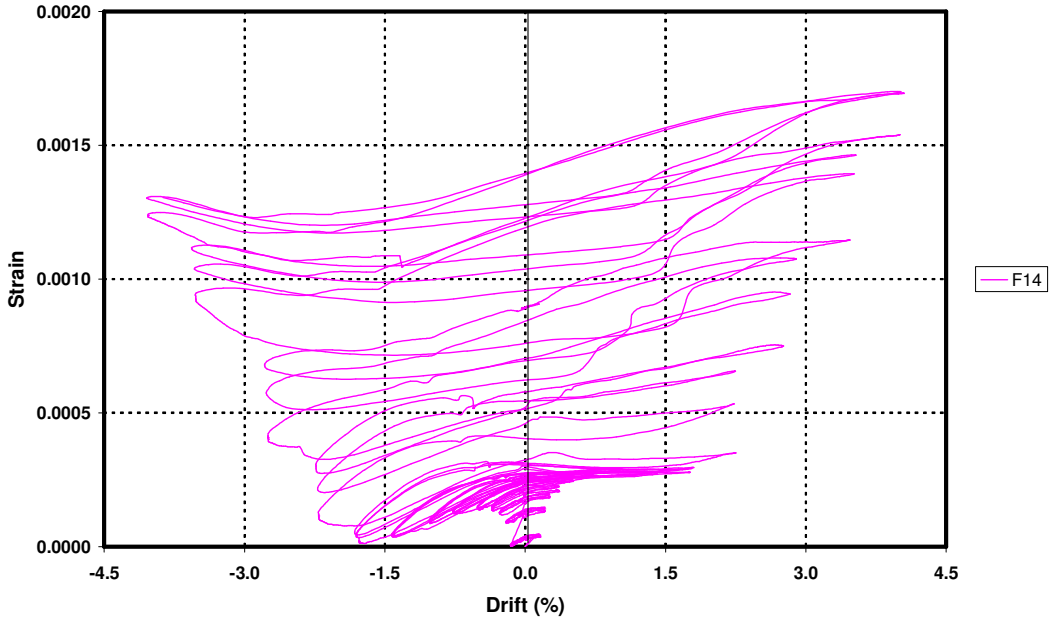

Figure 5.33. Strain versus drift response of transverse beam first anchorage strip

- **US3-CS-FRP2**

Total of 20 strain gages were mounted on FRP sheets in US3-CS-FRP2 as shown in Figure 3.20. FRP belt strain were not be able to measured directly in US3-CS-FRP1 because of the presence of L-shape FRP sheets on belt layers. It could be measured in US3-CS-FRP2 and the results are given in Figure 5.34. FRP belts worked efficiently up to the end of the test and strain level increased with increasing drift level. Maximum strain was around 5000 μЄ.

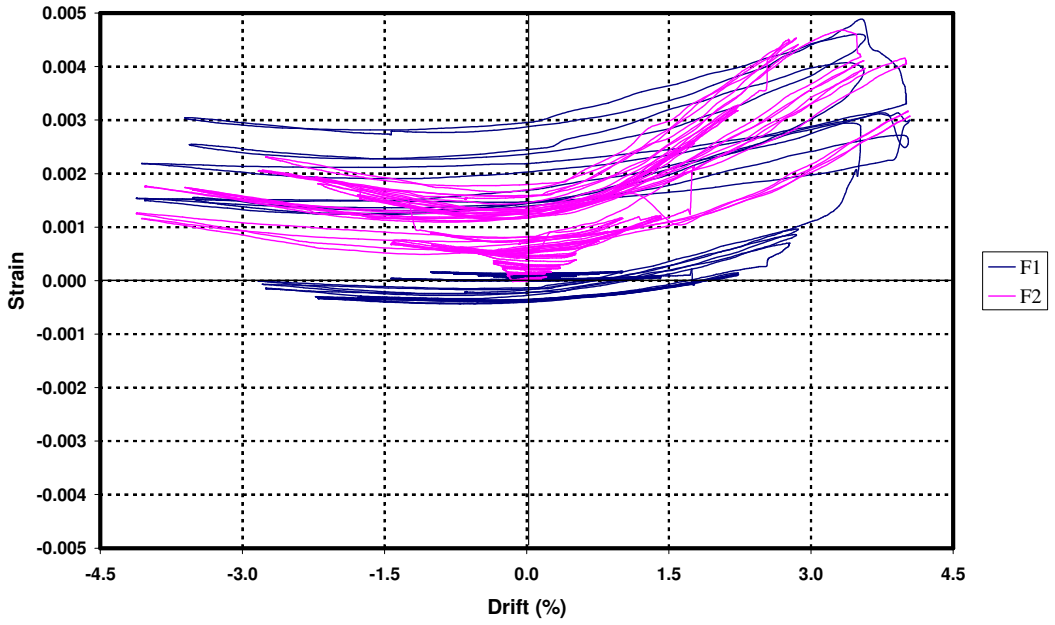

Figure 5.34. Strain vs. drift response of FRP belt

Maximum strain level on inner and outer L-shape FRP sheets was around 3000 μЄ as shown in Figure 5.35. It is obvious that strain level of gauge F17 was lower than that of gauge F6. Gauge F6 was closer to the top of the longitudinal beam and thus carried more tensile stresses, reasonably. Since FRP sheets can not carry compressive stresses, strain values in push direction of loading were approximately zero throughout the test for both gages. Column FRP wraps worked efficiently and stopped the damages of column close to the top and bottom of the joint region. Besides, anchorage strips on transverse beam carried resultant torsional stresses of slab contribution. Strain versus drift graphs are given

in Figures 5.36 and 5.37 for top column wrap and first anchorage strip on transverse beam, respectively.

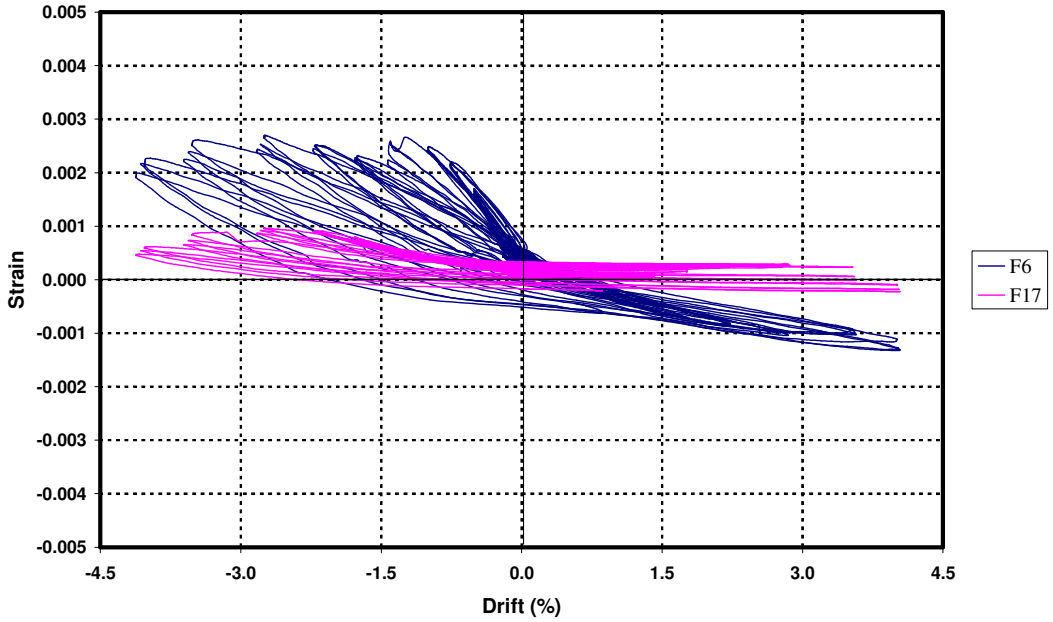

Figure 5.35. Strain versus drift response of L-shape FRP sheets

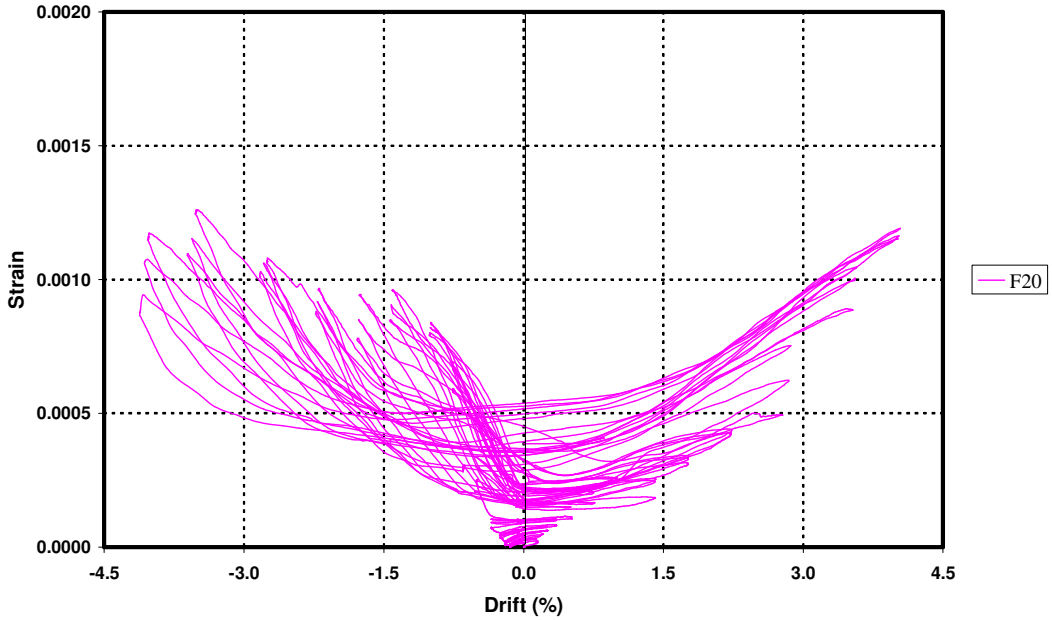

Figure 5.36. Strain versus drift response of column FRP wrap

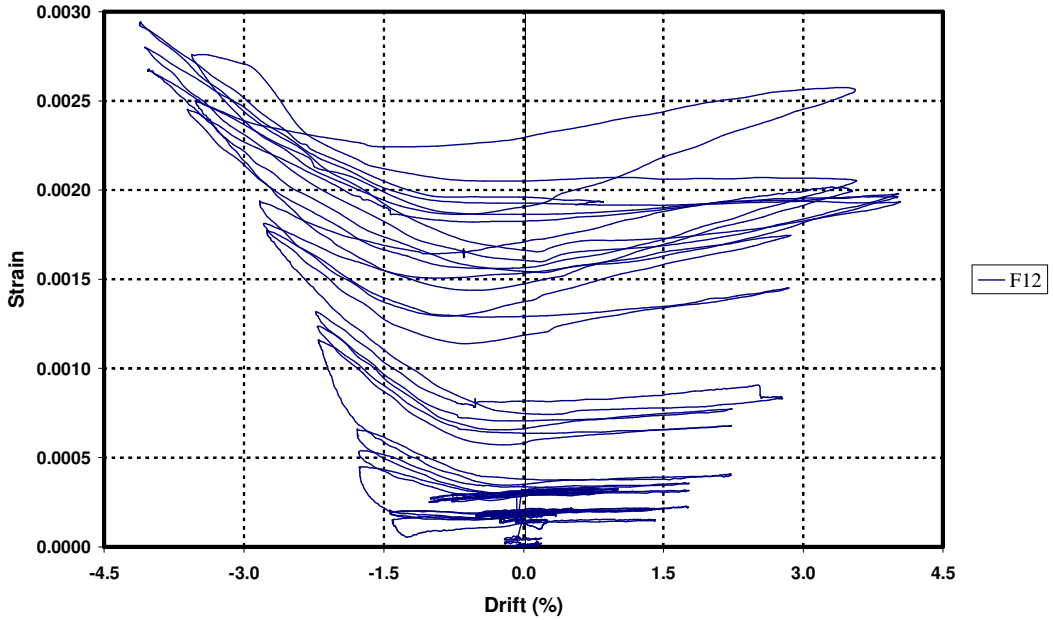

Figure 5.37. Strain versus drift response of transverse beam first anchorage strip

6. CONCLUSIONS

The following conclusions and key findings can be drawn on the basis of the results presented in this study:

- Bare RC corner beam-column joint specimens, with no transverse reinforcement in joint region and inadequately anchored beam bottom reinforcements, were exposed to brittle joint shear and bond-slip failures in pull and push direction of loading, respectively.
- Bond-slip failure was more critical than joint shear failures in terms of energy dissipation, stiffness and strength degradation characteristics.
- The presence of transverse beam increased the joint shear capacity of subassemblies but did not affect the bond-slip characteristics of inadequately anchored longitudinal beam bottom reinforcements.
- The inclusion of slab did not change the behavior in push direction of loading. On the other hand, maximum lateral load increased approximately 15% due to the contribution of slab in pull direction of loading. Slab contribution increased with the increasing drift level.
- FRP retrofitting application improved the overall behavior significantly. In retrofitted specimens, maximum lateral load increased approximately 2.5 times in push direction of loading and 20% in pull direction of loading. Beam hinging and hence a ductile behavior was maintained in pull direction of loading in US3-CS-FRP1. Joint shear failure was eliminated and brittle bond-slip failure was delayed to higher drift levels when it was compared with control specimens. In US3-CS-FRP2, joint shear and bond-slip failures were delayed to an acceptable drift level.
- Energy dissipation potential of deficient RC corner beam-column joints with floor slab was improved by CFRP application. Cumulative energy dissipated in retrofitted specimens was approximately 150% more than bare specimens.
- In addition to improved energy dissipation potential, CFRP application also achieved better stiffness degradation characteristic. Stiffness values of retrofitted specimens were higher than those of control specimens throughout the test. Besides, retrofitted

specimens maintained some of initial stiffness in both direction of loading at the end of the test, while control specimens had approximately zero stiffness after the occurrence of bond-slip failures in early drift levels in push direction of loading.

- During the experimental research, it was also observed that maximum strain level of CFRP sheets with epoxy resin were around 40% of the ultimate strain which were given by manufacturer.
- A proper FRP retrofitting technique was developed for 3D RC corner beam-column-slab joints which may also be applied to real structures.

REFERENCES

ACI T1.1 01, 2001, “Acceptance Criteria for Moment Frames Based on Structural Testing”, American Concrete Institute.

ACI-ASCE Committee 318, 2002, “Building Code Requirements for Reinforced Concrete (ACI 318-02) and Commentary (ACI 318R-02)”, American Concrete Institute, Farmington Hills, 443 pp.

ACI-ASCE Committee 352, 2002, “Recommendations for Design of Beam-Column Joints in Monolithic Reinforced Concrete Structures (ACI 352R-02)”, American Concrete Institute.

Altay, S., Parvin, A., Yalcin, C., and Kaya, O. 2007, “Evaluation of Existing Bond-Slip Models for R/C Joints,” the 9th Canadian Conference on Earthquake Engineering (9CCEE) Ottawa, ON.

Antonopoulos and Triantafillou, 2002, “Analysis of FRP-Strengthened RC Beam-Column Joints”, Journal of Composites for Construction, ASCE, Vol. 6, No. 1, pp. 41-51.

Antonopoulos, C. P. and T. C. Triantafillou, 2003, “Experimental Investigation of FRP-Strengthened RC Beam-Column Joints”, Journal of Composites for Construction, ASCE, Vol. 7, No. 1, pp. 39-49.

Balsamo, A., A. Colombo, G. Manfredi, P. Negro and A. Prota, 2005, “Seismic Behavior of a Full-Scale RC Frame Repaired Using CFRP Laminates”, Engineering Structures, Elsevier Ltd., Vol. 27, No. 5, pp. 769-780.

Beres, A., S. El-Borgi, R. White and P. Gergely, 1992, “Experimental Results of Repaired and Retrofitted Beam-Column Joint Tests in Lightly Reinforced Concrete Frame Buildings”, NCEER Report, NCEER-92-0025.

Beres, A., S. P. Pessiki, R. N. White and P. Gergely, 1996, “Implications of Experiments on Seismic Behavior of Gravity Load Designed RC Beam-to-Column Connections”, Earthquake Spectra, EERI, Vol. 12, No. 2, pp. 185-198.

Cheung, P. C., T. Paulay and R. Park, 1991, “New Zealand Tests on Full-Scale Reinforced Concrete Beam-Column-Slab Subassemblages Designed for Earthquake Resistance”, Design of Beam-Column Joints for Seismic Resistance (SP-123), American Concrete Institute, Detroit, pp. 1-37.

Di Franco, M. A., D. Mitchell, P. Paultre, 1995, “Role of Spandrel Beams on Response of Slab-Beam-Column Connections”, Journal of Structural Engineering, ASCE, Vol. 121, No. 3, pp. 408-419.

Durrani, A. J. and J. K. Wight, 1985, “Behavior of Interior Beam-to-Column Connections Under Earthquake Type Loading”, ACI Journal , Vol. 82, No. 3, pp. 343-349.

Durrani, A. J. and H. E. Zerbe, 1987, “Seismic Resitance of R/C Exterior Connections with Floor Slab”, Journal of Structural Engineering, ASCE, Vol. 113, No. 8, pp. 1850-1864.

Durrani, A. J. and J. K. Wight, 1987, “Earthquake Resistance of Reinforced Concrete Interior Connections Including a Floor Slab”, ACI Journal , Vol. 84, No. 5, pp. 400-406.

Ehsani, M. R. and J. K. Wight, 1985a, “Exterior Reinforced Concrete Beam-to-Column Connections Subjected to Earthquake-type Loading”, ACI Structural Journal, Vol. 82, No. 4, pp. 492-499.

Ehsani, M. R. and J. K. Wight, 1985b, “Effect of Transverse Beam and Slab on Behavior of Reinforced Concrete Beam-to-Column Connections", ACI Journal, Vol. 82, No. 2, pp. 188-195.

El-Amoury, T. and A. Ghobarah, 2002, “Seismic Rehabilitation of Beam-Column Joint Using CFRP Sheets”, Engineering Structures, Elsevier Ltd., Vol. 24, No. 11, pp. 1397-1407.

Engindeniz, M., L. F. Kahn and A. Zureick, 2005, “Repair and Strengthening of Reinforced Concrete Beam-Column Joints: State of the Art, ACI Structural Journal, Vol. 102, No. 2, pp. 1-14.

French, C. W. and J. P. Moehle, 1991, “Effect of floor slab on behavior of slab-beam-column connections”, Design of Beam-Column Joints for Seismic Resistance (SP-123), American Concrete Institute, Detroit, pp. 225-258.

Fujii, S. and S. Morita, 1991, “Comparison Between Interior and Exterior RC Beam-Column Joint Behavior”, Design of Beam-Column Joints for Seismic Resistance (SP-123), American Concrete Institute, Detroit, pp. 97-123.

Gergely, J., C. P. Pantelides and L. D. Reaveley, 2000, “Shear Strengthening of RCT-Joint Using CFRP Composites”, Journal of Composites for Construction, ASCE, Vol. 4, No. 2, pp. 56-64.

Ghobarah, A. and A. Said, 2002, “Shear Strengthening of Beam-Column Joints”, Engineering Structures, Elsevier Ltd., Vol. 24, No. 7, pp. 881-888.

Ghobarah, A. and T. El-Amoury, 2005, “Shear Strengthening of RCT-Joint Using CFRP Composites”, Journal of Composites for Construction, ASCE, Vol. 9, No. 5, pp. 408-416.

Granata, P.J. and Parvin, A., 2001, "An Experimental Study on Kevlar Strengthening of Beam-Column Connections," Composite Structures, Vol. 53, No. 2, pp. 163-171.

Kaku, T. and H. Asakusa, 1991a, “Bond and Anchorage of Bars in Reinforced Concrete Beam-Column Joints”, Design of Beam-Column Joints for Seismic Resistance (SP-123), American Concrete Institute, Detroit, pp. 401-423.

Kaku, T. and H. Asakusa, 1991b, “Ductility Estimation of Exterior Beam-Column Subassemblages in Reinforced Concrete Frames”, Design of Beam-Column Joints for Seismic Resistance (SP-123), American Concrete Institute, Detroit, pp. 167-186.

Moehle, J. P., 2000, “State of Research on Seismic Retrofit of Concrete Building Structures in the US”, US-Japan Symposium and Workshop on Seismic Retrofit of Concrete Structures.

Mukherjee, A. and M. Joshi, 2005, “FRPC Reinforced Concrete Beam-Column Joints Under Cyclic Excitation”, Composite Structures, Elsevier Ltd., Vol. 70, No. 2, pp. 185-199.

Pantazopoulou S. J. and C. W. French, 2001, “Slab Participation in Practical Earthquake Design of Reinforced Concrete Frames”, ACI Structural Journal, Vol. 98, No. 4, pp. 479-489.

Park, R., 1989, “Evaluation of Ductility of Structures and Structural Assemblages from Laboratory Testing”, Bulletin of the New Zealand National Society for Earthquake Engineering, Vol. 22, No. 3, pp. 155-166.

Paulay, T., R. Park, and M. J. N. Pristley, 1978, “Reinforced Concrete Beam-Column Joints under Seismic Actions”, ACI Journal , Vol. 75, No. 11, pp. 585-593.

Sin, M., 2004, Performance of Reinforced Concrete Edge Beam-Column-Slab Connections Subjected to Earthquake Loading, Ph.D. Dissertation, University of Illinois at Urbana, Champaign.

REFERENCES NOT CITED

Abrams, D. P., 1987, “Scale Relations for Reinforced Concrete Beam-Column Joints", ACI Structural Journal, Vol. 84, No. 6, pp. 502-512.

Paulay, T., 1986, “A Critique of the Special Provisions for Seismic Design of the Building Code Requirements for Reinforced Concrete (ACI 318-83)”, ACI Journal , Vol. 83, No. 2, pp. 274-283.

Bonacci, J. and S. Pantazopoulou, 1993, “Parametric Investigation of Joint Mechanics”, ACI Structural Journal , Vol. 90, No. 1, pp. 61-71.

French, C. W. and A. Boroojerdi, 1987, “Contribution of R/C Floor Slabs in Resisting Lateral Loads”, Journal of Structural Engineering, ASCE, Vol. 115, No. 1, pp. 1-18.

Goto, Y., O. Joh and T. Shibata, 1988, “Influence of Transverse Reinforcment in Beam Ends and Joints on the Behavior of R/C Beam-Column Subassemblages”, Proceeding of 9th WCEE, Japan, Vol. 4, pp. 585-590.

Hwang, S. J and H. J Lee, 1999, “Analytical Model for Predicting Shear Strength of Exterior Reinforced Concrete Beam-Column Joint for Seismic Resistance”, ACI Structural Journal, Vol. 96, No. 5, pp. 846-857.

Harajli, M. H., K. A. Soudki and T. Kudsi, 2006, “Shear Strengthening of RCT-Joint Using CFRP Composites”, Journal of Composites for Construction, ASCE, Vol. 10, No. 5, pp. 399-409.

Ichinose, T. 1991, “Interaction Between Bond at Beam Bars and Shear Reinforcement in RC Interior Joints”, Design of Beam-Column Joints for Seismic Resistance (SP-123), American Concrete Institute, Detroit, pp. 379-399.

Kim, J, J. M. LaFave, 2007, “Key Influence Parameters for The Joint Shear Behavior of Reinforced Concrete (RC) Beam-Column Connections”, Engineering Structures, Elsevier Ltd., Vol. 29, No. 10, pp. 2523-2539.

Kitayama, K., S. Otani and H. Aoyama 1991, “Development of Design Criteria for RC Interior Beam-Column Joints”, Design of Beam-Column Joints for Seismic Resistance (SP-123), American Concrete Institute, Detroit, pp. 97-123.

Meinheit, D. F. and J. O. Jirsa, 1981, “Shear Strength of RC Beam-Column Connections”, Journal of Structural Division, ASCE, Vol. 107, No. 11, pp. 2227-2244.

Prota, A., A. Nanni, G. Manfredi and E. Cosenza, 2000, “Seismic Upgrade of Beam-Column Joints with FRP Reinforcement”, Industria Italiana del Cemento, November 2000.